IMPROVEMENTS TO MECHANISM SYNTHESIS METHODS

A Dissertation Presented to the

Faculty of the Department of Mechanical Engineering

University of Houston

In Partial Fulfillment

of the Requirements for the Degree

Doctor of Philosophy

By

Robert T. Strong

May 1978

ACKNOWLEDGEMENTS

The author would like to express appreciation and thanks to his advisor, Dr. K. J. Waldron for his invaluable assistance and guidance before and throughout the preparation of this dissertation, to Dr. T. E. Shoup for his interest and help with the numerical algorithm, to the National Science Foundation for their financial support through grant ENG 75-20889 during the course of this work, and finally to Miss Cynthia Powers for her help in typing this dissertation.

TABLE OF CONTENTS

CHAPTER PAGE

LIST OF FIGURES

Figure		Page

Figure		Page

To my wife Sharyn,

my daughters Jennifer and Courtney,

and to Frank and Eleanor

CHAPTER 1

INTRODUCTION

Four-bar mechanisms are used quite extensively in industry to obtain unusual motions because they are simple and cheap to build and provide good service as compared to cams which are much more difficult to manufacture. However, cams have the advantage of being much easier to design than the four-bar mechanism. One type of linkage design is that of finding a mechanism which moves a lamina through a number of nominated positions. This type of synthesis is called motion generation or sometimes referred to as the plane path problem. This is the type of synthesis primarily studied in this dissertation. Several other types of synthesis problem, such as function generation and point path-angle synthesis can be transformed to motion generation problems.

The standard representation of a four-bar mechanism is illustrated in Figure 1-1. The mechanism is composed of two cranks, referred to as the driving crank and the driven crank, the base, and the coupler which connects the moving pivots of the two cranks. The slider-crank mechanism of Figure 1-2 is a special case of the four-bar mechanism in the sense that the driven crank can be considered to be infinite in length.

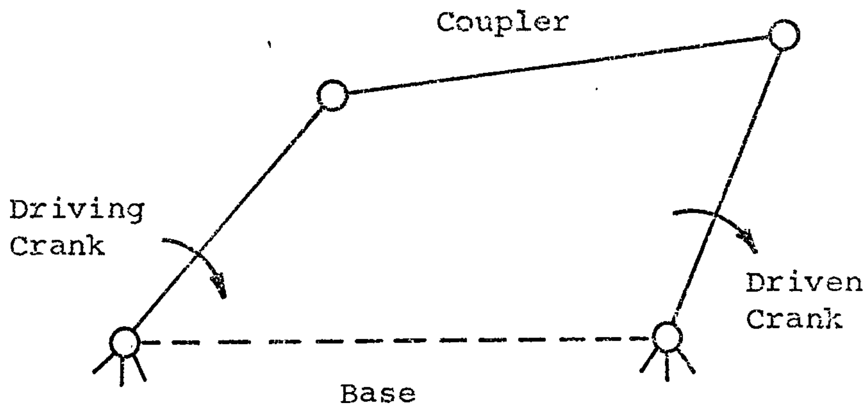

Four-bar linkage

Fig. 1-1

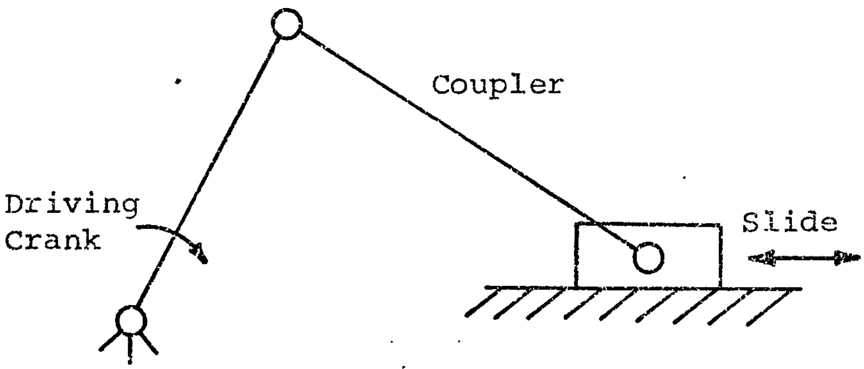

Slider-crank linkage

Fig. 1-2

In Germany, Burmester [1-1] used the concepts of poles, circle-point and center-point curves to develop methods for synthesizing mechanisms which would approximate straight line generation. These ideas were later extended by Alt [1-2], Beyer [1-3] and Hain [1-4]. The circle-point curve is the locus of all points in the fixed frame whose four positions all lie on a circle. If the circle is the locus for the moving pivot of a crank, then the fixed pivot lies at the center of that circle. Therefore, for each point on the circle-point curve there exists a point which represents the corresponding fixed pivot. The locus of these fixed pivots is called the center-point curve. Thus there is a one-to-one correspondence between points on these two curves.

A pole is the point in the fixed plane about which the moving lamina rotates for a pair of design positions. The image pole is the pole as seen relative to the moving plane. Because of the one-to-one correspondence there are points on the circle-point curve which correspond to the poles of the center-point curve. These points are called Q points [1-3] and their location both graphically and analytically is described in detail in Chapter 2. Likewise, the points on the center-point curve which correspond to the image poles can be found in the same manner. Both the circle-point and center-point curves are third degree curves which go through the two imaginary circle-points and center-points at infinity and thus intersect the asymptote once in the finite plane [1-3]. One point exists on the circle-point curve for which the radius of the circle on which its four positions lie is infinite. This point is called the Ball point [1-3]. Thus if the Ball point is chosen as the moving pivot for the crank, the trace of the moving pivot will be a straight line. Therefore since the fixed pivot of the crank must lie at infinity, the point on the center-point curve which corresponds to the Ball point on the circle-point curve must be at infinity. When designing a slider-crank mechanism for four finitely separated positions the moving pivot for the slide must be chosen as the Ball point. For the inverted slider-crank linkage, one chooses the circle-point at infinity as the moving pivot of the crank and the corresponding center-point is the fixed pivot. The moving pivot is now the slide for this mechanism which is called the turning block linkage, see Figure 1-3.

The circle-point curve, as mentioned earlier, is derived for four finitely separated design positions (FSP). Evidently, an infinite number of solutions are possible. For the motion generation synthesis problem it can be shown that the maximum number of design, or nominated positions, is five [1-3]. The five design position problem is solved by solving the four design position problem twice for two different sets of four of the five

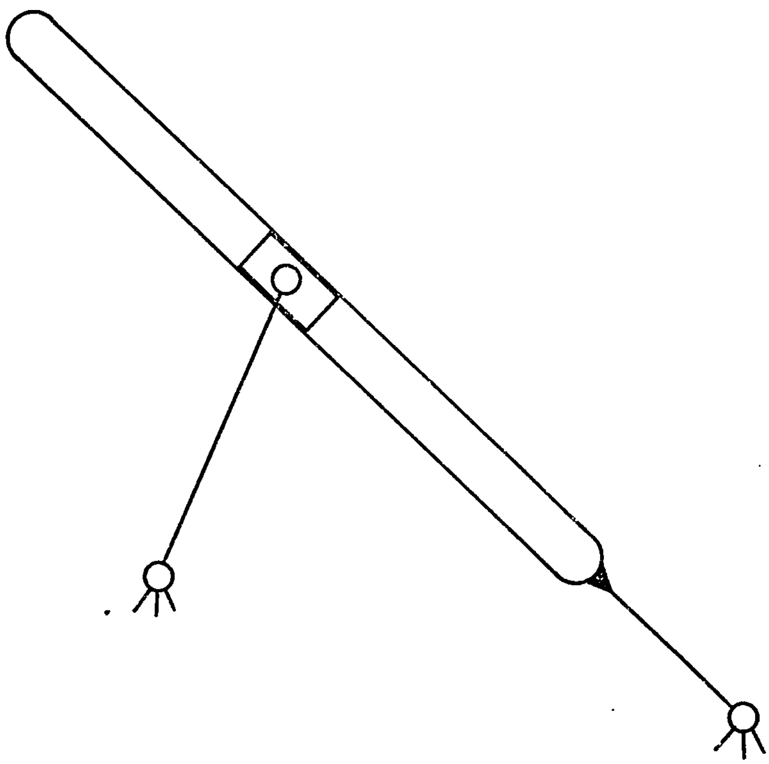

Turning block linkage

Fig. 1-3

design positions. For example, the common solutions to the motion generation problems using positions 1, 2, 3 and 4 and positions 1, 2, 3 and 5 are the only possible solutions to the five design position problem. Since the two curves are third degree curves there are a maximum of nine intersections or solutions. However, two of the intersections are the previously mentioned imaginary circle-points at infinity and three others are the common image poles (P'_{12}, P'_{13} and P'_{23}) for the two sets of four design positions chosen. Therefore there are a maximum of four solutions, known as the Burmester points, if all four solutions exist. The other possibilities are two solutions if two are imaginary or none if all four are imaginary. Thus if all four solutions exist there is a maximum of six linkages which may be designed for a 5FSP problem. However, it may happen that none of these linkages is a desirable solution. Therefore the probability of a practicable solution for a 5FSP problem is greatly reduced from that of a 4FSP problem.

For the 2FSP and 3FSP problems, any point in the plane may be chosen as the moving pivot of a crank and the fixed pivot is the center of a circle on which the moving pivot lies for the given design positions. In the two design position case there are an infinite number of fixed pivots corresponding to any point lying on the perpendicular bisector of the line joining those two positions. However, for the three design position problem only one circle can be drawn through three points. Therefore, there is only one choice for the fixed pivot of the crank. These two cases are illustrated in Figures 1-4 and 1-5.

The previous material, as indicated, was for a finite set of design positions. Mueller [1-5] developed numerous synthesis methods for infinitesimally separated position (ISP) problems. For ISP problems the instantaneous centers or poles are found by locating the intersection of the normal to the path tangent for each end of the coupler. The instantaneous centers are handled in the same manner as the poles for the FSP problems. When the ISP and FSP problems are combined, they are called multiply separated position (MSP) problems. Previous work in this area, using an analytical-numerical approach is that of Tesar and his associates [1-6 through 1-11]. Graphical solutions to MSP problems have been presented by Volmer [1-12], Dijksman [1-13], Hain [1-4] and Waldron [1-14]. Tesar and Carrero [1-15] have drawn together graphical solutions to FSP, ISP and MSP problems. Although the methods presented in this dissertation are formulated for FSP problems, they can be immediately applied to all MSP problems in a similar manner to those presented in Ref. [1-14].

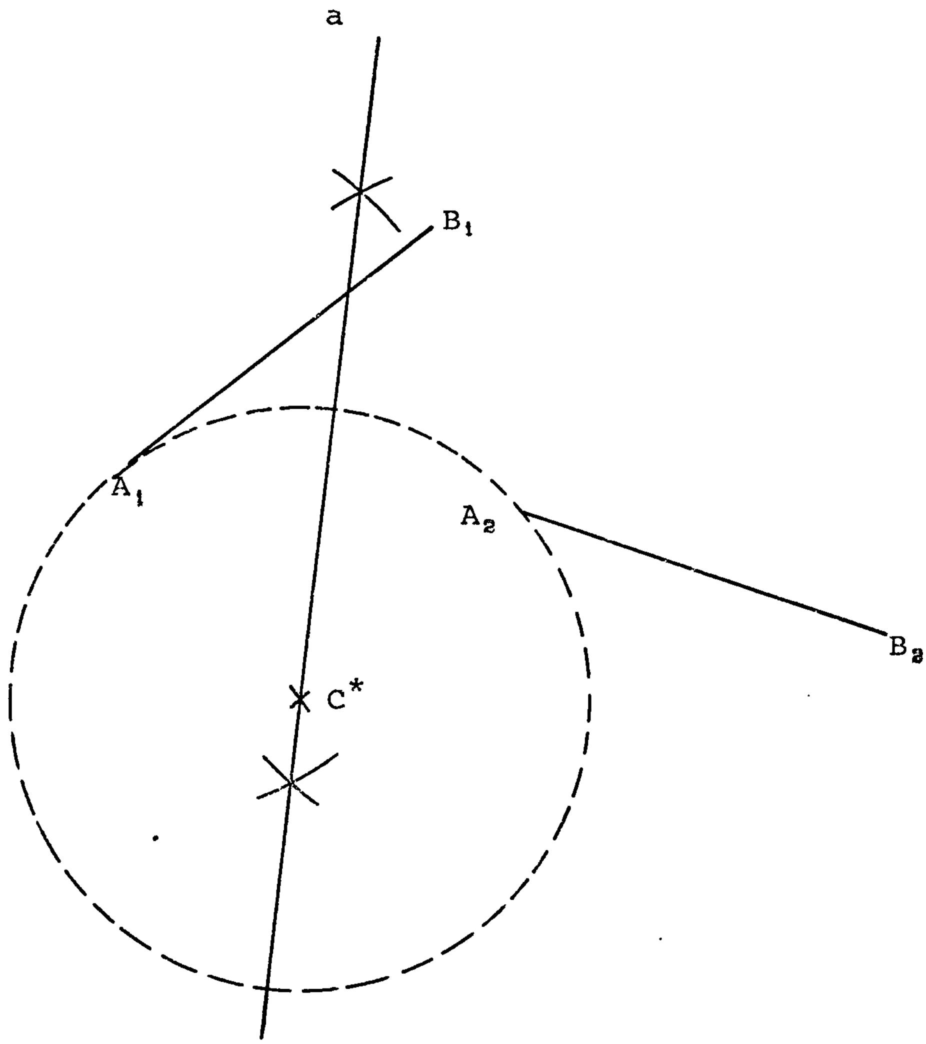

Determination of loci for finding center-point for two finitely separated design positions

Fig. 1-4

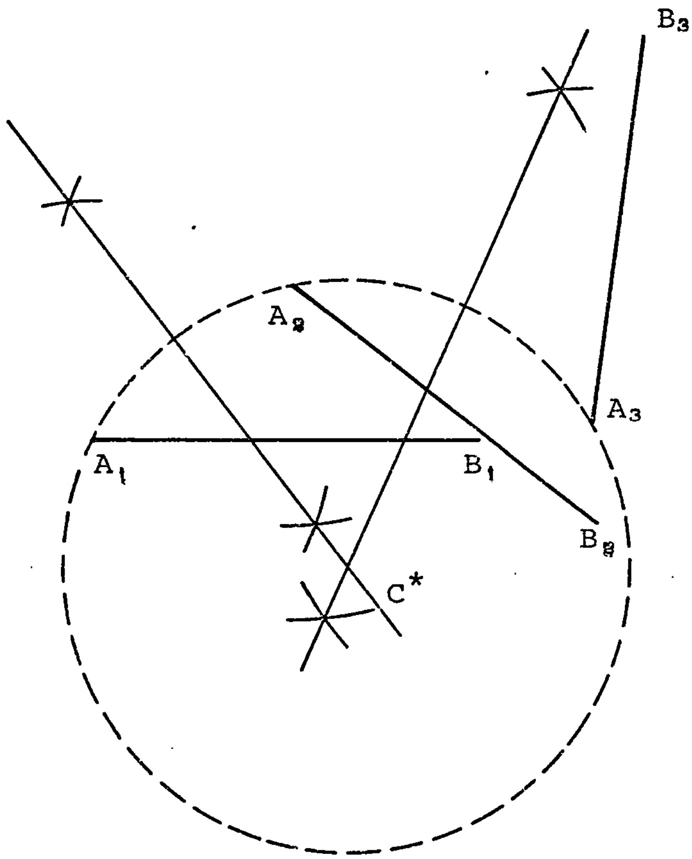

Determination of center-point for three finitely separated design positions

Fig. 1-5

If one of the joint angles, θ, is fixed, as shown in Figure 1-6, then the linkage may be arranged in one of the two possible positions indicated by the solid and broken lines. Note that the angles ψ between the remaining crank and the coupler for the two configurations (branches) have the same magnitude but are opposite in direction as indicated by the negative sign. For the linkage to get from one branch to the other, it must pass through one of the two transition configurations shown in Figure 1-7. In other words, for a transition from one branch to the other to occur, the linkage must pass through either the $\psi = 0^{\circ}$ or $\psi = \pi$ positions. Now if link 4 is assumed to have some rotation, ω_4, as shown in Figure 1-8 for either of the two transition configurations, then Kennedy's theorem [1-16] gives

$$\omega_2 = \omega_4 \frac{I_{14}I_{24}}{I_{12}I_{24}}$$

But since the instantaneous centers I_{14} and I_{24} are the same point, the angular velocity of link 2 is zero. Thus when a joint is passing through one of the transition positions, the opposite joint must have zero velocity. Therefore if link 2 is assumed to rotate completely, then ψ cannot pass through a transition position. Hence the range of ψ must be less than π. If link 2 in Figure 1-6 is assumed to rotate

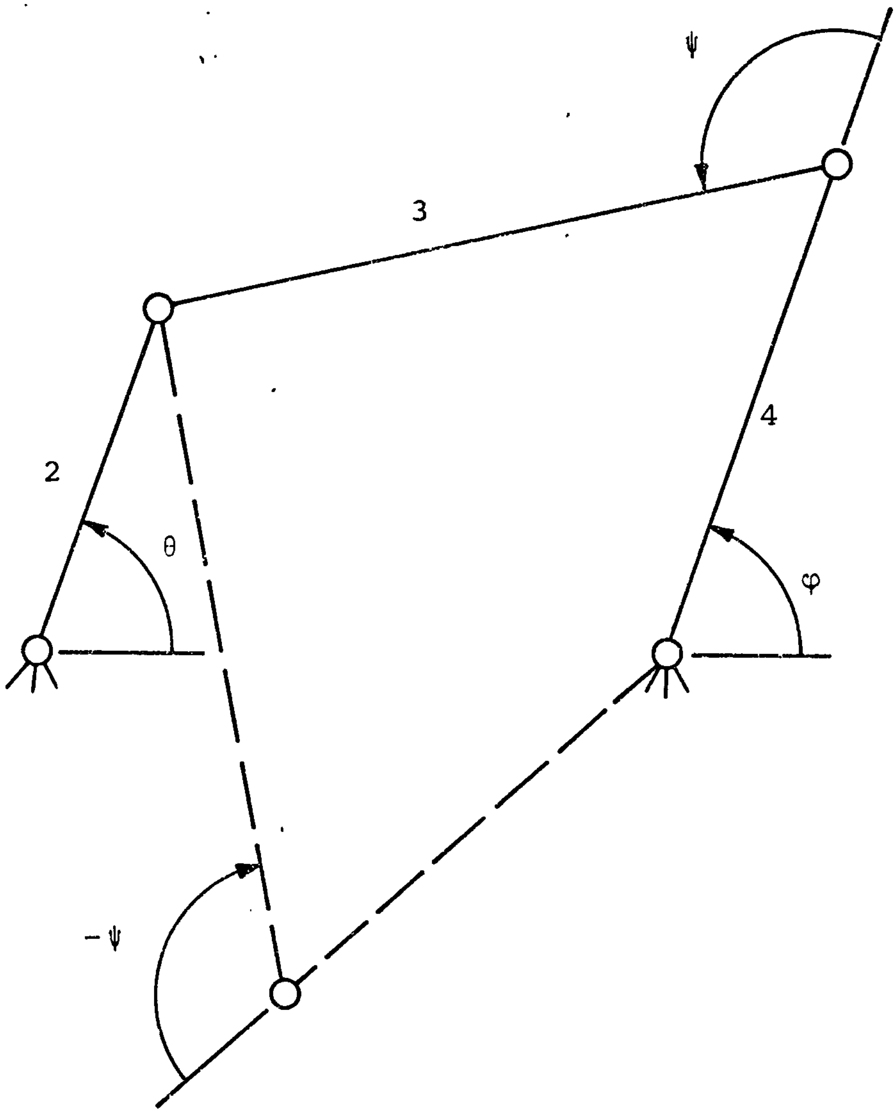

Definition of joint angles for four-bar linkage

Fig. 1-6

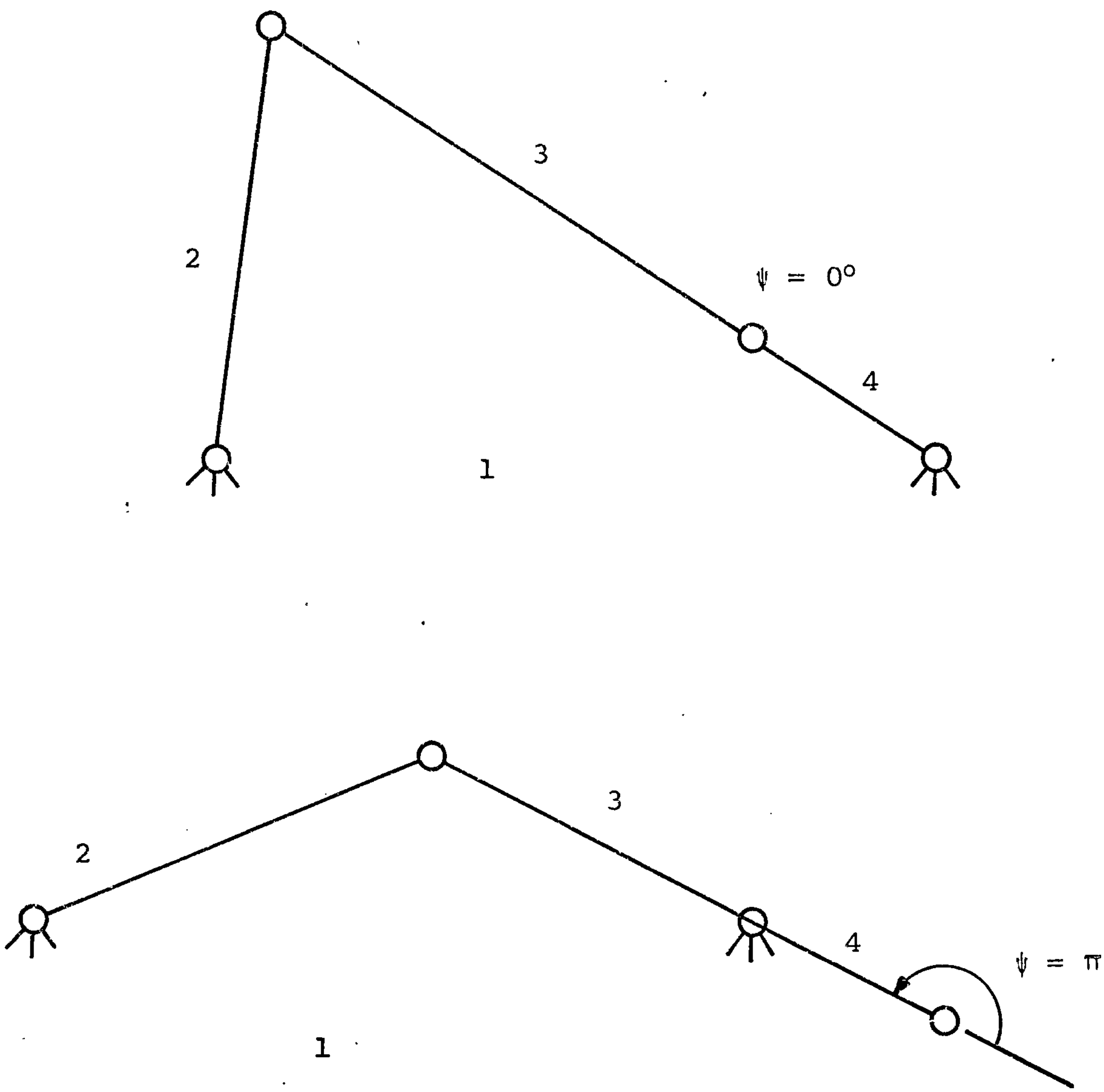

Transition configurations for four-bar linkage

Fig. 1-7

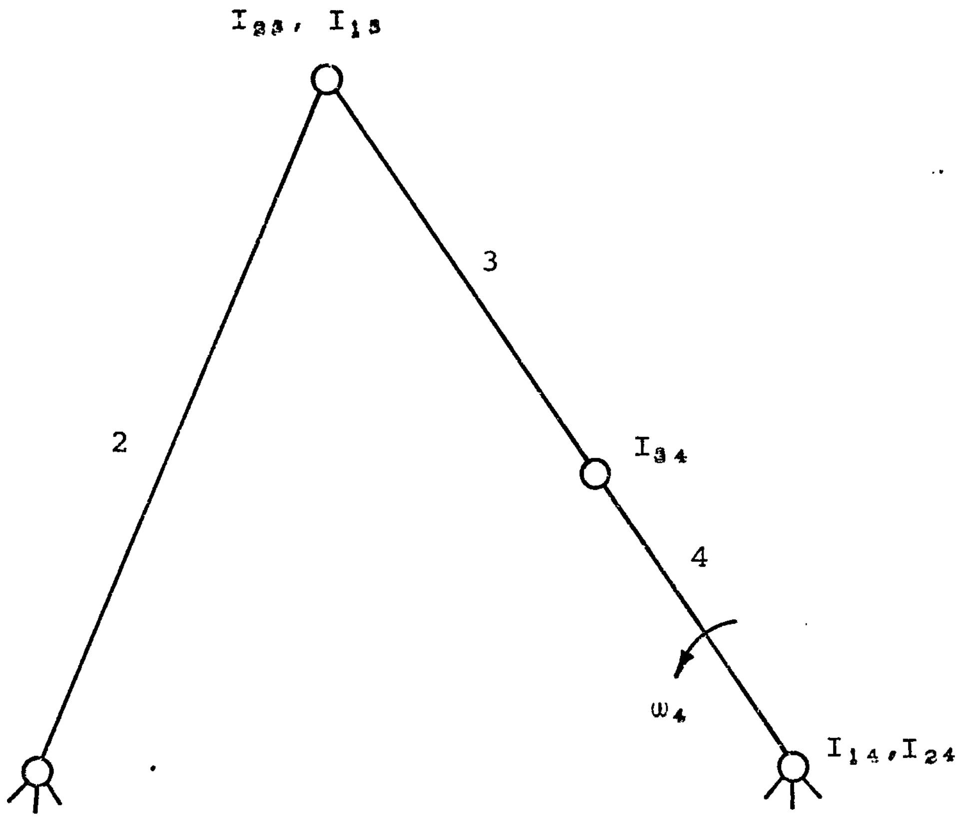

Location of instantaneous centers for four-bar linkage

Fig. 1-8

completely with respect to both links 1 and 3, then both ψ and φ are less than 180°, and one has the crank-rocker mechanism. Likewise if links 2 and 4 rotate completely relative to link 1, then the mechanism is a drag-link. Grashof's rules [1-17] provide a quick method for determining not only the type but also the class of the linkage. For a Class I linkage, the shortest link makes a complete rotation relative to each of the other three while they only oscillate relative to each other. And for the Class II linkage, no link makes a full rotation relative to any of the other links.

In theory, for four-bar mechanism synthesis there are an infinite number of choices for each of the two cranks. However, not all of the resulting mechanisms are practically usable. The crank-rocker and drag-link mechanism types are usually required because of the need for a continuously rotating input crank. Since other four-bar types occur as solutions in the Burmester synthesis, the location of the regions in which neither the crank-rocker nor the drag-link mechanisms exist would greatly reduce the trial and error needed to find practicable linkages. Previous work on this problem has been done by Beyer [1-3], Filemon [1-18] and Waldron [1-14, 1-19, 1-20].

In addition to the above problem, referred to as the "Grashof Problem", two other effects give rise to impractical solution linkages. These are referred to as the "order problem," and the "branch problem." The order problem arises when it is necessary that the mechanism go through the four design positions in some specified order. For four or more design positions, a continuously rotating crank will frequently drive the coupler through the design positions in the wrong order. Therefore it becomes important to identify regions of the solution space which give cranks which will drive the linkage through the design positions in the desired order. Previous work on this problem has been published by Modler [1-21], Waldron [1-14, 1-19] and Waldron and Strong [1-22 and Chapter 3].

In addition, the solution to the order problem has important implications for the Grashof problem. In a drag-link linkage both cranks not only have to rotate completely, but they must do so in the same direction and in the same order of rotation. Also, in a crank-rocker, the order of rotation of the crank relative to the coupler must be opposite the rotation of the crank relative to the base. Thus the solution of the order problem can be used to identify regions of the solution space in which these Grashof types cannot occur. Its use in this manner will be discussed in Chapter 5.

All linkages which satisfy the Grashof inequality display dual branched trajectories. It is possible for some design positions to be on one branch and the others on the second branch. Thus, this effect gives rise to true spurious solutions. This is the problem called the branch problem. Previous work on this problem has been done by Filemon [1-18], Waldron [1-14, 1-20] and Waldron and Strong [1-22 and Chapter 4].

The methods developed in Chapters 3 and 4 reveal a further improvement in the design of crank-rocker mechanisms by simply inverting the linkage onto the coupler and applying the techniques in a similar manner. The inverted branch solution requires the location of some more special points on the circle-point curve. These can be located very easily with the information already available from the previous work.

The circle-point equation is derived in Chapter 2 along with the necessary equations for locating all of the special points which are needed for the order and branch solutions. The generation of the circle-point curve is by means of an exact solution rather than by an approximate method such as the Newton-Raphson method. The Appendix contains a listing of the entire program along with some examples of the output data for both a single branch and double branch circle-point curve.

CHAPTER 2

NUMERICAL GENERATION OF CIRCLE POINT CURVE

2.1 Introduction

The circle-point curve is the locus of all points in a plane whose 4 positions lie on a circle. Thus, in theory, any point on this curve may be chosen as the moving pivot of a crank with the fixed pivot being the center of the circle on which the moving pivot lies in its four design positions. The following chapters, however, indicate that not all of these solutions are desirable ones for the designer to choose. Nevertheless, it is necessary to be able to obtain all points on the circle-point curve, which is in general, a cubic in both the abscissa and ordinate variables. This is the purpose of the numerical solution, along with the location of the special points - P'_{ij}, Q_{ij}, T_{ij}, U_{ij}, T^*_{ij} and U^*_{ij} - which lie on the circle-point curve. As indicated in the following chapters, these special points are all that are needed to restrict the circle-point curve to those segments which eliminate the branch problem and define the order of rotation.

Since the circle-point curve is asymptotic to a line which extends to infinity in both directions it may be difficult to compute the solutions because the orientation of the asymptote is unknown beforehand, making it difficult to know where to start the calculations. This problem can be resolved by merely rotating the axes so that the asymptote is parallel with the abscissa. Now a negative value of the abscissa may be chosen as the starting point and the corresponding value or values of the ordinate may be computed. Then the abscissa is incremented by a positive value and the calculations carried out again. This process may be repeated as many times as necessary to obtain a sufficient portion of the circle-point curve.

In general, the circle-point curve is either a single branch or double branch curve as shown in Figures 2.1-1 and 2.1-2, respectively. It may be seen from these figures that, if the starting abscissa is chosen to be a sufficiently large negative value there is only one real value for the ordinate. As the calculation progresses along the abscissa to more positive values, a region is encountered where all three values of the ordinate are real. Finally, for still more positive abscissae, the curve reverts back to having only one real ordinate value. Therefore the computer program must be able to detect the region in which the calculations are being made since only the real roots are desired. As will be seen later, this is a simple procedure requiring only a

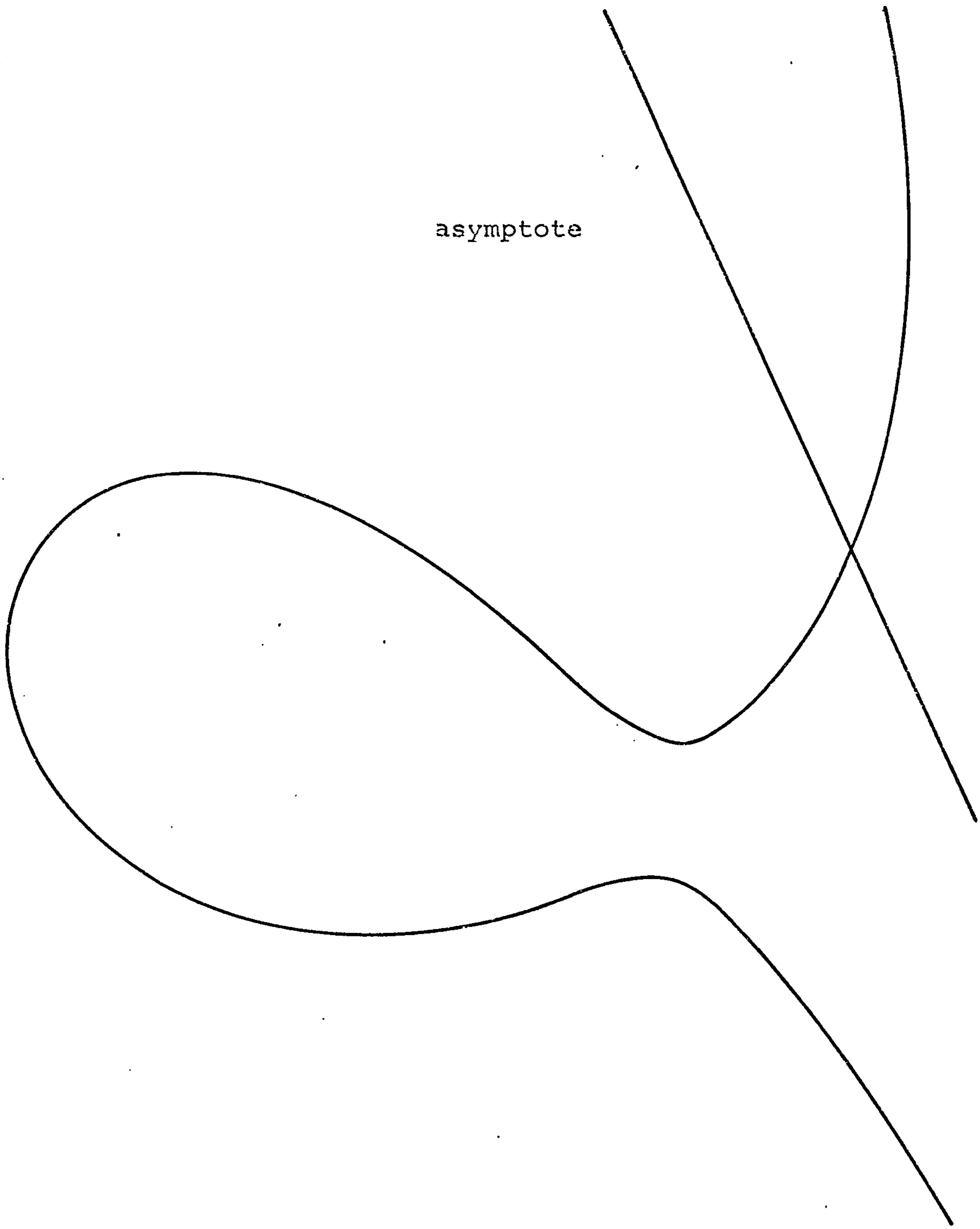

Example of single branch type of circle-point curve

Fig. 2.1-1

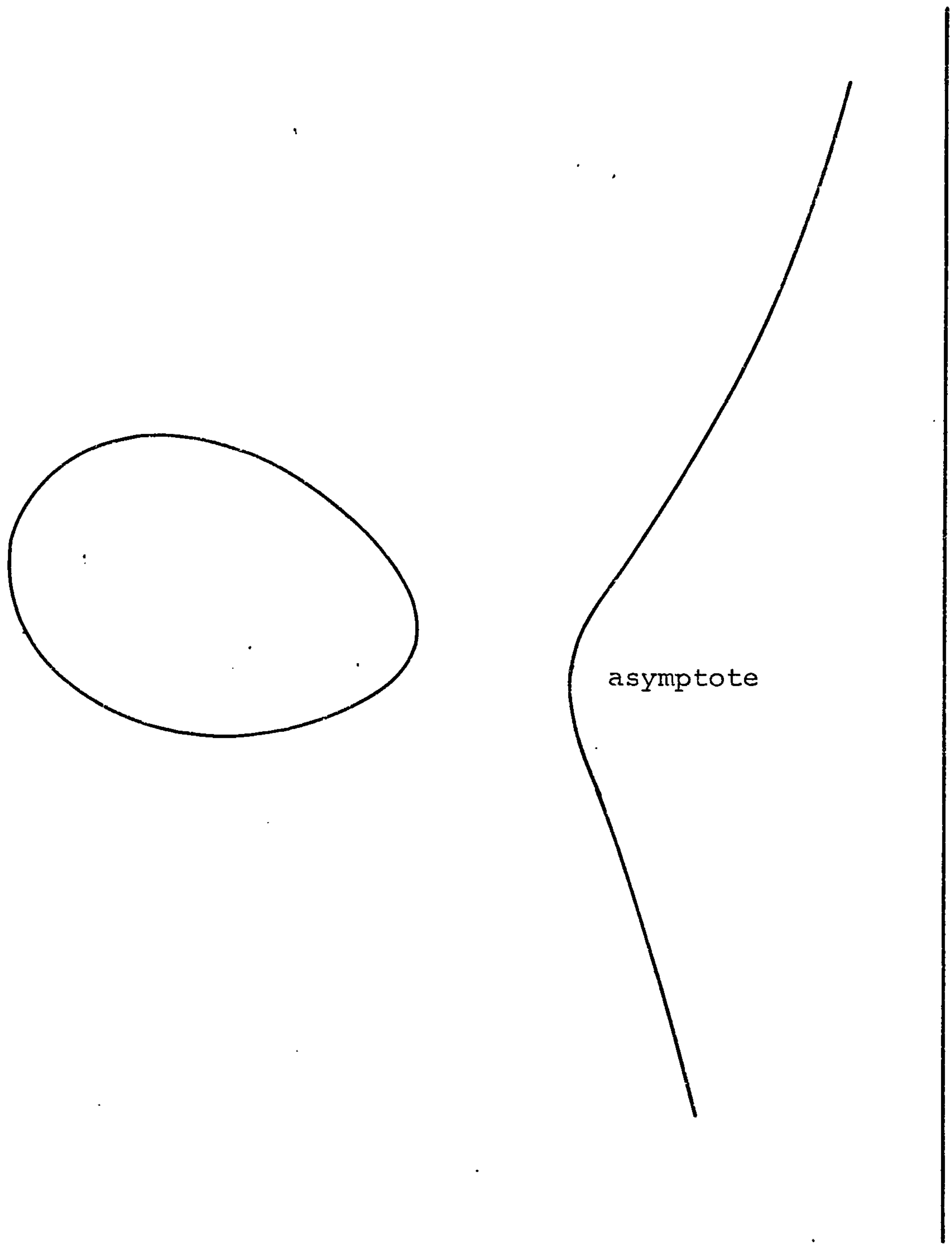

Example of double branch type of circle-point curve

Fig. 2.1-2

check to see if the discriminant is positive or negative. A positive value for the discriminant yields one real root while a negative or zero value yields three real roots with at least two being equal for the zero case.

In addition to the locus of solutions to the circle-point curve the special points which lie on the curve are also computed. The first of these are the image poles. Since the image poles are found from the poles, it is first necessary to determine the poles. Figure 2.1-3(a) shows the line AB, which represents a rigid body, in the i and j^{th} positions. In order to find the point in the fixed plane about which AB rotates in going from position i to position j, the perpendicular bisectors between points A_i and A_j and likewise B_i and B_j are constructed as shown in Figure 2.1-3(b) and labelled a and b, respectively. The intersection of lines a and b is the center of pure rotation of body AB between the i^{th} and j^{th} positions. This point is called the pole and is denoted as P_{ij}. Thus a pole is the point in the fixed and moving plane which is coincident in both of a pair of design positions. The image poles are the locations of the poles relative to a reference frame fixed on the moving body and plotted on the first design position. Since there are four design positions and the poles are defined by taking two at

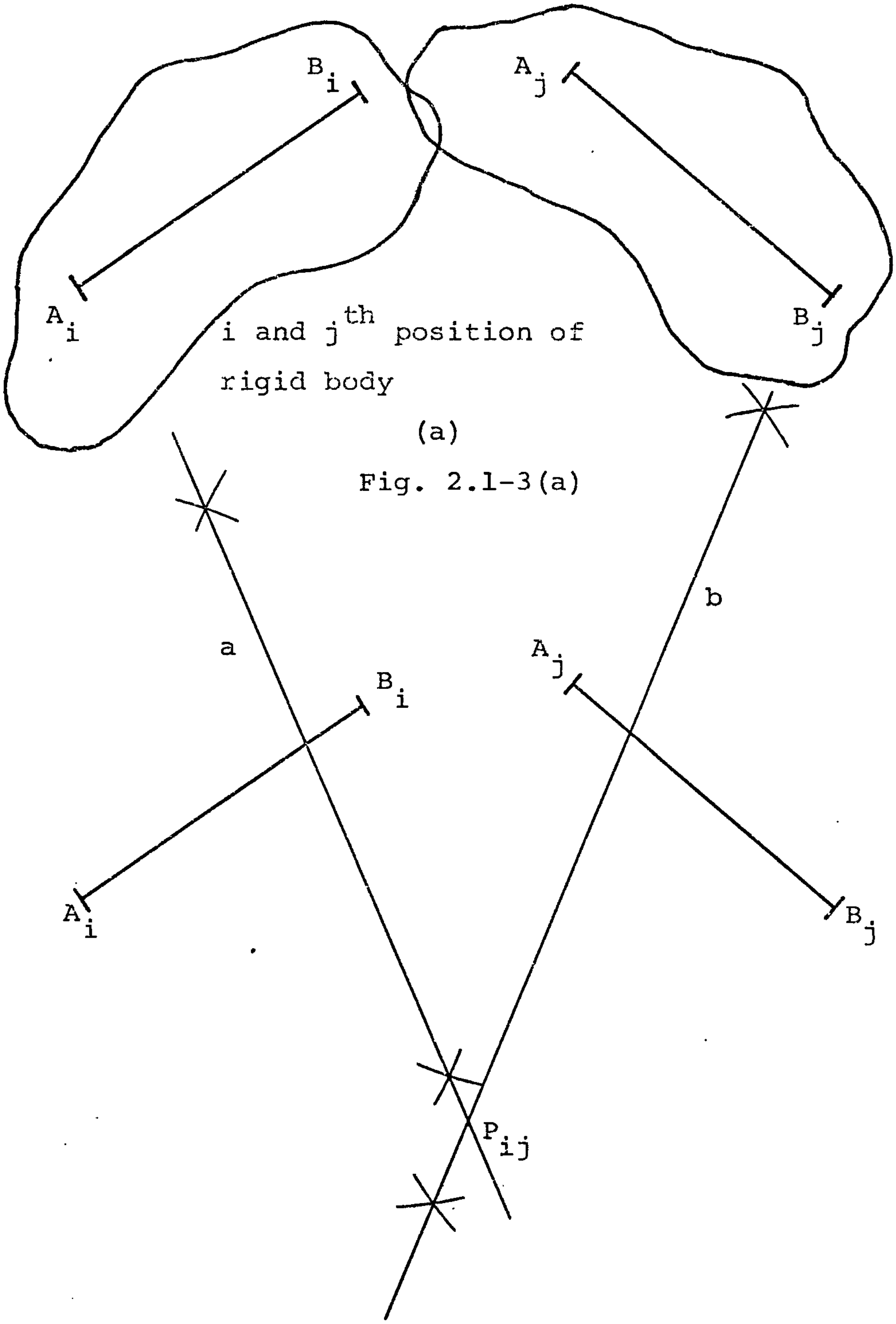

(a)

Fig. 2.1-3(a)

Construction for location of pole P_{ij}

Fig. 2.1-3(b)

a time, there are six poles and likewise six image poles. The notation for the image poles is P'_{ij}, thus the six image poles are P'_{12}, P'_{13}, P'_{14}, P'_{23}, P'_{24} and P'_{34}. Another way of looking at the image poles is that each is the point in the moving lamina which corresponds to a pole in the fixed lamina, thus the three image poles with one of the subscripts being 1 are in the same locations as the corresponding poles.

Two poles which have no common subscript are called opposite poles. The six poles when taken in pairs such that the subscripts are 1, 2, 3 and 4 in any order form three pairs of opposite poles ($P_{12}P_{34}$, $P_{13}P_{24}$ and $P_{14}P_{23}$). Figure 2.1-4 shows the opposite poles connected by solid lines. When two pairs of opposite poles are taken as the diagonals of a quadrilateral, it is called an opposite-pole quadrilateral or quadrangle. Figure 2.1-5 shows the three opposite-pole quadrilaterals formed by using the three opposite pole pairs of Figure 2.1-4. The sides of the opposite-pole quadrilateral are indicated by broken lines. The sides of the quadrilaterals are called adjacent poles. Notice that adjacent poles have one subscript which is common and that the adjacent poles for the opposite side have the same noncommon subscripts as the first. For example, from Figure 2.1-5(a) the side formed by adjacent poles P_{12} and P_{13}

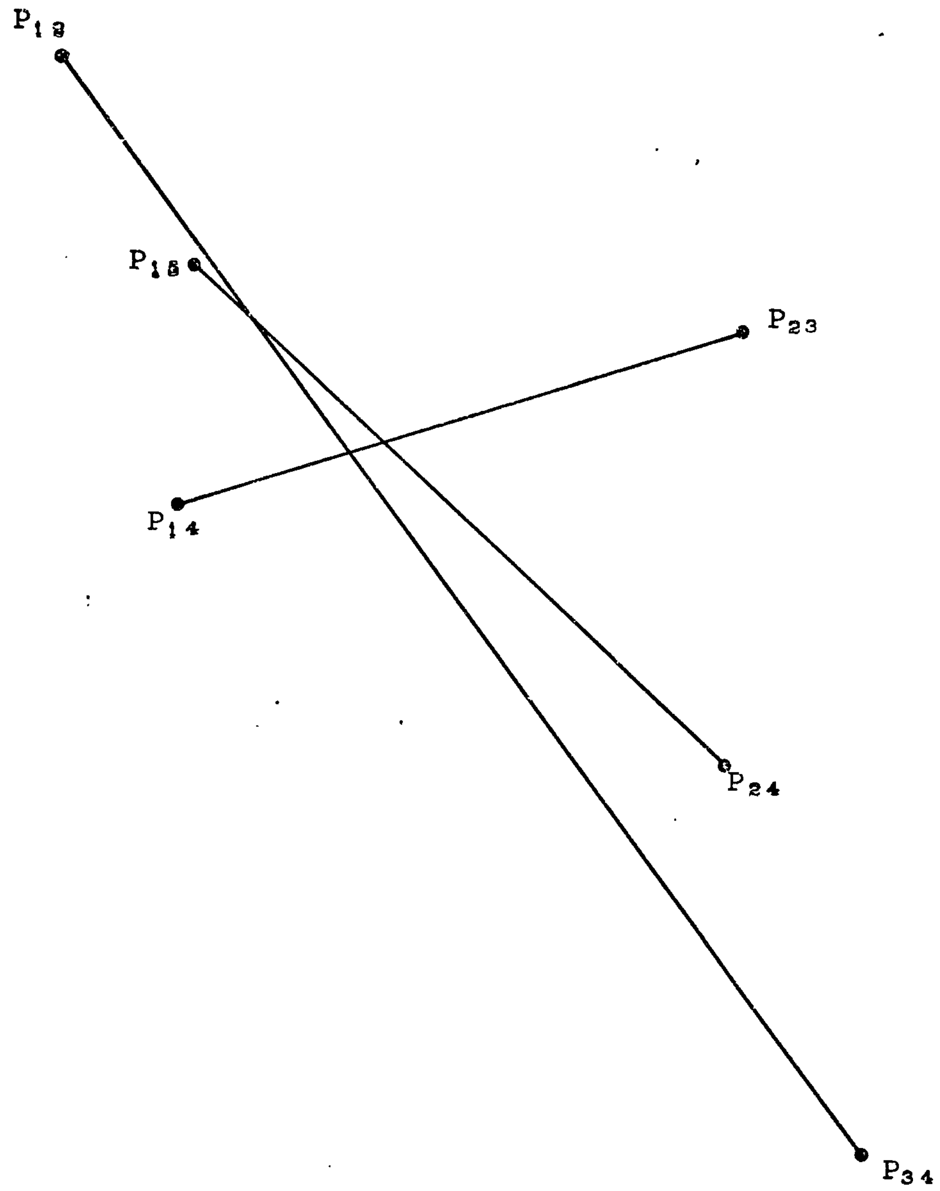

Three pairs of opposite poles

Fig. 2.1-4

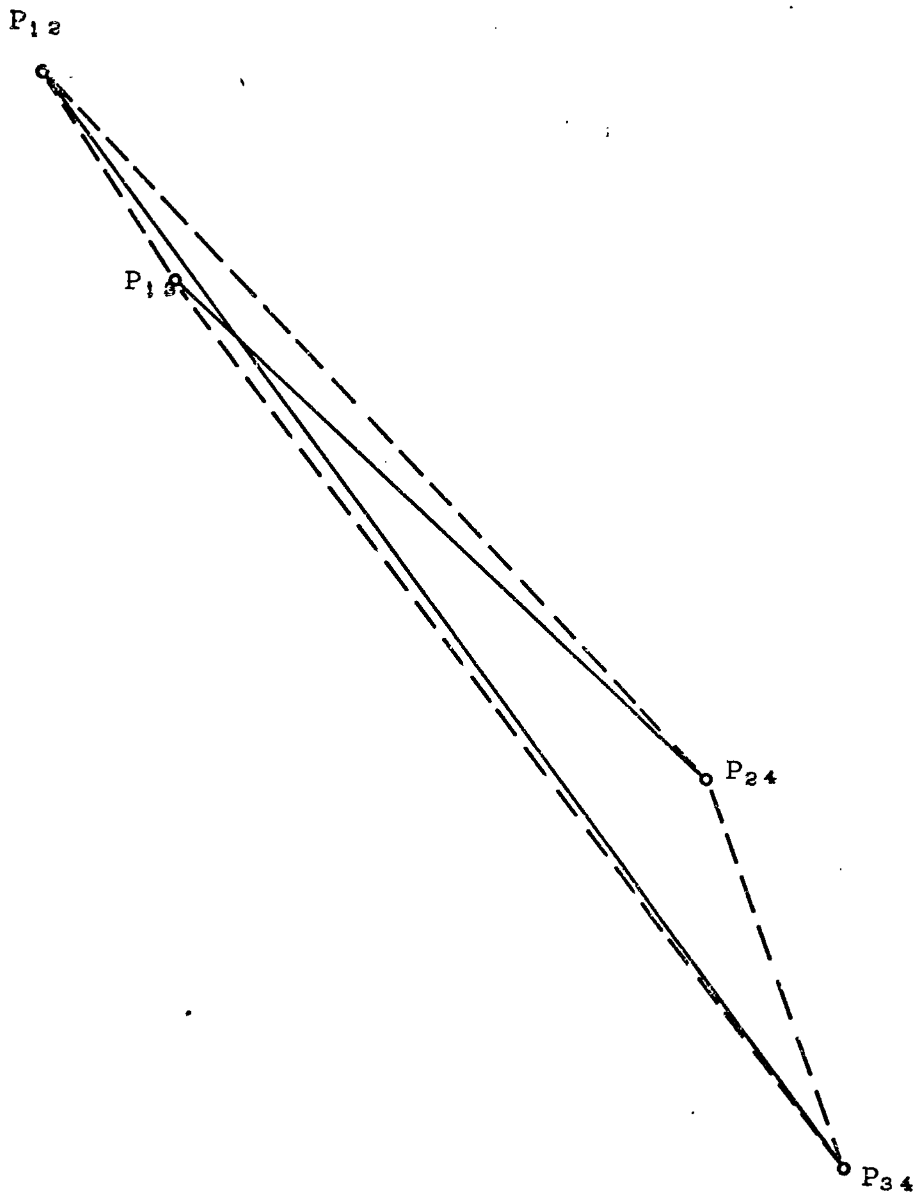

Opposite pole quadrilateral using

P_{12}, P_{13}, P_{24} and P_{34}

Fig. 2.1-5(a)

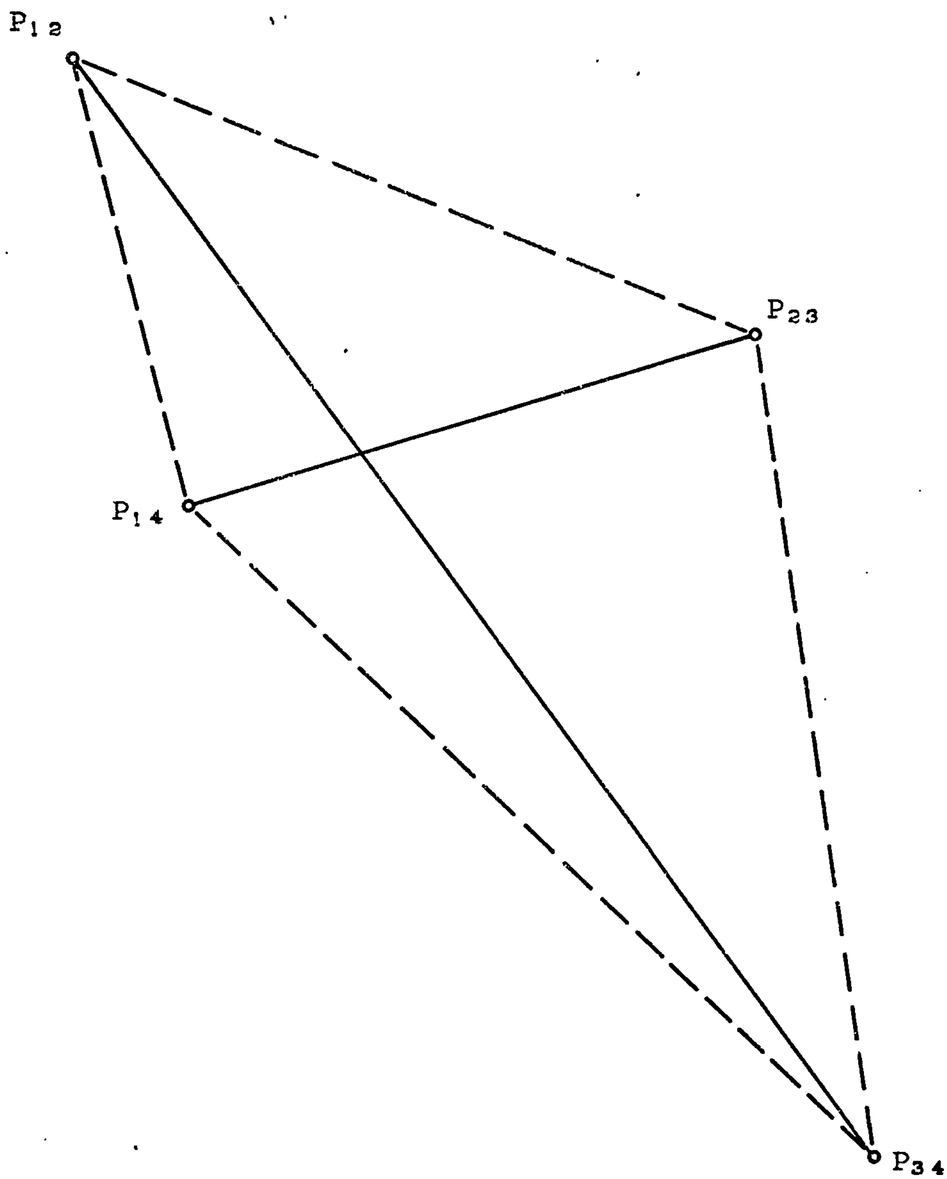

Opposite pole quadrilateral using P_{12}, P_{14}, P_{23} and P_{34}

Fig. 2.1-5(b)

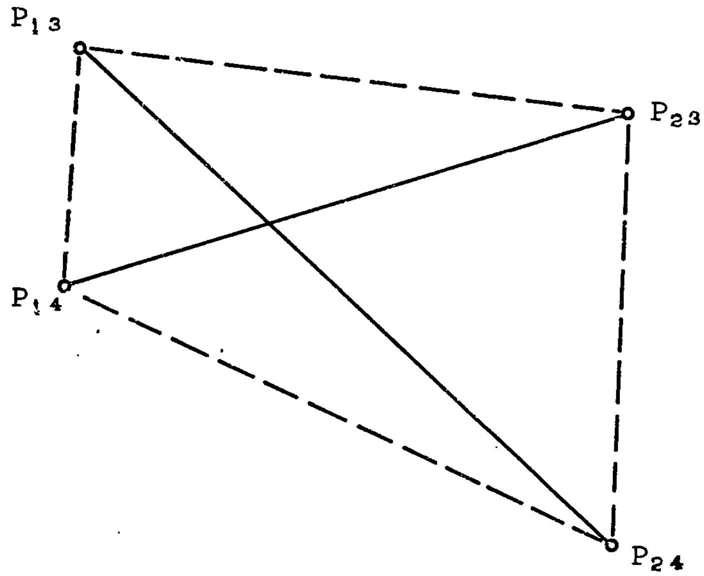

Opposite pole quadrilateral using P_{13}, P_{14}, P_{23} and P_{24}

Fig. 2.1-5(c)

have subscripts 23 as uncommon. Likewise the opposite side is adjacent poles P_{24} and P_{34} which again have 23 as uncommon subscripts. In the first case 1 was common and in the second case 4 was the common subscript. Since each quadrilateral yields two pairs of sides with the same uncommon subscript, there will be six pairs of sides for all three opposite-pole quadrilaterals with subscripts the same as for the poles. Because the image poles have the same subscripts as the poles, the same procedure may be performed using the image poles. If the opposite sides formed by the adjacent image poles are extended until they intersect, these intersections are called Q_{ij}. Thus the six Q_{ij} points so determined are Q_{12}, Q_{13}, Q_{14}, Q_{23}, Q_{24} and Q_{34}. These six points in addition to the six image poles all lie on the circle-point curve [2-1].

Now if circles are drawn with the adjacent image pole pairs at the ends of their diameters, then the intersection of those two circles with the same uncommon subscripts are T_{ij} and U_{ij}. However, not all of these pairs of circles will intersect. Thus there is a maximum of twelve T_{ij} and U_{ij} points with the same subscripts as the image poles. All of the T_{ij} and U_{ij} points which exist also lie on the circle point curve [2-2].

The image pole circle is a circle on which lie three image poles whose subscripts represent only three of the four design positions. Thus image pole circles may be formed by using subscripts 123 ($P'_{12}P'_{23}P'_{13}$), subscripts 124 ($P'_{12}P'_{24}P'_{14}$), subscripts 134 ($P'_{13}P'_{34}P'_{14}$) or subscripts 234 ($P'_{23}P'_{34}P'_{24}$). Figure 2.1-6 shows the four image pole circles obtained from the six image poles. Note that all four circles intersect at one point called the Ball point which is indicated by $\mathfrak{B}$ and also lies on the circle-point curve [2-1].

If the circle-point curve is drawn, then the only one of the image pole circles needs to be constructed to find the Ball point. It is located at the fourth intersection of the circle with the curve (the other three being the image poles). Likewise, only one of the two circles defining the T_{ij} and U_{ij} points needs to be constructed if the circle-point curve has been constructed. These points are located at the third and fourth intersections of the circle with the curve.

Figure 2.1-7 defines ψ, the angle which the coupler makes with the crank; also θ, the angle which the coupler makes with the base; and φ, the angle which the crank makes with the base. The value for ψ_{ij} is found from the equation $\psi_{ij} = \theta_{ij} - \varphi_{ij}$ when φ_{ij} is $\pm\ \pi$ such that $-\pi < \psi_{ij} < \pi$. This is presented in more detail in Chapter 5. Since θ_{ij} may be

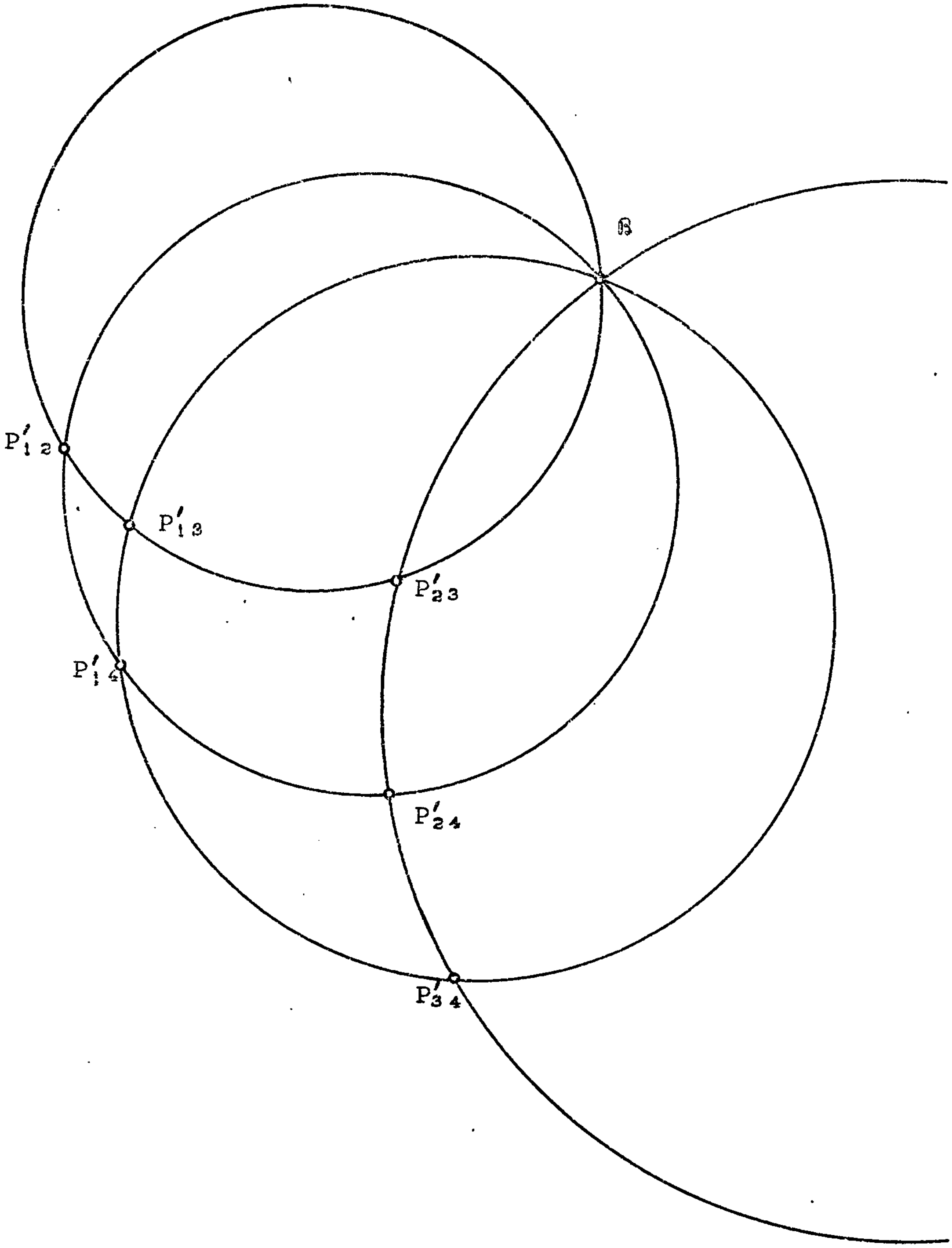

Image pole circles defining Ball point

Fig. 2.1-6

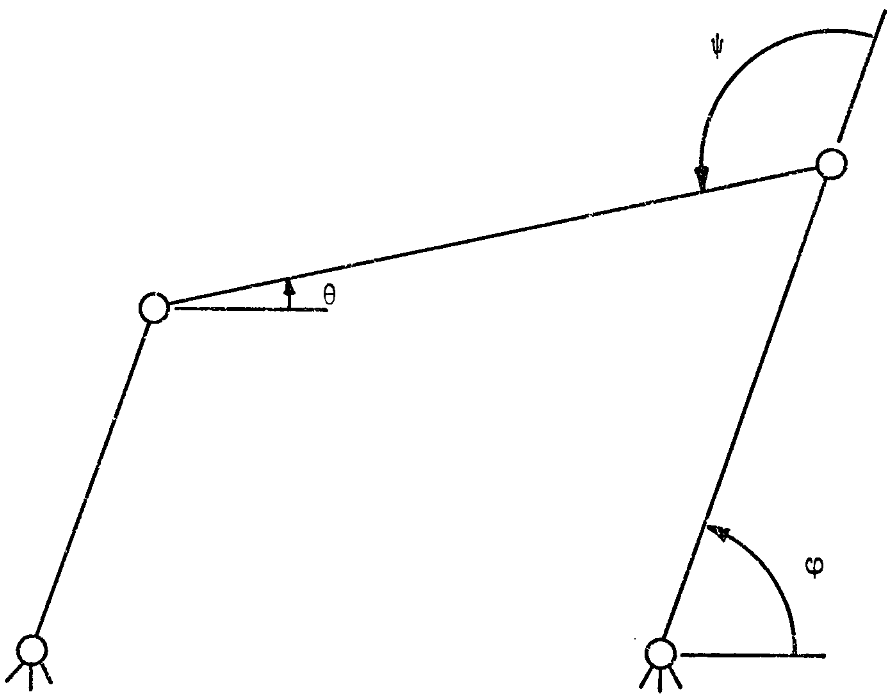

Definition of angles for a four-bar linkage

Fig. 2.1-7

found from the design positions, then the ψ_{ij}'s can be calculated. Using these angles and the adjacent poles the circles can be constructed locating T^*_{ij} and U^*_{ij}, if they exist. The special points T^*_{ij} and U^*_{ij} are the intersections of two circles on which adjacent pole pairs lie but are not the diameters as was the case for T_{ij} and U_{ij}, see Fig. 2.1-8. For the circle using P'_{12} and P'_{23}, the center is C^2_{13}, and likewise for the circle on P'_{14} and P'_{34} the center would be C^4_{13}. Now the angles formed by $P'_{12}C^2_{13}P'_{23}$ and $P'_{14}C^4_{13}P'_{34}$ are ψ_{13}, where ψ_{13} is the change in ψ from position 1 to position 3. Again, if the circle-point curve is defined only one of these circles need be constructed to locate T^*_{ij} and U^*_{ij} as the third and fourth intersections of the circle with the circle-point curve.

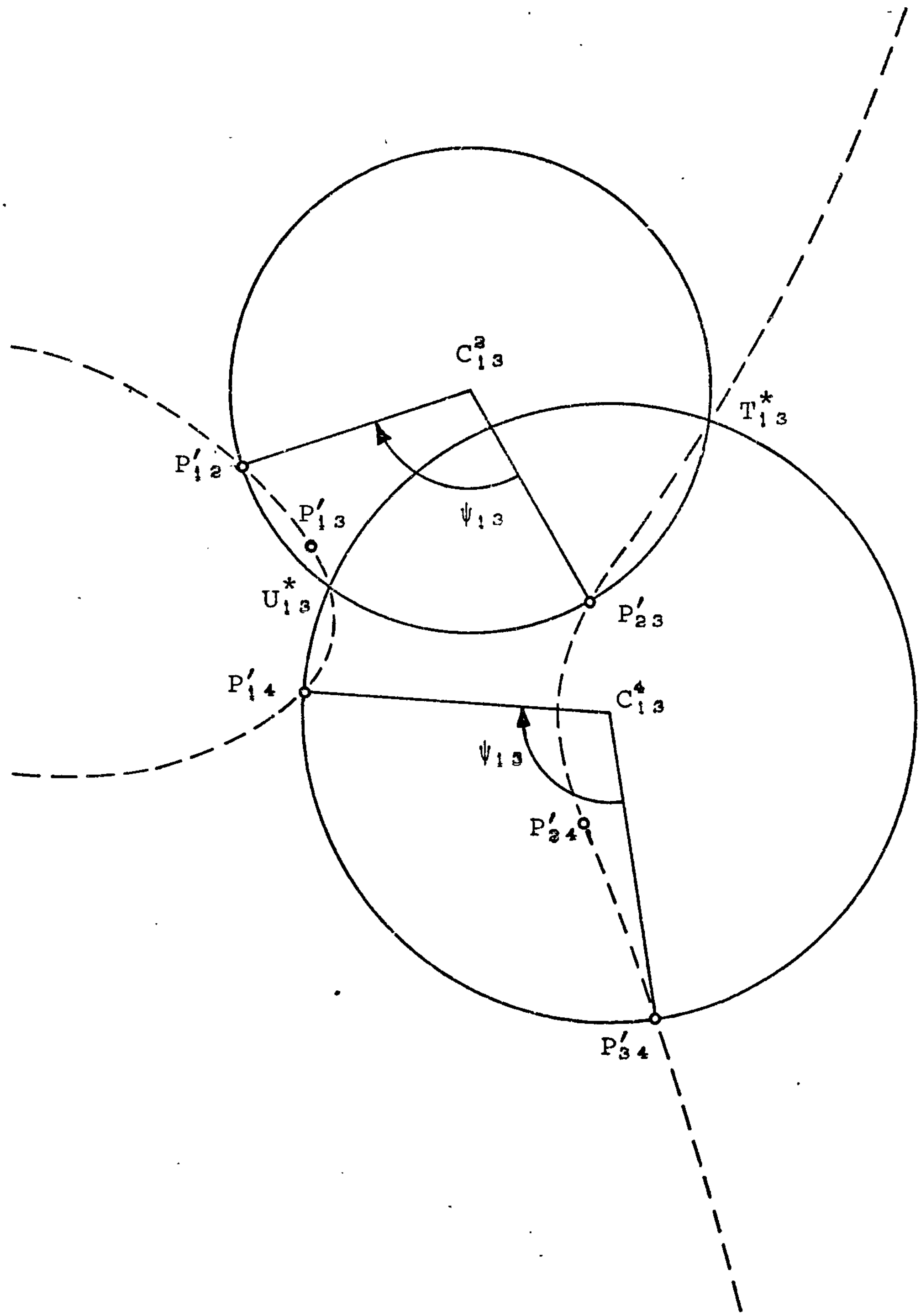

Location of T_{13}^{*} and U_{13}^{*} for $\psi_{ij} > 0^{\circ}$ ($\psi_{ij} = \theta_{ij} - \pi$ for $0 < \theta_{ij} < \pi$ and $\psi_{ij} = \theta_{ij} + \pi$ for $-\pi < \theta_{ij} \leq 0$)

Fig. 2.1-8

2.2 Derivation of Circle-Point Equation

The rigid body is represented by the line AB in the fixed XYZ reference frame, Figure 2.2-1. The xyz coordinate system is fixed to AB such that the origin is point A and the x-axis lies along AB. The coordinates of a point P in the rigid body are

$$\begin{aligned} X &= p + x\cos\theta - y\sin\theta \\ Y &= q + x\sin\theta + y\cos\theta \end{aligned} \tag{2.2-1}$$

where p and q are the coordinates of the point A in the XYZ coordinate system.

If the coordinates of the circle-point are (x,y) and the coordinates of the center-point are (x*,y*), then the equation for a circle is

$$(x - x^*)^2 + (y - y^*)^2 = R^2 \tag{2.2-2}$$

where R is the radius of the circle. Now if we let the fixed and moving coordinate systems coincide in the first design position then $p_1 = q_1 = \theta_1 = 0$. Thus equation (2.2-1) becomes for i = 2,3,4

$$\begin{aligned} X_i &= p_i + x\cos\theta_i + y\sin\theta_i \\ Y_i &= q_i + x\sin\theta_i + y\cos\theta_i \end{aligned} \tag{2.2-3}$$

Substitution of equation (2.2-3) into equation (2.2-2) yields

$$\begin{aligned} &(p_i + x\cos\theta_i + y\sin\theta_i - x^*)^2 + \\ &(q_i + x\sin\theta_i + y\cos\theta_i - y^*)^2 = R^2 \end{aligned} \tag{2.2-4}$$

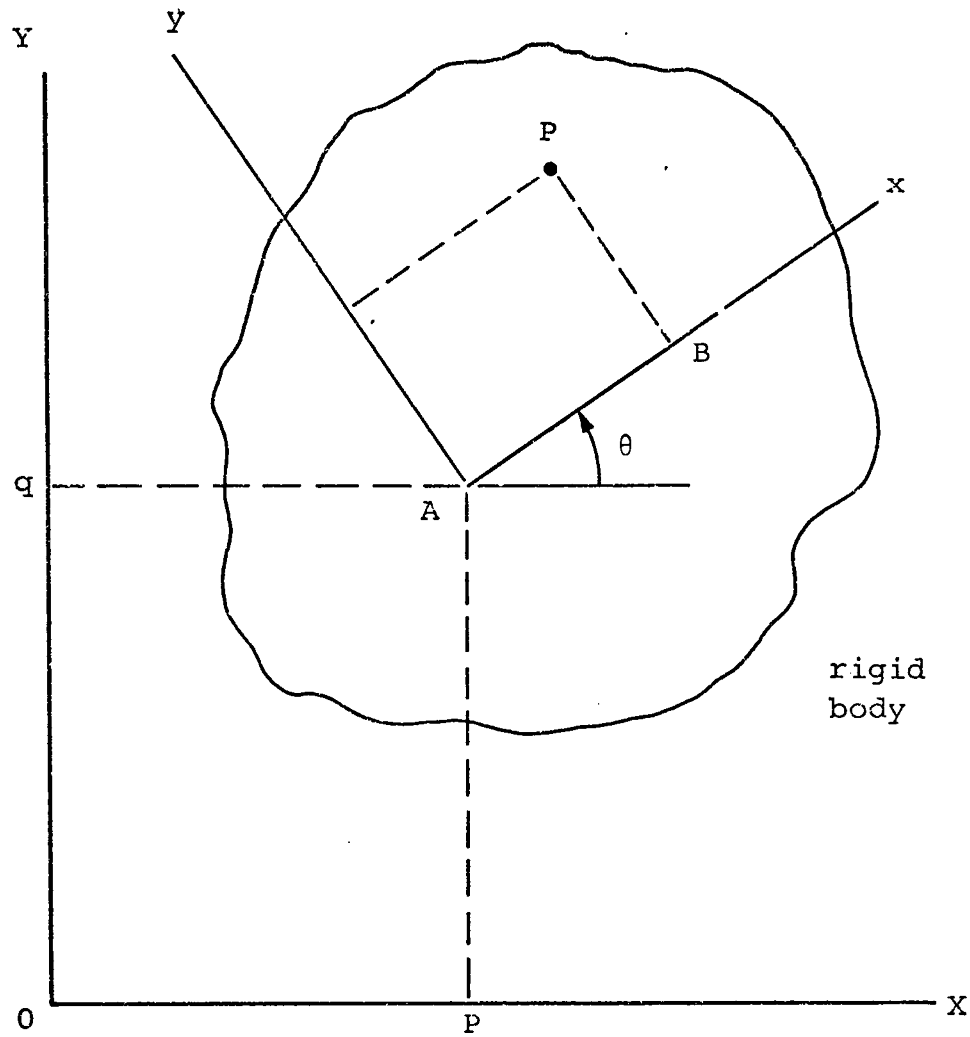

Fixed and moving reference frames

Fig. 2.2-1

Since $p_1 = q_1 = \theta_1 = 0$, then equation (2.2-4) yields for the first design position

$$(x - x^*)^2 + (y - y^*)^2 = R^2 \tag{2.2-5}$$

Equating the left hand sides of equations (2.2-4) and (2.2-5) and rearranging yields

$$\begin{aligned}[][x(1 - \cos\theta_i) + y \sin\theta_i - p_i]x^* + [y(1 - \cos\theta_i) - x \sin\theta_i - q_i]y^* \\ + x(p_i \cos\theta_i + q_i \sin\theta_i) + y(q_i \cos\theta_i - p_i \sin\theta_i) + \\ \tfrac{1}{2}(p_i^2 + q_i^2) = 0\end{aligned} \tag{2.2-6}$$

Let

$$\begin{aligned} a_i &= 1 - \cos\theta_i \\ b_i &= \sin\theta_i \\ c_i &= p_i \cos\theta_i + q_i \sin\theta_i \\ d_i &= q_i \cos\theta_i - p_i \sin\theta_i \\ e_i &= \tfrac{1}{2}(p_i^2 + q_i^2) \end{aligned} \tag{2.2-7}$$

Substitution of equation (2.2-7) into equation (2.2-6) yields

$$\begin{aligned}(xa_i + yb_i - p_i)x^* + (ya_i - xb_i - q_i)y^* \\ + xc_i + yd_i + e_i = 0\end{aligned} \tag{2.2-8}$$

Adopting the following notation

$$|u_i \ v_i \ w_i| = \begin{vmatrix} u_2 & v_2 & w_2 \\ u_3 & v_3 & w_3 \\ u_4 & v_4 & w_4 \end{vmatrix}$$

the nontrivial solution of equation (2.2-8) requires

$$|(a_i x + b_i y - p_i)(-b_i x + a_i y - q_i)(c_i x + d_i y + e_i)| = 0 \tag{2.2-9}$$

which upon expansion and rearrangement yields the circle-point equation

$$(Ax + By)(x^2 + y^2) + Cxy + Dx^2 + Ey^2 + \\ Fx + Gy + H = 0 \tag{2.2-10}$$

where the coefficients of equation (2.2-10) are defined as

$$A = -|a_i\ b_i\ c_i|$$

$$B = |b_i\ a_i\ d_i|$$

$$C = -|a_i\ q_i\ d_i| - |b_i\ q_i\ c_i| + |p_i\ b_i\ d_i| - |p_i\ a_i\ c_i|$$

$$D = -|a_i\ b_i\ E_i| - |a_i\ q_i\ c_i| + |p_i\ b_i\ c_i|$$

$$E = |b_i\ a_i\ e_i| - |b_i\ q_i\ d_i| - |p_i\ a_i\ d_i|$$

$$F = -|a_i\ q_i\ e_i| + |p_i\ b_i\ e_i| + |p_i\ q_i\ c_i|$$

$$G = -|b_i\ q_i\ e_i| - |p_i\ a_i\ e_i| + |p_i\ q_i\ d_i|$$

$$H = |p_i\ q_i\ e_i|$$

As discussed earlier the axes will now be rotated through an angle α to make the computation of the solutions to equation (2.2-10) better suited for the computer. Thus

$$x = u\cos\alpha - v\sin\alpha \\ y = u\sin\alpha + v\cos\alpha \tag{2.2-11}$$

Returning to equation (2.2-10) and dividing by x^2 yields

$$(Ax + By)\left(1 + \frac{y^2}{x^2}\right) + C\left(\frac{y}{x}\right) + D + E\left(\frac{y}{x}\right)^2 + \\ F\left(\frac{1}{x}\right) + G\left(\frac{y}{x^2}\right) + H\left(\frac{1}{x^2}\right) = 0 \tag{2.2-12}$$

Now let x become large, then equation (2.2-12) reduces to

$$(Ax + By) + D = 0 \tag{2.2-13}$$

If the angle of rotation were such that the term in parenthesis in equation (2.2-13) was dependent on y only, then equation (2.2-13) would be a function of y alone and would yield the value of the intercept of the asymptote with the y-axis. Substitution of equation (2.2-11) into Ax + By yields

$$Ax + By = (A\cos\alpha + B\sin\alpha)u - (A\sin\alpha - B\cos\alpha)v \qquad (2.2\text{-}14)$$

Therefore for equation (2.2-14) to be a function of v only, we see that the coefficient of u must vanish or

$$A\cos\alpha + B\sin\alpha = 0$$

so,

$$\tan\alpha = -\frac{A}{B} \qquad (2.2\text{-}15)$$

From equation (2.2-15) in conjunction with the identity $\sin^2\alpha + \cos^2\alpha = 1$ we get

$$\sin\alpha = \frac{A}{\sqrt{A^2 + B^2}} \quad \text{and} \quad \cos\alpha = -\frac{B}{\sqrt{A^2 + B^2}} \qquad (2.2\text{-}16)$$

Substitution of equations (2.2-11) and (2.2-16) into equation (2.2-10) and rearranging yields

$$\begin{aligned} B'(u^2 + v^2)v + C'uv + D'u^2 + E'v^2 + \\ F'u + G'v + H' = 0 \end{aligned} \qquad (2.2\text{-}17)$$

where

$$B' = \sqrt{A^2 + B^2}$$

$$C' = \frac{C(B^2 - A^2) + 2ABD - 2ABE}{(B')^2}$$

$$D' = \frac{EA^2 + DB^2 - ABC}{(B')^2}$$

$$E' = \frac{DA^2 + EB^2 + ABC}{(B')^2}$$

$$F' = \frac{BF - AG}{B'}$$

$$G' = \frac{AF + BG}{B'}$$

$$H' = H$$

Now if equation (2.2-17) is divided by u^2 and then u is very large the result is the v intercept of the asymptote which is

$$(v)_{asymptote} = -\frac{D'}{B'} \tag{2.2-18}$$

Since the computer starts with a given value for u and continues to vary it by some preset increment, equation (2.2-17) becomes a cubic equation in v. Rearranging equation (2.2-17) into the standard form for a cubic results in

$$v^3 + a_1 v^2 + a_2 v + a_3 = 0 \tag{2.2-19}$$

where

$$a_1 = \frac{E'}{B'}$$

$$a_2 = \frac{B'u^2 + C'u + G'}{B'}$$

$$a_3 = \frac{D'u^2 + F'u + H'}{B'}$$

Let

$$Q = \frac{3a_2 - a_1{}^2}{9} \tag{2.2-20a}$$

$$R = \frac{9a_1 a_2 - 27a_3 - 2a_1{}^3}{54} \tag{2.2-20b}$$

$$S = \sqrt[3]{R + \sqrt{D}} \tag{2.2-20c}$$

$$T = \sqrt[3]{R - \sqrt{D}} \tag{2.2-20d}$$

$$D = Q^3 + R^2 \tag{2.2-20e}$$

The three conditions which determine the reality of the solutions are: D less than zero; equal to zero; or greater than zero.

i) $D > 0$, one real root exists

$$v_1 = S + T - \frac{a_1}{3} \tag{2.2-21}$$

ii) $D = 0$, all three roots are real with at least two equal

$$\varphi = \cos^{-1} \frac{|R|}{\sqrt{-Q^3}} \tag{2.2-22}$$

$$v_1 = 2\sqrt{|Q|}\ \cos\left(\frac{\varphi}{3}\right) - \frac{a_1}{3} \tag{2.2-23a}$$

$$v_2 = 2\sqrt{|Q|}\ \cos\left(\frac{\varphi + 2\pi}{3}\right) - \frac{a_1}{3} \tag{2.2-23b}$$

$$v_3 = 2\sqrt{|Q|}\ \cos\left(\frac{\varphi + 4\pi}{3}\right) - \frac{a_1}{3} \tag{2.2-23c}$$

iii) $D < 0$, all three roots are real and unequal

$$\varphi = \cos^{-1} \frac{|R|}{\sqrt{-Q^3}} \tag{2.2-24}$$

$$v_1 = 2\sqrt{|Q|}\ \cos\left(\frac{\varphi}{3}\right) - \frac{a_1}{3} \tag{2.2-25a}$$

$$v_2 = 2\sqrt{|Q|}\ \cos\left(\frac{\varphi + 2\pi}{3}\right) - \frac{a_1}{3} \tag{2.2-25b}$$

$$v_3 = 2\sqrt{|Q|}\ \cos\left(\frac{\varphi + 4\pi}{3}\right) - \frac{a_1}{3} \tag{2.2-25c}$$

In order to determine whether the circle-point curve is a single branch or double branch curve, it is only necessary to investigate the region in which there are three real solutions or, in other words, cases ii) and iii). Equation (2.2-17) when rearranged so that u is the variable rather than v yields a quadratic equation in u.

$$\begin{aligned}(B'v + D')u^2 + (C'v + F')u + \\ (B'v^3 + E'v^2 + G'v + H') = 0\end{aligned} \qquad (2.2\text{-}26)$$

Since all values of u must be real, the discriminant of this quadratic equation must be equal to or greater than zero which requires

$$D = (C'v + F')^2 - 4(Bv' + D')(B'v^3 + E'v^2 + G'v + H') \geq 0 \qquad (2.2\text{-}27)$$

Expansion of equation (2.2-27) and arrangement of the resulting quartic in standard form yields

$$a_1 v^4 + 4a_2 v^3 + 6a_3 v^2 + 4a_4 v + a_5 \geq 0 \qquad (2.2\text{-}28)$$

where

$$a_1 = 4(B')^2$$

$$a_2 = B'(D' + E')$$

$$a_3 = \frac{-(C')^2 + 4B'G' + 4D'E'}{6}$$

$$a_4 = -\frac{C'F'}{2} + 4B'H' + D'G'$$

$$a_5 = -(F')^2 + 4D'H'$$

Equation (2.2-28) will have either two real roots or four real roots. The number of real roots gives the number of real lines parallel to the asymptote and tangent to the circle-point curve. It follows, then, that the single branch curve will give two real roots while the double branch curve will give four real roots. The discriminant for the quartic is

$$D = (a_1 a_5 - 4a_2 a_4 + 3a_3^2)^3 - 27(a_1 a_3 a_5 + 2a_2 a_3 a_4 - a_1 a_4^2 - a_5 a_2^2 - a_3^3)^2 \tag{2.2-29}$$

Therefore the two cases of interest are

i) $D < 0$, 2 real roots, thus a single branch circle-point curve

ii) $D > 0$, 4 real roots, and thus a double branch circle-point curve.

2.3 Derivation of Image Pole Equations

Rewriting equation (2.2-1) in matrix form we have for the i^{th} position

$$\begin{Bmatrix} X_i \\ Y_i \end{Bmatrix} = \begin{bmatrix} \cos\theta_{1i} & -\sin\theta_{1i} \\ \sin\theta_{1i} & \cos\theta_{1i} \end{bmatrix} \begin{Bmatrix} x \\ y \end{Bmatrix} + \begin{Bmatrix} p_{1i} \\ q_{1i} \end{Bmatrix} \tag{2.3-1}$$

and likewise for the j^{th} position

$$\begin{Bmatrix} X_j \\ Y_j \end{Bmatrix} = \begin{bmatrix} \cos\theta_{1j} & -\sin\theta_{1j} \\ \sin\theta_{1j} & \cos\theta_{1j} \end{bmatrix} \begin{Bmatrix} x \\ y \end{Bmatrix} + \begin{Bmatrix} p_{1j} \\ q_{1j} \end{Bmatrix} \tag{2.3-2}$$

Since the image pole is the position in the moving lamina where $X_i = X_j$ and $Y_i = Y_j$ then the xy coordinates of the ij^{th} image pole are computed by equating equations (2.3-1) and (2.3-2) and letting $x = x'_{ij}$ and $y = y'_{ij}$ thus

$$\begin{bmatrix} \cos\theta_{1i} & -\sin\theta_{1i} \\ \sin\theta_{1i} & \cos\theta_{1i} \end{bmatrix} \begin{Bmatrix} x'_{ij} \\ y'_{ij} \end{Bmatrix} + \begin{Bmatrix} p_{1i} \\ q_{1i} \end{Bmatrix} = \begin{bmatrix} \cos\theta_{1j} & -\sin\theta_{1j} \\ \sin\theta_{1j} & \cos\theta_{1j} \end{bmatrix} \begin{Bmatrix} x'_{ij} \\ y'_{ij} \end{Bmatrix} + \begin{Bmatrix} p_{1j} \\ q_{1j} \end{Bmatrix} \tag{2.3-3}$$

Rearranging equation (2.3-3) we have

$$\begin{bmatrix} (\cos\theta_{1i} - \cos\theta_{1j}) & -(\sin\theta_{1i} - \sin\theta_{1j}) \\ (\sin\theta_{1i} - \sin\theta_{1j}) & (\cos\theta_{1i} - \cos\theta_{1j}) \end{bmatrix} \begin{Bmatrix} x'_{ij} \\ y'_{ij} \end{Bmatrix} = \begin{Bmatrix} p_{1j} - p_{1i} \\ q_{1j} - q_{1i} \end{Bmatrix} = \begin{Bmatrix} p_{ij} \\ q_{ij} \end{Bmatrix} \tag{2.3-4}$$

Now solving for the xy coordinates of the image poles we obtain

$$\begin{Bmatrix} x'_{ij} \\ y'_{ij} \end{Bmatrix} = \frac{1}{2(1-\cos\theta_{ij})} \begin{bmatrix} (\cos\theta_{1i}-\cos\theta_{1j}) & (\sin\theta_{1i}-\sin\theta_{1j}) \\ -(\sin\theta_{1i}-\sin\theta_{1j}) & (\cos\theta_{1i}-\cos\theta_{1j}) \end{bmatrix} \begin{Bmatrix} p_{ij} \\ q_{ij} \end{Bmatrix} \tag{2.3-5}$$

2.4 Derivation of Equations Defining Ball Point

As indicated in Section 2.1 the Ball point, $\mathcal{B}$, is one of the special points which lies on the circle-point curve. It is the fourth intersection of tne image pole circle with the circle-point curve. The image pole circle is the circle on which three image poles with subscripts P'_{ij}, P'_{jk} and P'_{ik} all lie. These three points also lie on the cruve. Another way of finding the Ball point is to construct two image pole circles. One of the two intersections of these two circles will be the common image pole and the other intersection will be the Ball point. For example using image poles P'_{12}, P'_{23} and P'_{13} for one circle and P'_{12}, P'_{24} and P'_{14} for the other circle, it is obvious that one intersection will be P'_{12}. This latter approach is the one which the numerical solution will use to locate the Ball point.

The circle through the image poles P'_{ij}, P'_{jk} and P'_{ik} is found by determining the intersection of pairs of the image poles. For image poles P'_{ij} and P'_{jk} the perpendicular bisector goes through the midpoint of a line connecting the two image poles and has a slope which is the negative inverse of the slope for the line through P'_{ij}

and P'_{jk} since it must be perpendicular to that line. Thus the perpendicular bisector must go through

$$\bar{x}_{jk} = \frac{x_{ij} + x_{jk}}{2} \tag{2.4-1}$$

$$\bar{y}_{jk} = \frac{y_{ij} + y_{jk}}{2}$$

with a slope of

$$\bar{m}_{jk} = -\frac{x_{jk} - x_{ij}}{y_{jk} - y_{ij}} \tag{2.4-2}$$

Likewise, for the image poles P'_{ij} and P'_{ik} we get for the midpoint and slope

$$\bar{x}_{ik} = \frac{x_{ij} + x_{ik}}{2}$$

$$\bar{y}_{ik} = \frac{y_{ij} + y_{ik}}{2} \tag{2.4-3}$$

$$\bar{m}_{ik} = -\frac{x_{ik} - x_{ij}}{y_{ik} - y_{ij}} \tag{2.4-4}$$

The intercepts for the above two cases are

$$\bar{b}_{jk} = \bar{y}_{jk} - \bar{m}_{jk}\bar{x}_{jk} \tag{2.4-5}$$

and

$$\bar{b}_{ik} = \bar{y}_{ik} - \bar{m}_{ik}\bar{x}_{ik} \tag{2.4-6}$$

Therefore the equations for the two perpendicular bisectors become

$$\bar{y}_K = \bar{m}_{jk}\bar{x}_K + \bar{b}_{jk} \tag{2.4-7}$$

and

$$\bar{y}_K = \bar{m}_{ik}\bar{x}_K + \bar{b}_{ik} \tag{2.4-8}$$

The simultaneous solution to equations (2.4-7) and (2.4-8) is the location of the center of a circle on which the image poles P'_{ij}, P'_{jk}, P'_{ik} all lie. Thus,

$$\bar{x}_K = \frac{\bar{b}_{jk} - \bar{b}_{ik}}{\bar{m}_{ik} - \bar{m}_{jk}} \tag{2.4-9}$$

$$\bar{y}_K = \frac{\bar{m}_{ik}\bar{b}_{jk} - \bar{m}_{jk}\bar{b}_{ik}}{\bar{m}_{ik} - \bar{m}_{jk}} \tag{2.4-10}$$

For the three image poles P'_{ij}, $P'_{j\ell}$, $P'_{i\ell}$ we get, by a similar derivation

$$\bar{x}_L = \frac{\bar{b}_{j\ell} - \bar{b}_{i\ell}}{\bar{m}_{i\ell} - \bar{m}_{j\ell}} \tag{2.4-11}$$

$$\bar{y}_L = \frac{\bar{m}_{i\ell}\bar{b}_{j\ell} - \bar{m}_{j\ell}\bar{b}_{i\ell}}{\bar{m}_{i\ell} - \bar{m}_{j\ell}} \tag{2.4-12}$$

where

$$\bar{m}_{j\ell} = - \frac{x_{j\ell} - x_{ij}}{y_{j\ell} - y_{ij}} \tag{2.4-13}$$

$$\bar{b}_{j\ell} = \bar{y}_{j\ell} - \bar{m}_{i\ell}\bar{x}_{j\ell}$$

with

$$\bar{x}_{j\ell} = \frac{x_{ij} + x_{j\ell}}{2}$$

$$\bar{y}_{j\ell} = \frac{y_{ij} + y_{j\ell}}{2} \tag{2.4-14}$$

and

$$\bar{m}_{i\ell} = -\frac{x_{i\ell} - x_{ij}}{y_{i\ell} - y_{ij}}$$

$$\bar{b}_{i\ell} = \bar{y}_{i\ell} - \bar{m}_{i\ell}\bar{x}_{i\ell} \tag{2.4-15}$$

with

$$\bar{x}_{i\ell} = \frac{x_{ij} + x_{i\ell}}{2}$$

$$\bar{y}_{i\ell} = \frac{y_{ij} + y_{i\ell}}{2} \tag{2.4-16}$$

Thus the radius squared for each circle is

$$\bar{r}_K^2 = \frac{(x_{ij} - \bar{x}_K)^2 + (y_{ij} - \bar{y}_K)^2}{4} \tag{2.4-17}$$

$$\bar{r}_L^2 = \frac{(x_{ij} - \bar{x}_L)^2 + (y_{ij} - \bar{y}_L)^2}{4} \tag{2.4-18}$$

The equations for the two circles defining the Ball point are

$$(x - \bar{x}_K)^2 + (y - \bar{y}_K)^2 = \bar{r}_K^2 \tag{2.4-19}$$

and

$$(x - \bar{x}_L)^2 + (y - \bar{y}_L)^2 = \bar{r}_L^2 \tag{2.4-20}$$

Upon expansion of these two equations and subtraction of equation (2.4-20) from (2.4-19) we get

$$2(\bar{x}_L - \bar{x}_K)x + 2(\bar{y}_L - \bar{y}_K)y = (\bar{x}_L^2 - \bar{x}_K^2) + (\bar{y}_L^2 - \bar{y}_K^2) - (\bar{r}_L^2 - \bar{r}_K^2) \tag{2.4-21}$$

which is the equation of the line defined by the intersections of the two circles. Solving equation (2.4-21) for x and substituting into equation (2.4-19) yields a quadratic equation in y with the following solution

$$y_{\beta} = \frac{\bar{y}_K + \bar{x}_K K_1 - K_1 K_2}{1 + K_1{}^2} \pm \sqrt{\left(\frac{\bar{y}_K + \bar{x}_K K_1 - K_1 K_2}{1 + K_1{}^2}\right)^2 - \frac{\bar{x}_K^2 + \bar{y}_K^2 - \bar{r}_K^2 - 2\bar{x}_K K_2 + K_2{}^2}{1 + K_1{}^2}} \tag{2.4-22}$$

where

$$K_1 = \frac{\bar{y}_K - \bar{y}_L}{\bar{x}_L - \bar{x}_K} \tag{2.4-23}$$

$$K_2 = \frac{\bar{x}_L^2 - \bar{x}_K^2 + \bar{y}_L^2 - \bar{y}_K^2 + \bar{r}_K^2 - \bar{r}_L^2}{2(\bar{x}_L - \bar{x}_K)} \tag{2.4-24}$$

One of the solutions to equation (2.4-22) will be the y coordinate for the Ball point and the other will be the y coordinate for P'_{ij}. Using the appropriate solution, the x coordinate is

$$x_{\beta} = K_1 y_{\beta} + K_2 \tag{2.4-25}$$

2.5 Derivation of Equations Defining Q_{ij}, T_{ij} and U_{ij}

As previously mentioned, Q_{ij} is the intersection of two lines passing through the opposite sides of the opposite-pole quadrilateral. Thus Q_{ij} is the intersection of the line through P'_{ik} and P'_{jk} with the line through $P'_{i\ell}$ and $P'_{j\ell}$. The equation of a line passing through the image poles P'_{ik} and P'_{jk} must satisfy the following conditions

$$y'_{ik} = m_k x'_{ik} + b_k$$

and (2.5-1)

$$y'_{jk} = m_k x'_{jk} + b_k$$

Solving equations (2.5-1) for the slope and intercept yields

$$m_k = \frac{y'_{ik} - y'_{jk}}{x'_{ik} - x'_{jk}} \tag{2.5-2}$$

$$b_k = \frac{x'_{ik}y'_{jk} - x'_{jk}y'_{ik}}{x'_{ik} - x'_{jk}}$$

In a similar manner for image poles $P'_{i\ell}$ and $P'_{j\ell}$ we get

$$m_\ell = \frac{y'_{i\ell} - y'_{j\ell}}{x'_{i\ell} - x'_{j\ell}}$$

(2.5-3)

$$b_\ell = \frac{x'_{i\ell}y'_{j\ell} - x'_{j\ell}y'_{i\ell}}{x'_{i\ell} - x'_{j\ell}}$$

Therefore the equations which define Q_{ij} are

$$y^Q_{ij} = m_k x^Q_{ij} + b_k \tag{2.5-4}$$

and

$$y^Q_{ij} = m_\ell x^Q_{ij} + b_\ell \tag{2.5-5}$$

Since Q_{ij} is the point which satisfies both equation (2.5-4) and equation (2.5-5) we need only equate the right hand sides of the two equations and solve for x^Q_{ij}, and then use either equation (2.5-4) or (2.5-5) to compute y^Q_{ij}. The results of these manipulations are the xy coordinates of Q_{ij}.

$$x^Q_{ij} = \frac{b_k - b_\ell}{m_\ell - m_k} \tag{2.5-6}$$

$$y^Q_{ij} = \frac{m_\ell b_k - m_k b_\ell}{m_\ell - m_k} \tag{2.5-7}$$

T_{ij} and U_{ij} are the intersections, if they exist, of two circles having as their respective diameters the opposite sides of an opposite image-pole quadrilateral. Thus, T_{ij} and U_{ij} are the intersections of the circle having diameter $P'_{ik}P'_{jk}$ with the circle having diameter $P'_{i\ell}P'_{j\ell}$. The equation of the circle with diameter P'_{ik} is

$$(x - x_K)^2 + (y - y_K)^2 = r^2_K \tag{2.5-8}$$

where x_K and y_K are the coordinates of the center of the circle and r_K is the radius determined from

$$x_K = \frac{x_{ik} + x_{jk}}{2} \tag{2.5-9a}$$

$$y_K = \frac{y_{ik} + y_{jk}}{2} \tag{2.5-9b}$$

$$r^2_K = \frac{(x_{jk} - x_{ik})^2 + (y_{jk} - y_{ik})^2}{4} \tag{2.5-9c}$$

In a similar manner for the circle with diameter $P'_{i\ell}P'_{j\ell}$ we get

$$(x - x_L)^2 + (y - y_L)^2 = r_L^2 \tag{2.5-10}$$

where

$$x_L = \frac{x_{i\ell} + x_{j\ell}}{2} \tag{2.5-11a}$$

$$y_L = \frac{y_{i\ell} + y_{j\ell}}{2} \tag{2.5-11b}$$

$$r_L^2 = \frac{(x_{j\ell} - x_{i\ell})^2 + (y_{j\ell} - y_{i\ell})^2}{4} \tag{2.5-11c}$$

After expanding equations (2.5-8) and (2.5-10) and subtracting equation (2.5-10) from (2.5-8), the result is the equation of a straight line passing through the intersections of the two circles.

$$\begin{aligned} 2(x_L - x_K)x + 2(y_L - y_K)y = (x_L^2 - x_K^2) + \\ (y_L^2 - y_K^2) - (r_L^2 - r_K^2) \end{aligned} \tag{2.5-12}$$

Equation (2.5-12) may be solved for x (or y) and this result substituted into either equation (2.5-8) or (2.5-10) to obtain a quadratic equation in y (or x). The solutions to this quadratic equation are the y coordinates for T_{ij} and U_{ij}. The test to check for the existence of these intersections requires the discriminant to be equal to or greater than zero. The quadratic equation derived in this manner is

$$y_{ij}^{T,U} = \frac{y_K + x_K C_1 - C_1 C_2}{1 + C_1^2} \pm \sqrt{\left(\frac{y_K + x_K C_1 - C_1 C_2}{1 + C_1^2}\right)^2 - \frac{x_K^2 + y_K^2 - r_K^2 - 2x_K C_2 + C_2^2}{1 + C_1^2}} \tag{2.5-13}$$

where

$$C_1 = \frac{y_K - y_L}{x_L - x_K} \tag{2.5-14}$$

$$C_2 = \frac{x_L^2 - x_K^2 + y_L^2 - y_K^2 + r_K^2 - r_L^2}{2(x_L - x_K)} \tag{2.5-15}$$

Substitution of equation (2.5-13) into (2.5-12) yields the x coordinate for T_{ij} and U_{ij}.

$$x_{ij}^{T,U} = C_1\ y_{ij}^{T,U} + C_2 \tag{2.5-16}$$

If all six pairs of circles intersected, then six T_{ij} and six U_{ij} points would result. However, since nothing guarantees this to be so, there may be some values of T_{ij} and U_{ij} which do not exist. All that is required for this evaluation is to check the discriminant of equation (2.5-13). A negative value for the discriminant means that the circles do not intersect thus T_{ij} and U_{ij} do not exist, and a positive value means that T_{ij} and U_{ij} do exist.

2.6 Derivation of Equations Defining T^*_{ij} and U^*_{ij}

Since T^*_{ij} and U^*_{ij} are the intersections of two circles, the approach is the same as used to determine T_{ij} and U_{ij}. However, as can be seen from Figure 2.1-8, the image poles P'_{ik} and P'_{jk} are not at the ends of the diameter of the circle and likewise for $P'_{i\ell}$ and $P'_{j\ell}$. Instead of $\psi_{ij} = \pi$ as is the case for T_{ij} and U_{ij}, it will be shown in Chapter 5 that $\psi_{ij} <$ π. In fact $\psi_{ij} = \theta_{ij} - \varphi_{ij}$ where $\varphi_{ij} = \pm \pi$ so

$$\psi_{ij} = \theta_{ij} \mp \pi \tag{2.6-1}$$

where $-\pi$ is used if θ_{ij} is positive and $+\pi$, if θ_{ij} is negative, so $-\pi \leq \psi_{ij} \leq \pi$. θ_{ij} is the change in the angle of the coupler relative to the base between the i and j positions. These values may be computed from the four design positions. Therefore the ψ_{ij} values are easily determined. Figure 2.6-1 illustrates the determination of T^*_{ij} and U^*_{ij} when ψ_{ij} is negative, while Figure 2.1-8 was for ψ_{ij} being positive (ψ_{ij} is assumed positive if clockwise). All that is needed to determine T^*_{ij} and U^*_{ij} are the radius and xy coordinates for each of the two circles. The square of the radius for the circle is

$$(r^*_K)^2 = \frac{(x'_{jk} - x'_{ik})^2 + (y'_{jk} - y'_{ik})^2}{4 \sin^2(\frac{1}{2}\ \psi_{ij})} \tag{2.6-2}$$

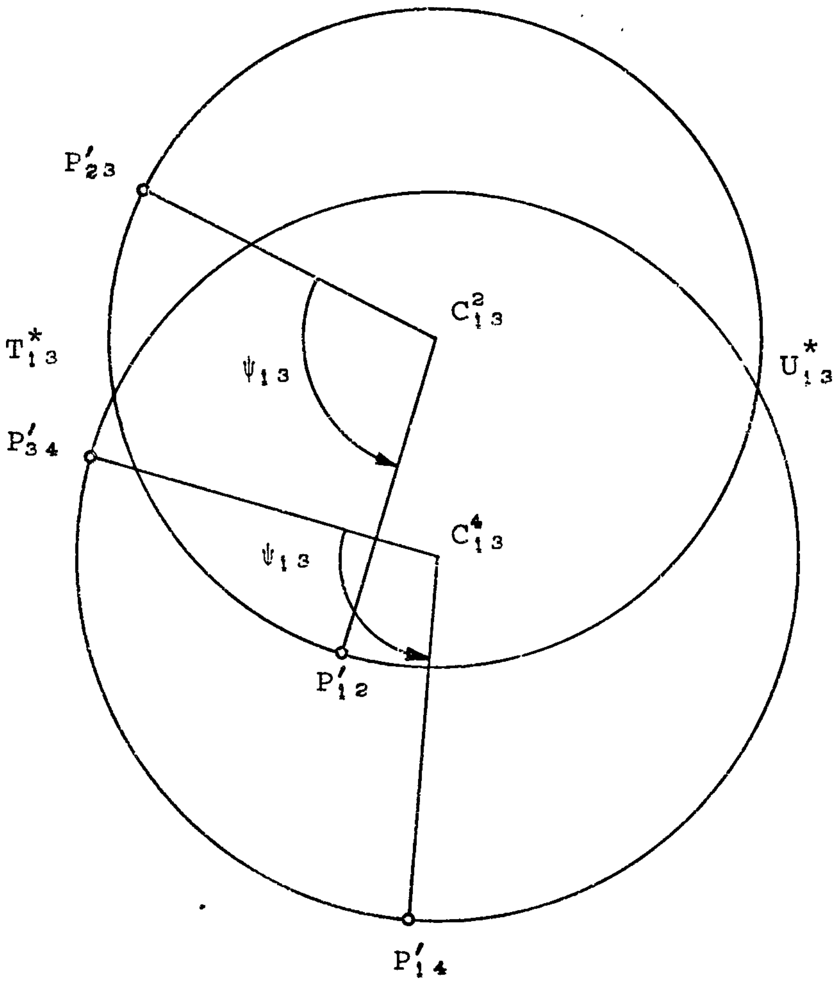

Location of T^*_{13} and U^*_{13} for $\psi_{ij} < 0°$

Fig. 2.6-1

and likewise for the other circle

$$(r^*_L)^2 = \frac{(x'_{j\ell} - x'_{i\ell})^2 + (y'_{j\ell} - y'_{i\ell})^2}{4 \sin^2(\frac{1}{2}\ \psi_{ij})} \tag{2.6-3}$$

The center of the circle is located at the intersection of the lines passing through the two image poles and having opposite slopes. The slope of the line through P'_{ik} is

$$m^*_{K_i} = \tan(\varphi_K - \beta_{ij}) \tag{2.6-4}$$

where $\tan\varphi_K$ is the slope of a line through the image poles P'_{ik} and P'_{jk} and

$$\beta_{ij} = \frac{\psi_{ij} \mp \pi}{2} \tag{2.6-5}$$

with $-\pi$ if $\psi_{ij} > 0$ and $+\pi$ if $\psi_{ij} < 0$. The slope of the line through P'_{jk} is

$$m^*_{K_j} = \tan(\varphi_K + \beta_{ij}) \tag{2.6-6}$$

The equation for the intercept of a line passing through a given point is $b = y_1 - mx_1$ thus for the line through P'_{ik}

$$b^*_{K_i} = y_{ik} - m^*_{K_i} x_{ik} \tag{2.6-7}$$

Likewise for the line through P'_{jk}

$$b^*_{K_j} = y_{jk} - m^*_{K_j} x_{jk} \tag{2.6-8}$$

Applying equations (2.5-6) and (2.5-7), the coordinates for the center of the circle on which P'_{ik} and P'_{jk} lie are

$$x_K^* = \frac{b_{K_i}^* - b_{K_j}^*}{m_{K_j}^* - m_{K_i}^*} \tag{2.6-9}$$

$$y_K^* = \frac{m_{K_j}^* b_{K_i} - m_{K_i}^* b_{K_j}^*}{m_{K_j}^* - m_{K_i}^*} \tag{2.6-10}$$

Similarly for the circle using $P'_{i\ell}$ and $P'_{j\ell}$ we get

$$x_L^* = \frac{b_{L_i}^* - b_{L_j}^*}{m_{L_j}^* - m_{L_i}^*} \tag{2.6-11}$$

$$y_L^* = \frac{m_{L_j}^* b_{L_i}^* - m_{L_i}^* b_{L_j}^*}{m_{L_j}^* - m_{L_i}^*} \tag{2.6-12}$$

where

$$m_{L_i}^* = \tan(\varphi_L - \beta_{ij}) \tag{2.6-13}$$

$$m_{L_j}^* = \tan(\varphi_L + \beta_{ij}) \tag{2.6-14}$$

$$b_{L_i}^* = y_{i\ell} - m_{L_i}^* x_{i\ell} \tag{2.6-15}$$

$$b_{L_j}^* = y_{j\ell} - m_{L_j}^* x_{j\ell} \tag{2.6-16}$$

Now using equations (2.5-13) through (2.5-16) the xy coordinates for T_{ij}^* and U_{ij}^* are

$$y_{ij}^{T^*,U^*} = \frac{y_K^* + x_K^* C_1^* - C_1^* C_2^*}{1 + (C_1^*)^2} \pm \sqrt{\left[\frac{y_K^* + x_K^* C_1^* - C_1^* C_2^*}{1 + (C_1^*)^2}\right]^2 - \frac{(x_K^*)^2 + (y_K^*)^2 - (r_K^*)^2 - 2x_K C_2^* + (C_2^*)^2}{1 + (C_1^*)^2}} \tag{2.6-17}$$

$$x_{ij}^{T^*,U^*} = C_1^* y_{ij}^{T^*,U^*} + C_2^* \tag{2.6-18}$$

where

$$C_1^* = \frac{y_K^* - y_L^*}{x_L^* - x_K^*} \tag{2.6-19}$$

$$C_2^* = \frac{(x_L^*)^2 - (x_K^*)^2 + (y_L^*)^2 - (y_K^*)^2 + (r_K^*)^2 - (r_L^*)^2}{2(x_L^* - x_K^*)} \tag{2.6-20}$$

2.7 Summary

The input data for the computer program are the xy coordinates of the four design positions, the initial value for u and the value of the incremental change in u. When the computations reach the region with three real solutions, the incremental change for u is reduced to better define that region. Then as the program enters again into a region with a single real ordinate, the increment is returned to the original value. The coordinates of the design positions are printed for both the original coordinate system and the final rotated system. The coefficients of the circle-point equation are listed for both the axes aligned with the first design position and the final axes. The values for θ_{ij} are tabulated along with the value for the asymptote. Finally the image poles, Q_{ij}, T_{ij}, U_{ij}, T^*_{ij} and U^*_{ij}, along with the numerical solutions are tabulated for the final rotated axes. The equations in matrix form for rotation of all these points into the final system are

$$\begin{Bmatrix} u_{ij} \\ v_{ij} \end{Bmatrix} = \begin{bmatrix} \cos\alpha & \sin\alpha \\ -\sin\alpha & \cos\alpha \end{bmatrix} \begin{Bmatrix} x_{ij} \\ y_{ij} \end{Bmatrix} \qquad (2.7\text{-}1)$$

where α is defined by equation (2.2-15).

Figure 2.7-1 is an example of a single branch curve with all of the special points as determined from the numerical

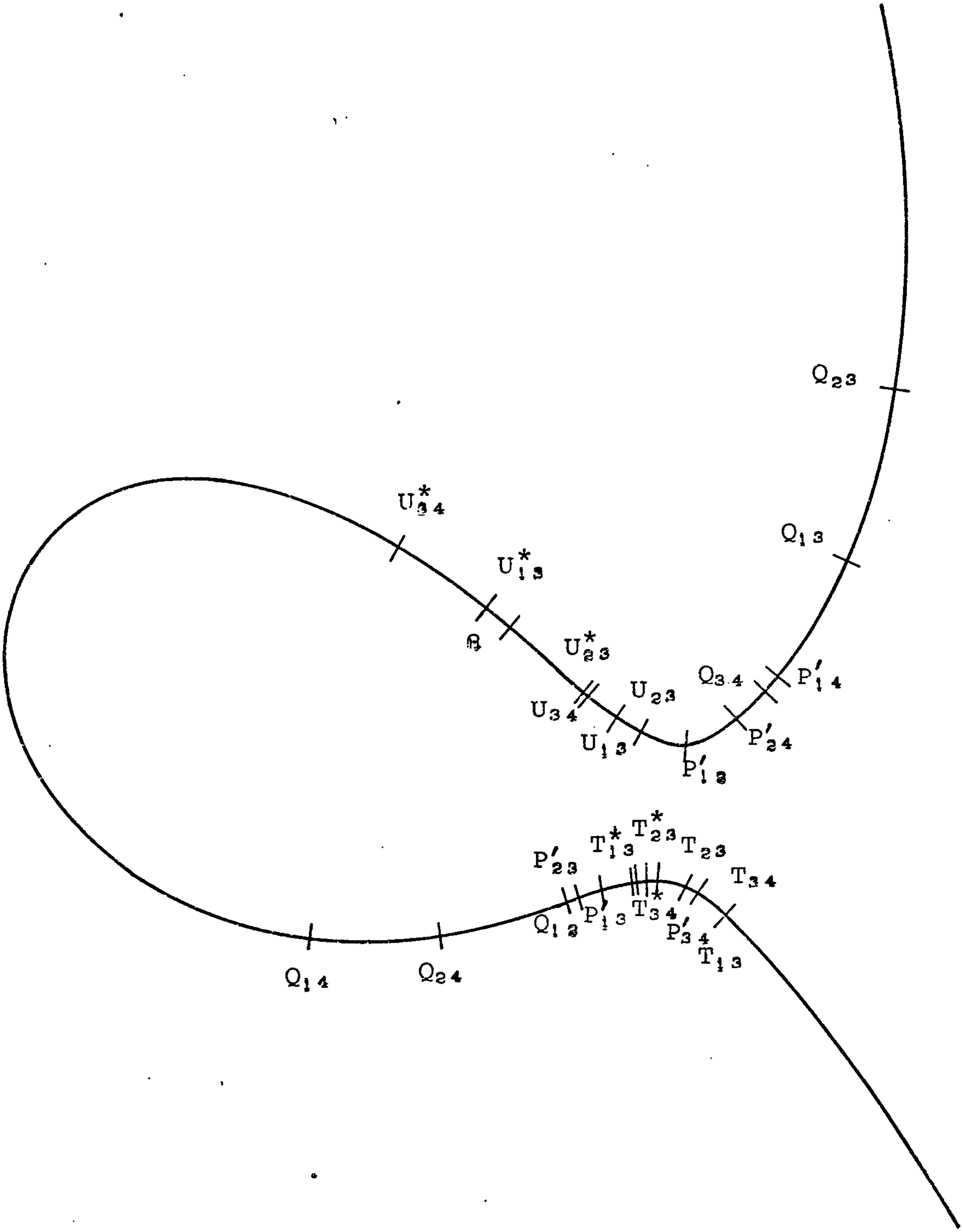

Single branch circle-point curve with all special points indicated

Fig. 2.7-1

solution, while Fig. 2.7-2 is an example of a double branch curve. For a listing of the computer program and the output data see the Appendix.

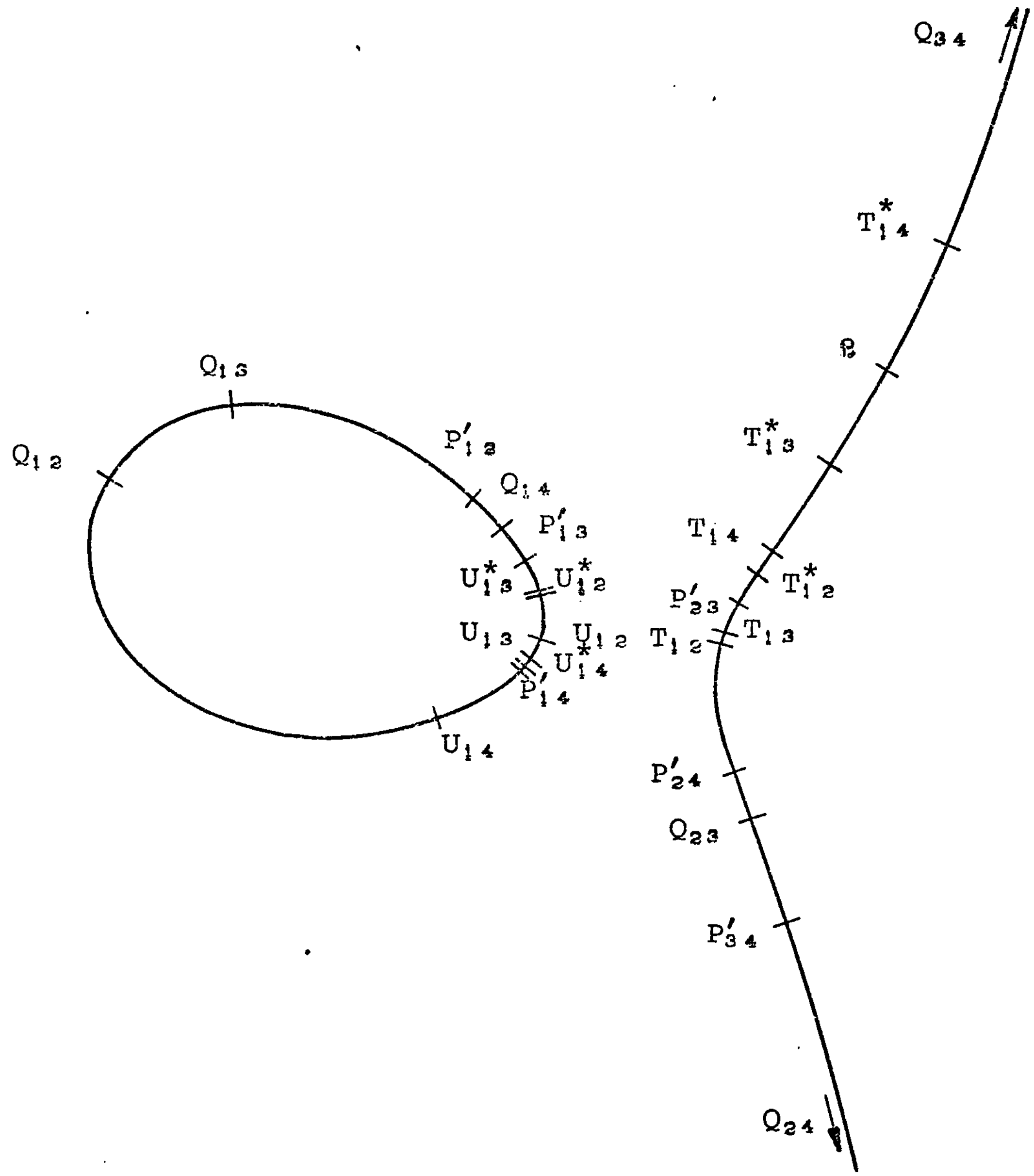

Double branch circle-point curve with all special points indicated.

Fig. 2.7-2

CHAPTER 3

SOLUTION TO THE ORDER PROBLEM

3.1 Introduction

As indicated in Chapter 1, the selection of solution linkages which pass through the design positions in a specified order when driven by a continuously rotating crank is known as the order problem. This problem along with the branch problem, which is discussed in the following chapter, has been a source of frustration for linkage designers for many years. Recently, Waldron [3-1, 3-2] has published a method of solving this problem which builds on earlier work by Modler [3-3].

For this solution [3-2] it is necessary that the circle-point curve be plotted and the image poles and Ball point marked on it. The six image poles divide the curve into six segments, on each of which the order is constant, since the two ends which go to infinity are regarded as a single segment with the point at infinity lying on it. The term "sense" denotes the difference between forward and reverse sequence. That is, 1234 and 1432 have the same order but opposite sense. If the order and sense for any one point of the curve is known, the order and sense for all points on the curve may be determined. For a double branch curve, it is necessary to know the order and sense at one point on each branch.

Starting at a point on the curve where the order and sense are known and following along the curve in either direction, the order is changed everytime an image pole is passed by interchanging the two positions corresponding to the subscripts of that image pole. When the Ball point is passed the order remains the same but the sense is reversed.

A convenient starting point for both order and sense is the point at infinity. The center-point corresponding to this circle-point is the Ball point of the center-point curve. The crank defined by these two points does not rotate relative to the coupler making the angular displacements, φ_{ij}, of the crank relative to the base equal to the angular displacements, θ_{ij}, of the coupler relative to the base. If the angles θ_{ij} have not been explicitly stated in the design data they can be readily obtained from that data. When the design positions are given as four plotted positions of a line segment, the angles θ_{ij} and the order and sense at the point at infinity can be obtained using the simple auxiliary diagram shown in Figure 3.1-1. For the example shown, the order when using a clockwise sense is 1234.

In the case of a single branch curve, simply follow along the curve from the point at infinity interchanging the positions corresponding to the subscripts of each image pole

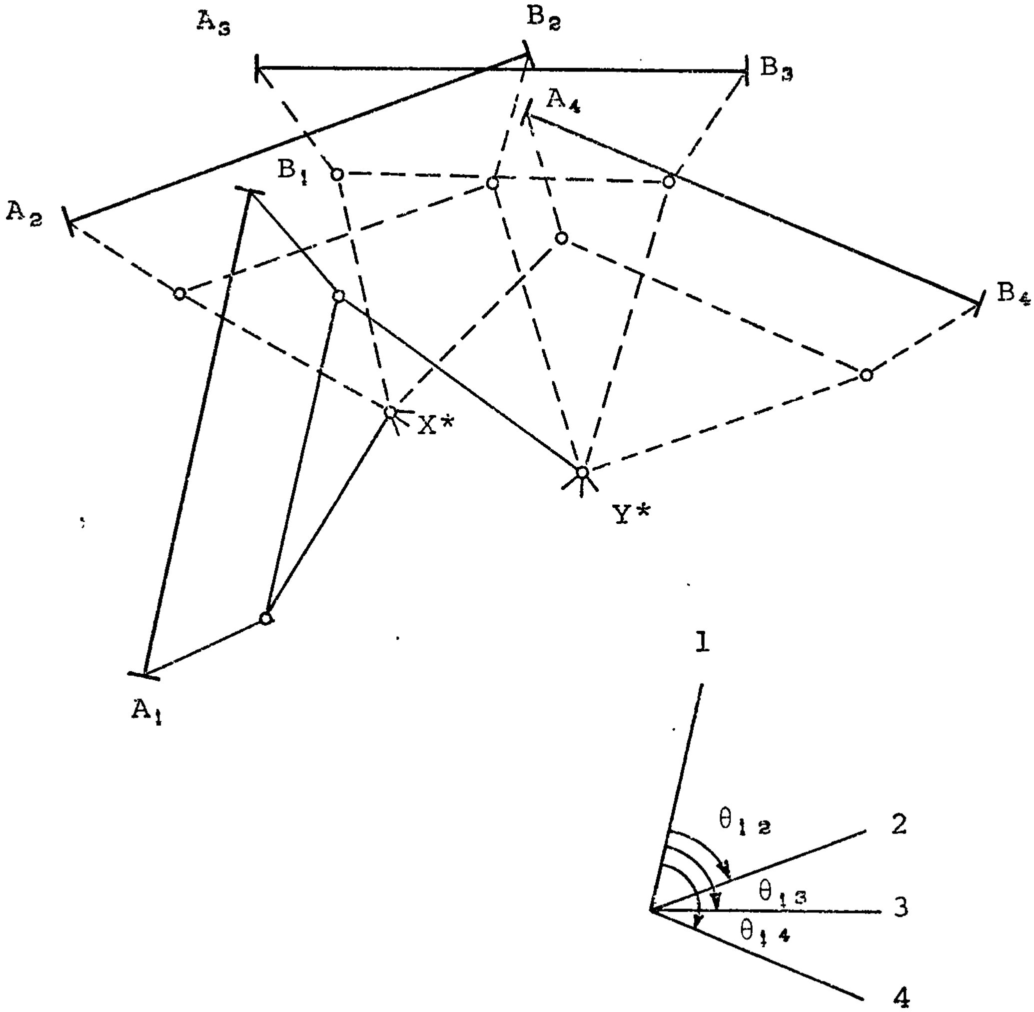

Order and sense of circle-point at infinity

Fig. 3.1-1

as it is passed and reversing the entire sequence of positions when passing the Ball point. This gives both order and sense everywhere on the curve.

In the case of a two branch curve this procedure only works for the open branch. In order to get both order and sense on the closed branch it is necessary to plot the four successive positions of one point on that branch to determine the order at that point. This can then be used as a starting point to determine order every where on that branch.

The ambiguity in the direction of rotation of the crank is usually unimportant from a practical point of view. However, there are occasions when it is important, or even essential, to have a specified direction of crank rotation. An example occurs when a drag-link solution is sought. In that case both cranks must be capable of driving the linkage through the design positions in the specified order when they are continuously rotated, and the direction of rotation must be the same for both cranks. A simple method for resolving the ambiguity in rotation direction is given below.

3.2 Method of Solution

The order problem for motion generation with three finitely separated positions will be examined first. Here the only question is whether the crank rotates clockwise or anti-clockwise in driving the linkage through the design positions in the prescribed order. The locus of circle-points which give cranks having infinite length is a circle; the circle on which the three image poles P_{12}, P_{13} and P'_{23} lie [3-4]. In crossing this circle the center of curvature passes to infinity and returns from infinity in the opposite direction. This results in a reversal of the direction of rotation. Indeed this is the only way the direction of crank rotation through the design positions can reverse. Therefore, the image pole circle divides the plane into two areas. Circle points chosen in each of these areas all give cranks which must rotate in the same direction to drive the linkage through the design positions in the prescribed order.

It remains to develop a means of determining the direction of rotation in one of these areas. This is done by considering the circle-points at infinity. The circle-points at infinity correspond to the center-points which lie on the pole circle. The physical form of a crank whose circle-point lies at infinity and whose center-point lies on the pole circle is a turning block. Thus, there is no rotation between the coupler and crank, and the rotation of the crank relative to the base is identical to that of the coupler relative to the base. Therefore, circle-points everywhere outside the image pole circle give cranks whose direction of rotation through the design positions is the same as that of the coupler. Circle-points everywhere inside the image pole circle give cranks which rotate through the design positions of the linkage in the reverse direction to that of the coupler.

Turning now, to the four position problem, as was shown in Ref. [3-2], the sequence in which a crank drives the linkage through the design positions is easily determined by inspection of the subscripts of the image poles which bound the segment of circle-point curve on which its moving pivot lies. However, the direction in which the linkage proceeds through that sequence is ambiguous. For example, if the circle point lies on a segment bounded by P_{13} and P'_{23}, then 3 must lie between 1 and 2 in the sequence. Thus the order is 1324 or 1423*. In order to determine which is the correct order, three image poles are selected whose subscripts form the pattern P'_{ij}, P'_{ik}, P'_{jk}. That is, only 3 different subscripts appear. The image pole circle through those three image poles is drawn. Circle-points outside that circle give cranks which rotate

*Remember that the order continuously repeats. That is 1324 ≡ 3241 ≡ 2413 ≡ 4132 ≡ 1324. The convention of always starting with position 1 is adopted here.

through positions ijk in the same direction the coupler rotates through those positions, while circle-points inside the circle give the opposite direction of rotation. This is sufficient to resolve the ambiguity as to the sense of rotation since the sense of rotation through any 3 positions determines the sense of rotation through all four. Note that this is a generalization of the method used in Ref. [3-2] of using the Ball point to resolve the ambiguity. That technique was only effective for single branch circle-point curves. The Ball point lies on the image pole circle. In fact, it is located either by finding the fourth intersection of an image pole circle with the circle-point curve or by finding the second intersection of two image pole circles. Thus no additional construction is needed for the present method. It is simply a matter of extracting more information from the same construction. The implementation of this technique is demonstrated in the example below.

3.3 Example of Order Mapping

A linkage is to be designed to move a lamina through 4 design positions shown in Figure 3.3-1 by four positions A_1B_1, A_2B_2, A_3B_3, A_4B_4 of a line segment fixed in the lamina. It should pass through the design positions in the order 1234 when driven by a crank rotating clockwise. Figure 3.3-1 also shows the image poles and circle-point curve derived from the design positions.

We start by choosing three image poles such that their subscripts have the pattern ij, ik, jk and draw the image pole circle on which they lie. Figure 3.3-2 shows the image pole circle for P_{12}, P_{13}, P'_{23}. The fourth intersection of the circle with the circle-point curve locates the Ball point β. The order within the segment of the circle-point curve bounded by P_{12} and P_{13} must be such that position 1 lies between positions 2 and 3, thus the order is either 1243 or 1342. According to the method described here, the order outside the image pole circle will be 123 and within the circle it will be 132. Therefore since the segment lies within the circle, the order must be 1342. The remaining portions of the closed branch segment of the circle-point curve may now be identified by proceeding around the curve in either direction and reversing the order of the two positions

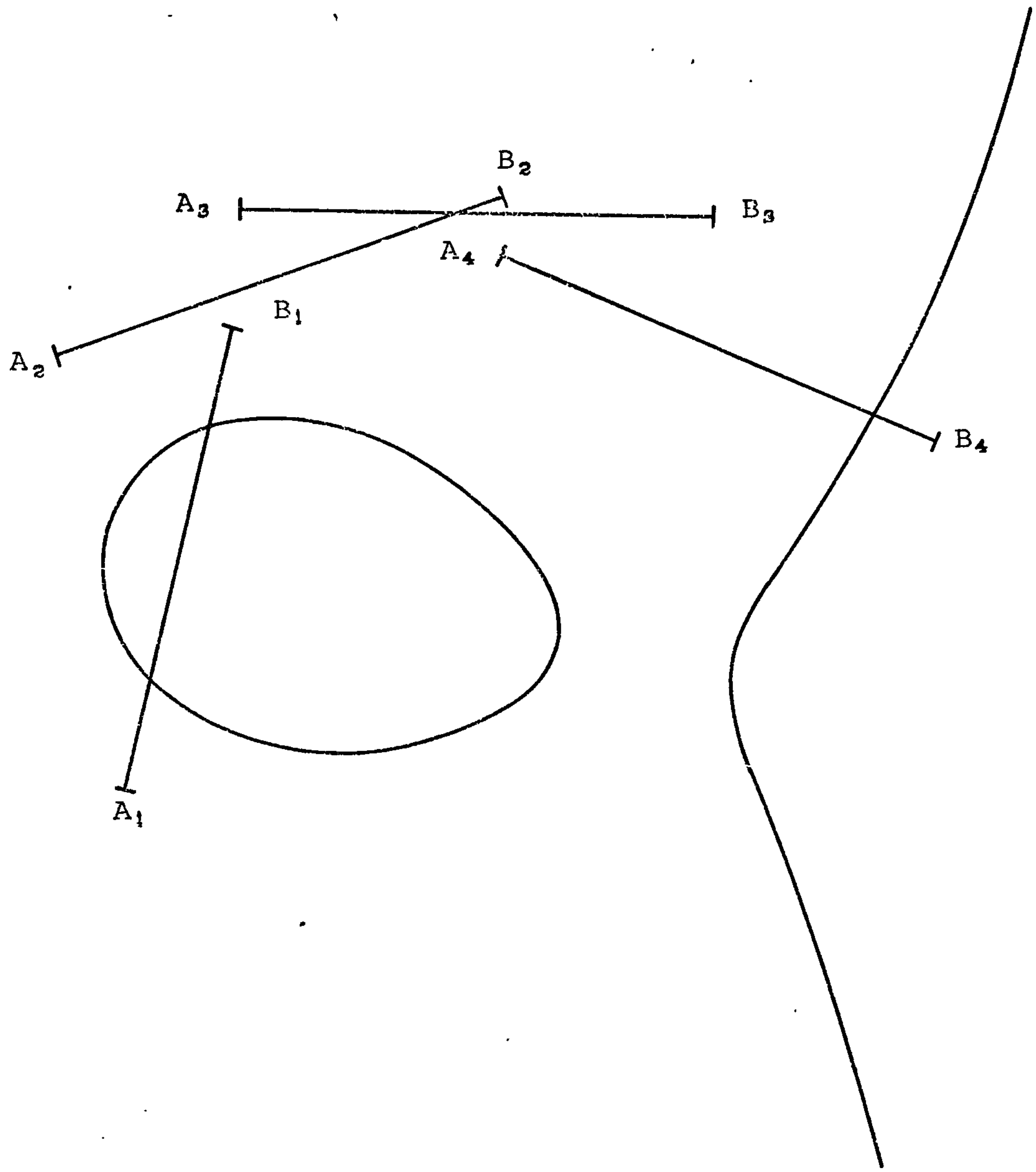

Circle-point curve and image poles for four design positions

Fig. 3.3-1

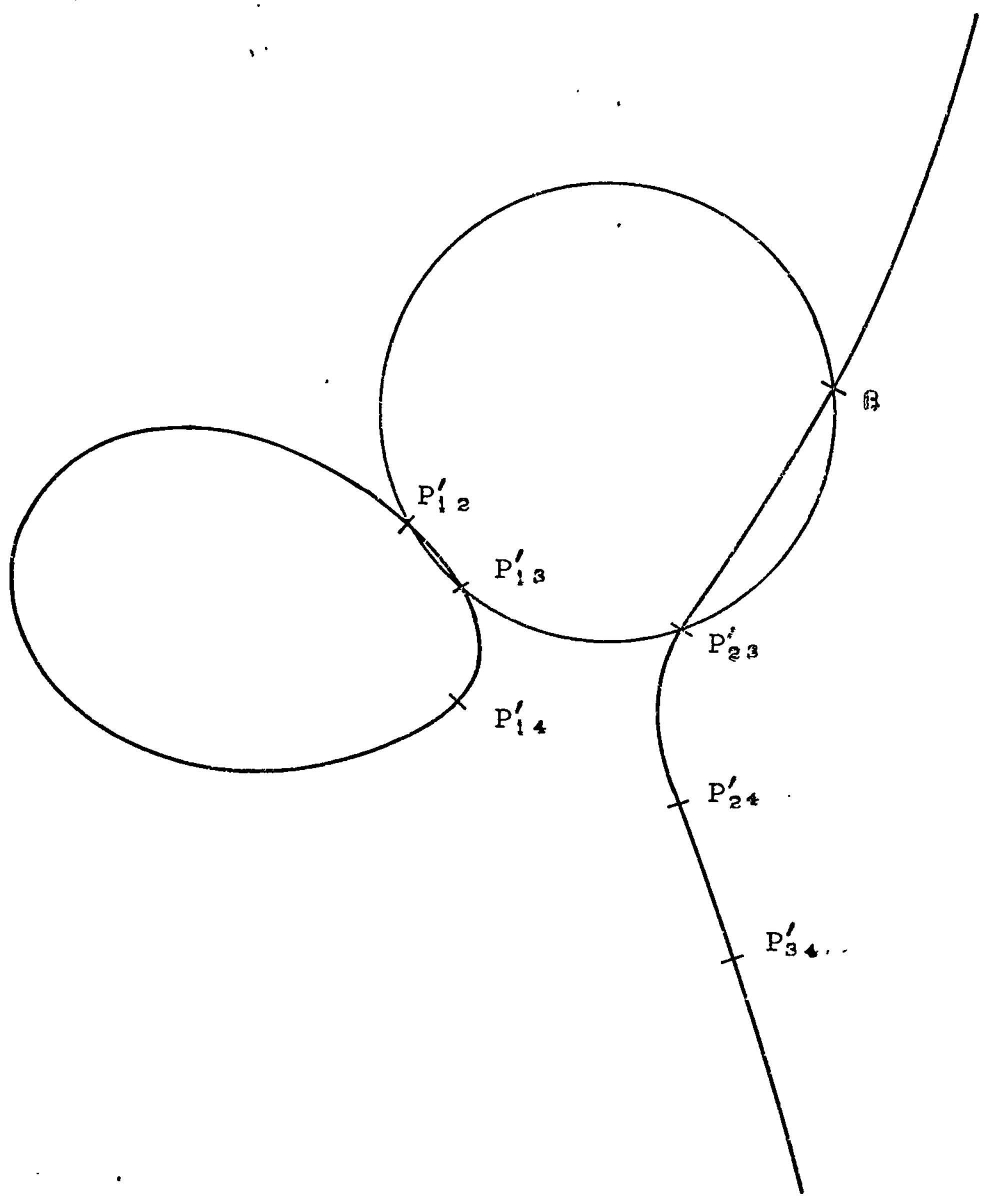

Determination of Ball point using image pole circle and circle-point curve

Fig. 3.3-2

which correspond to the subscripts of each of the image poles as they are encountered [3-2]. For the open branch segment bounded by P'_{23} and P'_{24}, we see that position 2 must be between positions 3 and 4; thus the order is either 1324 or 1423. Since this segment lies outside the image pole circle, the order must be 1423. The order for the remaining segments are determined exactly as for the closed branch segment. When the Ball point is passed, the sense is reversed. Figure 3.3-3 shows the order for each segment of the circle-point curve.

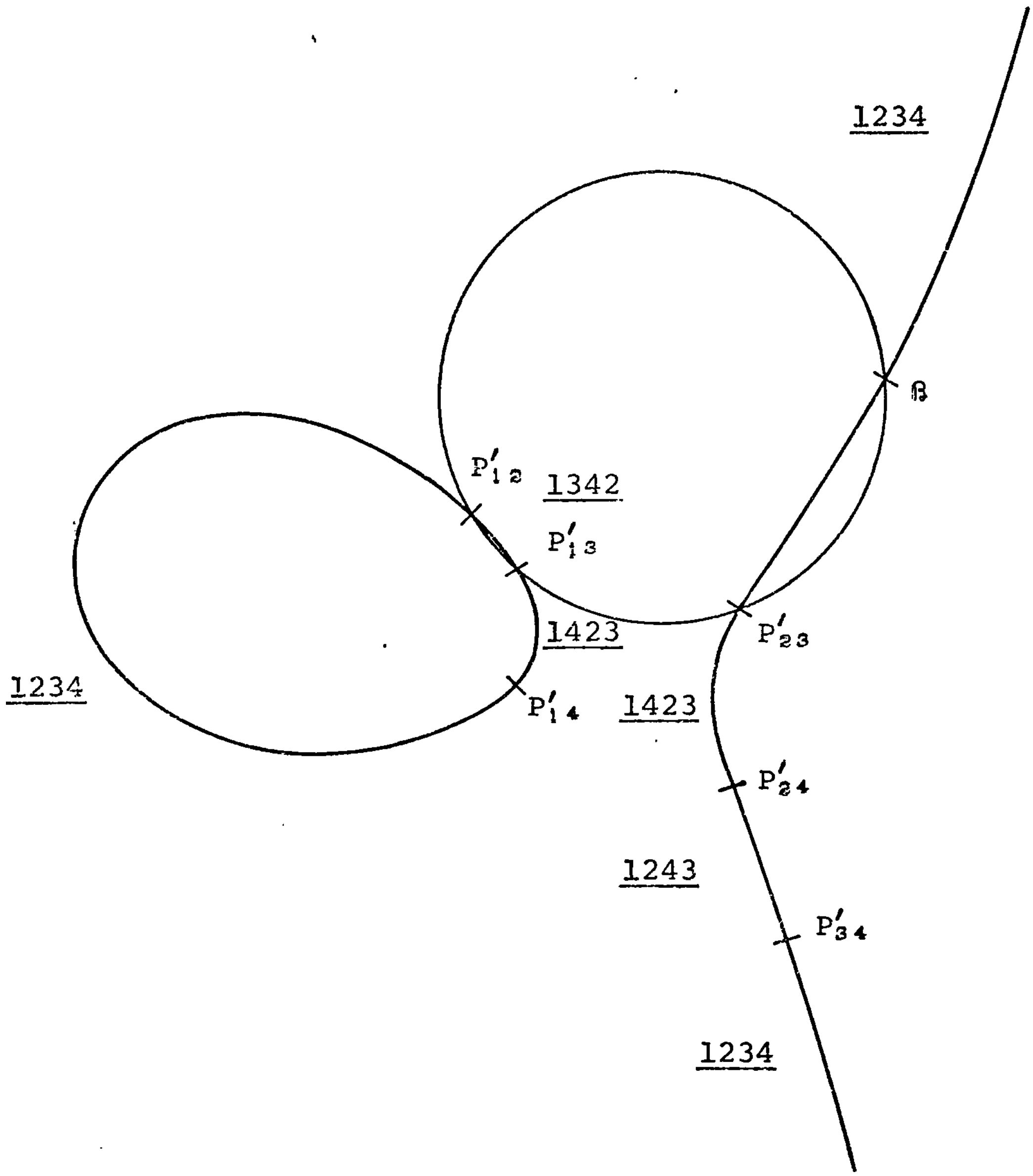

Order of rotation for each segment of circle-point curve

Fig. 3.3-3

3.4 Summary

The solution of the order problem presented here significantly simplifies the solution of the order problem presented in Ref. [3-2]. The order technique resolves the ambiguity as to the sense of crank rotation left by the subscript inspection method of Ref. [3-2]. Unlike the trial point method suggested in that paper, the technique presented here requires no additional construction since, it is assumed, an image pole circle would have been drawn, in any case, to locate the Ball point.

CHAPTER 4

SOLUTION TO THE BRANCH PROBLEM

4.1 Introduction

The branch problem of Burmester's four-bar linkage synthesis method is the problem of selecting solution linkages which do not need to change assembly configuration in order to pass through the design positions.

The solution to the branch problem given in Ref. [4-1] requires a rather cumbersome technique for keeping track of the signs of the 6 angular displacements Ψ_{ij} of the coupler relative to the driven crank as the linkage moves between the design positions.

There are regions of the circle-point curve on which the points give only spurious solutions if selected as driven crank pivots. On the remainder of the curve, spurious solutions can still result depending on the choice of driving crank. In order to locate those regions for which only solutions are possible Table 4-1 is used. Figure 4.1-1 shows the example used for Table 4-1. In the first part of Table 4-1, the points $\mathfrak{B}$, Q_{ij}, T_{ij} and U_{ij} which lie on the closed branch of the curve are listed in the order in which they are passed in going around that branch in either direction starting from $\mathfrak{B}$. Opposite $\mathfrak{B}$ in the Table are entered the six pairs of

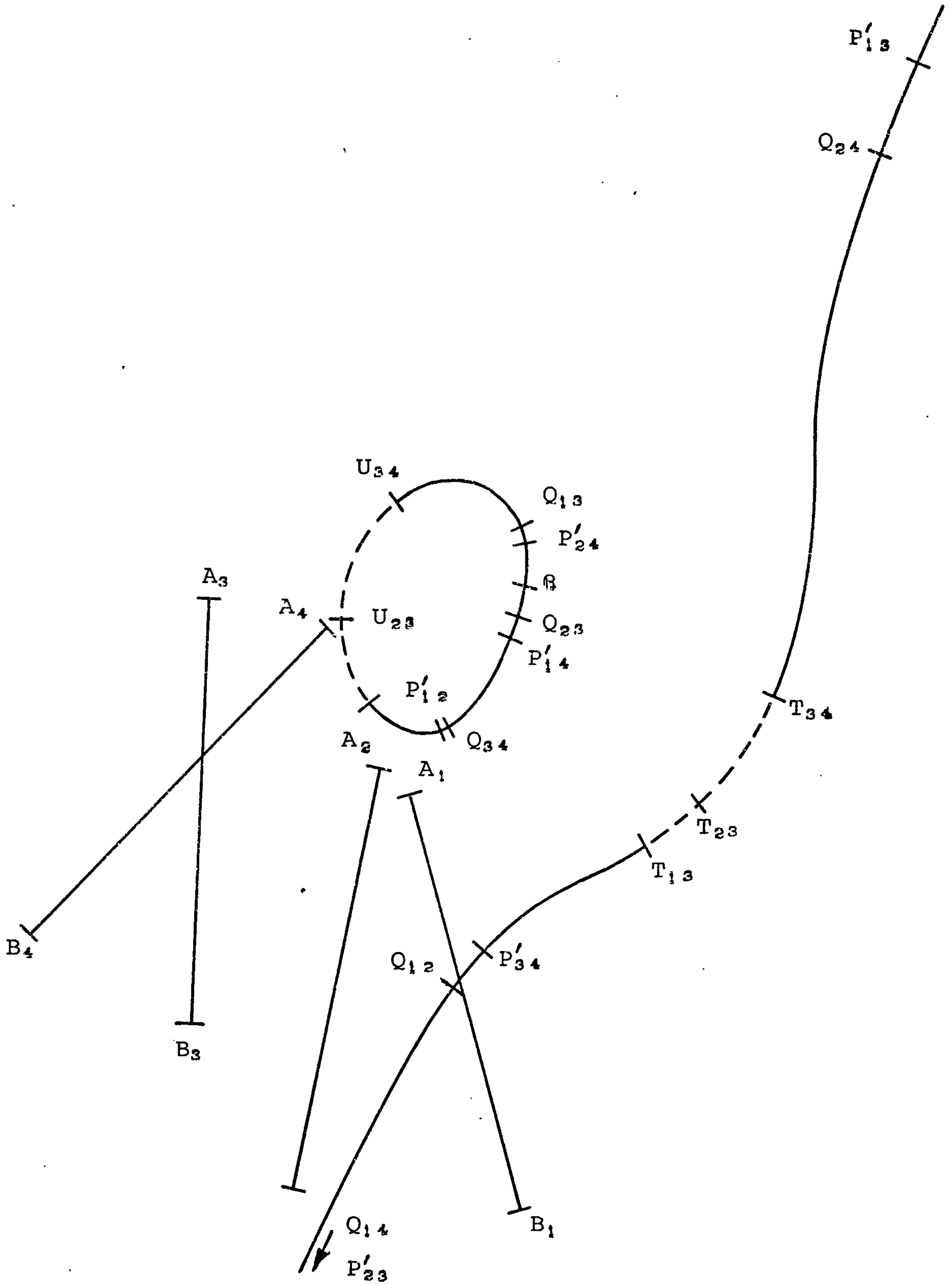

Example for branch solution using table method

Fig. 4.1-1

subscripts of the angular displacements θ_{12}, θ_{13}, θ_{14}, θ_{23}, θ_{24} and θ_{34} of the coupler. The order in which each pair of subscripts is written is that for which the corresponding angle is positive (counterclockwise). If θ_{ij} is counterclockwise, ij is entered and if θ_{ij} is clockwise, then ji is entered. The signs of the angular displacements at $\mathcal{B}$ are read off the auxiliary diagram of Figure 4.1-1. Proceeding down the table as each point Q_{ij}, T_{ij} or U_{ij} is passed the number pair corresponding to its subscripts are reversed. The remaining number pairs are entered in the same order as on the preceding line. For example, when Q_{23} is passed the pair 32 is reversed to 23. When $\mathcal{B}$ is reached again the six number pairs will have returned to their starting order.

Each row of number pairs is now inspected for a number which is in the first position in all three of its appearances. If such a number is present, there will also be a number which appears in the second position in all three of its appearances. For the segment of the curve between Q_{34} and U_{13} the number pairs are 21, 31, 41, 32, 42, 34. It can be seen that 3 is in the first position whenever it appears and 1 is in the second position whenever it appears. When such a number pair is present it is entered in the right hand column of the table. The segments corresponding to rows on the table

TABLE 4-1

Closed Branch

ß	21	31	41	23	42	43	41
Q_{23}	21	31	41	32	42	43	41
Q_{34}	21	31	41	32	42	34	31
U_{13}	21	13	41	32	42	34	—
U_{23}	21	13	41	23	42	34	—
U_{34}	21	13	41	23	42	43	43
Q_{13}	21	31	41	23	42	43	41
ß							

Open Branch

S	21	13	41	23	24	43	23
Q_{24}	21	13	41	23	42	43	43
T_{34}	21	13	41	23	42	34	—
T_{23}	21	13	41	32	42	34	—
T_{13}	21	31	41	32	42	34	31
Q_{12}	12	31	41	32	42	34	32
Q_{14}	12	31	14	32	42	34	32
S							

in which there is no number pair in the right hand column are those which give only spurious solutions. These segments are shown dotted in Figure 4.1-1.

On the other branch of the curve, there is no point like ß for which the six number pairs can immediately be entered in correct order. In order to obtain a starting point, select the point S which is beyond all points P_{ij}, T_{ij}, U_{ij} on that branch of the curve going toward infinity. Choose a pair of image poles with a common subscript such as $P'_{14}P'_{34}$ and draw a line through that image pole pair. Rotate the paper until S appears above the line and read the uncommon subscripts of the image poles from left to right as 13. This process is repeated until all six numbered pairs have been determined. The open branch portion of Table 4-1 shows the points Q_{ij}, T_{ij}, U_{ij} and S in the order which they appear in following along the curve. Proceed in either direction from S changing the orders of the number pairs in the same manner as on the closed branch. The orders obtained when approaching infinity on the two limbs of the curve should be the reverse of one another. As for the closed branch segment, number pairs which appear in the first and second positions in all appearances are entered in the right hand column. Also, those segments for which no such pair is present are shown dotted.

A much simpler technique is developed below which requires only inspection of the subscripts of points on the curve, somewhat after the style of the order solution of Ref. [4-2].

4.2 The Branch Problem

When working on the order problem the rotational displacements of a crank relative to the base are studied. Conversely, in the case of the branch problem the rotational displacements of the coupler relative to a crank are studied. Clearly, if the linkage is inverted onto its coupler, the rotations of the original coupler relative to the crank become minus the rotations of the crank relative to the new base. Just as the image poles divide the circle-point curve into segments on each of which all circle-points give the same order of rotation of the crank relative to the base, the poles divide the center-point curve into segments on each of which all center-points give the same order of rotation of the coupler relative to the crank. Now, the circle-point corresponding to the pole P_{ij} is the point Q_{ij} which lies at the intersection of the lines $P'_{ik}P'_{jk}$ and $P'_{il}P'_{jl}$. As was shown in Ref. [4-1], the points Q_{ij} are important in mapping regions of the circle-point curve on which the range of rotation through the design positions of the coupler relative to the crank is less than $180°$. One can now go further and say that the points Q_{ij} bound segments of the curve on which the order of rotation of the coupler relative to the crank is constant.

The points T_{ij}, U_{ij} at the intersections of the circles with diameters $P'_{ik}P'_{jk}$ and $P'_{il}P'_{jl}$ were shown in Ref. [4-1]

to be circle-points for which the angular displacement Ψ_{ij} of the coupler relative to the crank between positions i and j is 180°. If positions i and j are adjacent in the order of coupler rotation relative to the crank, as controlled by the Q_{ij}'s, T_{ij} or U_{ij} marks the boundary between segments of the curve on which the range of rotation of the coupler relative to the crank is greater than, or less than, 180° (Figure 4.2-1). If i and j are not adjacent in the order of coupler rotation relative to the crank, T_{ij} or U_{ij} can only lie on a segment of the curve on which the range of coupler rotation relative to the crank is greater than 180° (Figure 4.2-2). Thus regions of the curve which give rotational ranges of the coupler relative to the crank less than 180° can be mapped as follows:

(i) Draw the circle-point curve and locate the points Q_{ij}, T_{ij}, U_{ij}.

(ii) The sequence (see Section 3.2) of coupler rotation relative to the crank is determined on each segment by inspection of the subscripts of the points Q_{ij} bounding it. If the bounding points are Q_{ij} and Q_{ik} then i lies between j and k in the sequence. Hence the sequence is iklj (or ijlk). It does not matter, for the present purpose, what the sense of the rotation is.

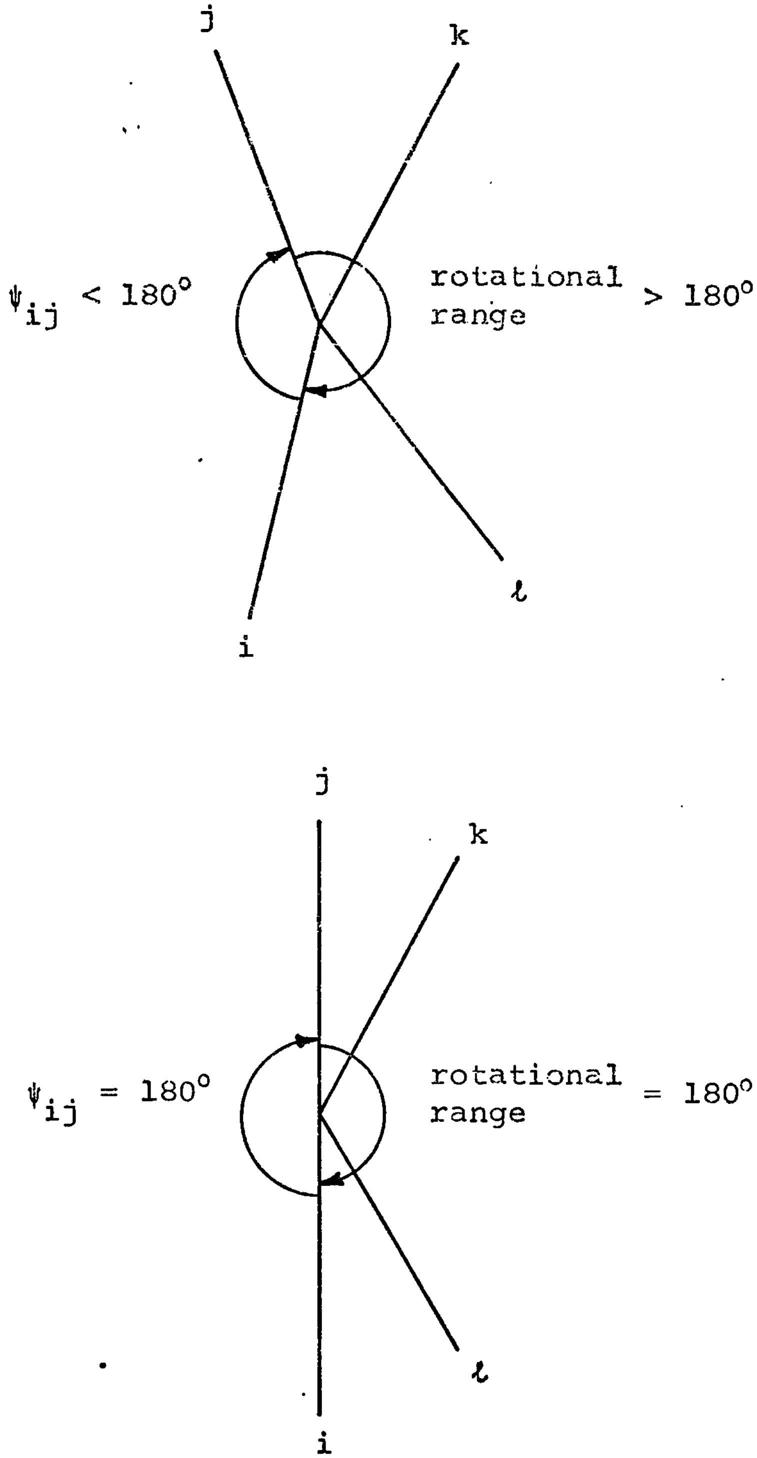

Rotational ranges of the coupler relative to the driven crank for order ijkℓ.

Fig. 4.2-1

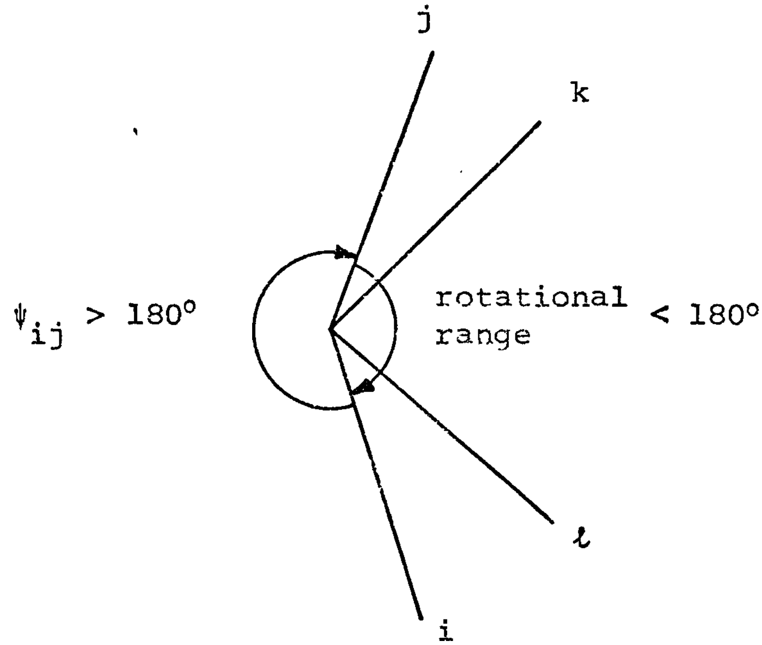

Fig. 4.2-1 (cont.)

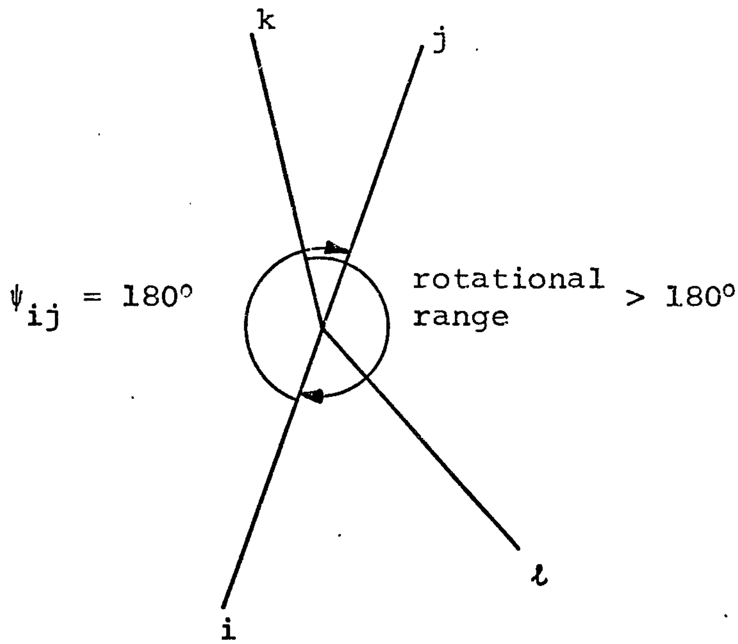

Rotational range of coupler relative to the driven crank for order ikjℓ with $\psi_{ij} = 180°$

Fig. 4.2-2

(iii) Inspect each point T_{ij} or U_{ij}. If its subscripts correspond to positions which are adjacent in the sequence on the segment on which it lies, then it marks a boundary between regions on which the angular range is greater than, or less than 180°. Next look for points T_{ij} and U_{ij} whose subscripts do not represent positions which are adjacent in the sequence. These must lie on segments for which the angular range is greater than 180°. By marking these segments as not permissible and alternately marking permissible and non-permissible segments between those points T_{ij} and U_{ij} distinguished as marking segment boundaries, it is now possible to map all permissible segments; that is , those which give angular ranges less than 180°.

(iv) On each segment distinguished as giving an angular range less than 180°, the design positions which give the extreme positions can be distinguished as follows:

Start from one end of the segment. Initially the extremal design positions are those corresponding to the subscripts of the point T_{ij} or U_{ij} marking the segment boundary. Following along the segment, every time a point Q_{ij} is encountered with one of its subscripts corresponding to one of the extremal positions, this position is exchanged with the position denoted by the other subscript of the point Q_{ij}

to obtain a new pair of extremal positions (i.e. if the extremal positions are 12 and Q_{13} is encountered the extremal positions become 23). At the other end of the segment, the current extremal positions should correspond to the subscripts of the point T_{ij} or U_{ij} bounding the segment on that end. Note that no T_{ij} or U_{ij} points can appear inside a segment on which the angular range is less than 180^0. Also note that encountering a Q_{ij} where neither i nor j is extremal does not affect this process. Such points represent a change in sequence of positions internal to the sequence only, and are of no interest in this application, since our concern is only with knowledge of the extremal positions as needed for the Filemon construction.

The above information is sufficient to permit selection of a suitable driven crank and to proceed to Filemon's construction [4-1,4-3] to obtain a suitable driving crank to ensure a solution free of branch change, provided it is of crank-rocker or drag-link type, and provided that it is driven by the designated driving crank.

4.3 Example of Branch Mapping

Figure 4.3-1 shows the circle-point curve used in the order problem example (section 3.3) along with the corresponding Q_{ij}, T_{ij}, U_{ij} points and the Ball point $\mathcal{B}$.

On the closed branch segment all the U_{ij} points lie on the segment bounded by Q_{12} and Q_{14}, thus the sequence is either 1234 or 1432. The subscripts for U_{ij} which represent boundaries between regions on which the angular range is greater than or less than 180° would be 12, 23, 34 and 14. The subscripts of U_{ij} points which lie on segments for which the angular range is greater than 180° would be 13 and 24. From Figure 4.3-1 the U_{ij} points are U_{12}, U_{13} and U_{14}, thus the segment of the circle-point curve on which U_{13} lies has an angular range greater than 180°, and U_{12} and U_{14} mark the limits of this segment.

The design positions which are the extreme positions for each segment are found by starting at U_{14} and working clockwise to U_{12} or starting at U_{12} and working counterclockwise to U_{14}. Starting at U_{12} the limits are 1 and 2 until Q_{14} is passed and then the limits are 4 and 2. When Q_{12} is passed the limits become 4 and 1. Note that no change occurs at Q_{13} since neither position 1 nor position 3 is extremal on this portion of the curve.

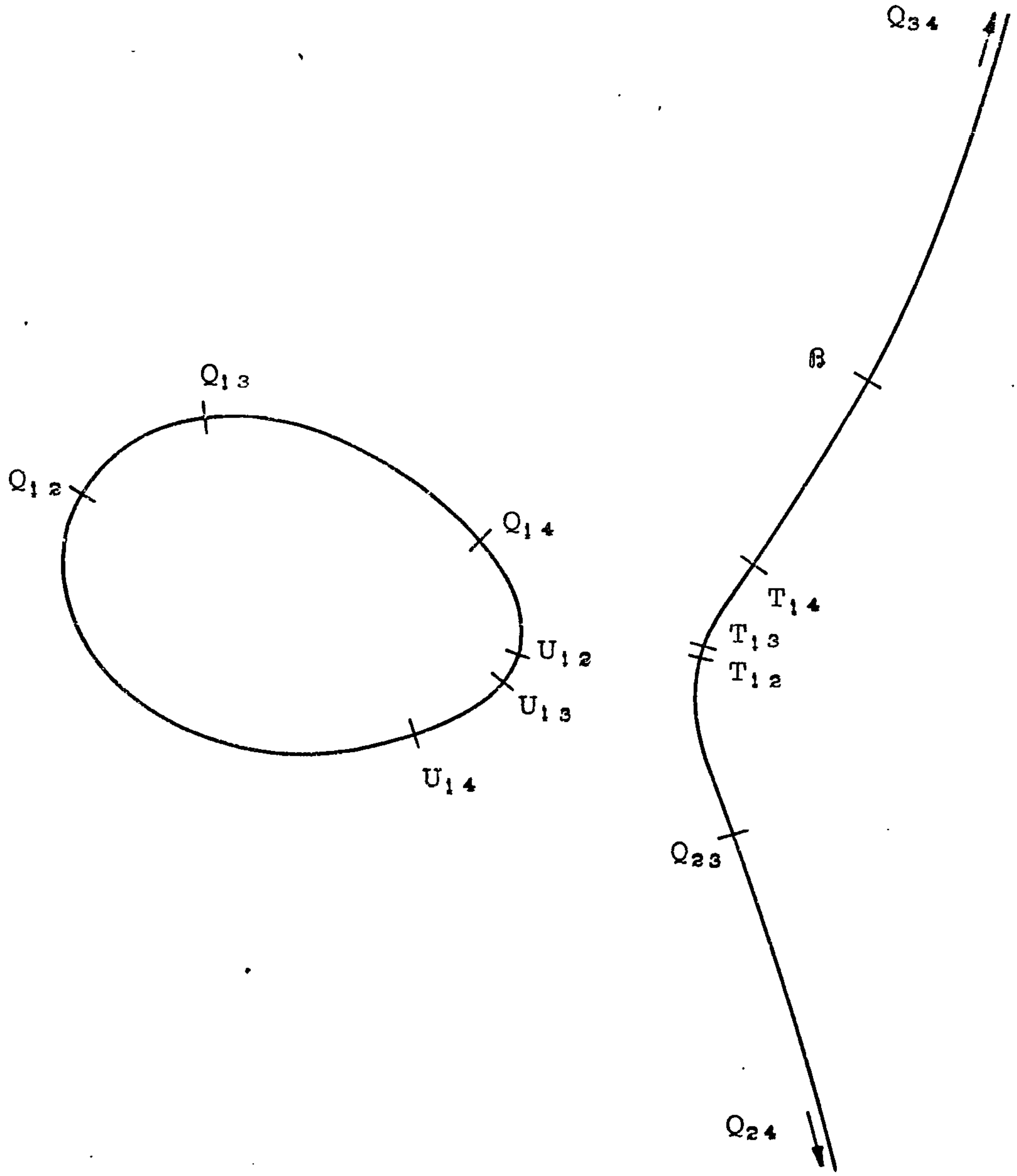

Circle-point curve with Q_{ij}, T_{ij} and U_{ij} points used for branch mapping

Fig. 4.3-1

For the open branch segment of the circle-point curve all of the T_{ij} points lie between Q_{34} and Q_{23}, thus the sequence would again be either 1234 or 1432. Using the same procedure as for the closed branch segment it is found that the only region of the open branch segment for which the angular range is greater than 180° is that segment on which T_{12}, T_{13} and T_{14} lie. Starting with T_{14} the extreme positions are 1 and 4 until Q_{34} is passed and then they become 1 and 3. On the other portion of the open branch segment the extreme positions are 1 and 2 until Q_{23} is passed and then they become 1 and 3. Figure 4.3-2 shows the circle-point curve with the extreme positions for each segment. The regions where the angular range is less than 180° are indicated by the solid lines.

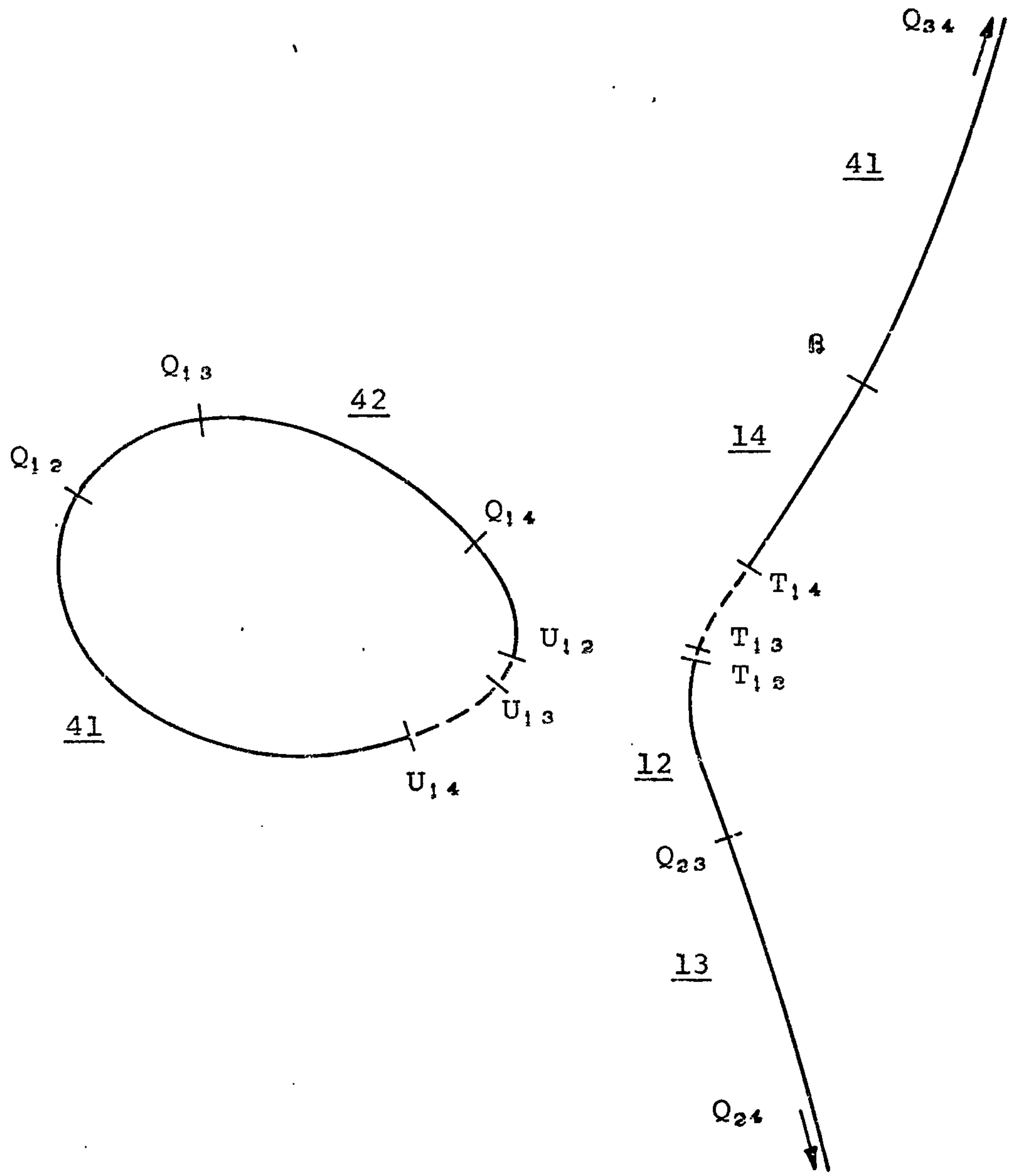

Regions of circle-point curve for $\psi_{ij} < 180^{\circ}$ (solid lines) and extreme positions

Fig. 4.3-2

4.4 Summary

A technique has been presented which significantly simplifies the solution of the branch problem presented in reference [4-1] making the solution a "by inspection" method. The branch mapping technique eliminates the need for a table, as required in Ref. [4-1], giving signs of the six angles Ψ_{ij} representing the angular displacement of the coupler relative to the driven crank between design positions i and j, on each segment of the curve. It permits location of permissible regions of the curve for the driven crank circle-points by inspection of the subscripts, first of the points Q_{ij} and then of the points T_{ij}, U_{ij}. The location of the points Q_{ij}, T_{ij} and U_{ij} and the use of the Filemon construction to complete the solution remains as described in Ref. [4-1].

CHAPTER 5

INVERSION OF ORDER AND BRANCH SOLUTIONS

5.1 Introduction

In Section 4.2 the linkage was inverted so the coupler became the base. It was found that the Q_{ij} points bound segments of the circle point curve on which the order of rotation of the coupler relative to the crank is constant. At that time there was no concern for the sense of the rotation as the objective was to determine the segments in which ψ_{ij} was less than 180°. In this chapter the inverted order solution will be completed in order to improve the selection for driven crank moving pivots when designing a crank-rocker mechanism.

If the branch solution is performed for the inverted linkage, then segments of the circle-point curve for which the rotation of the crank relative to the base, φ_{ij} (since the coupler of the inverted linkage is the base for the original linkage), is less than 180°. Thus by combining this new inverted branch solution with the improved branch solution of Chapter 4 we are able to further resolve the regions of the circle-point curve from which it is possible to design crank-rockers. In this case the inverted order solution is used in conjunction with the branch solutions.

5.2 Inverted Order Solution

When the linkage is inverted so the coupler becomes the base, the order problem is solved as described in Section 3.2 except that the center-point curve must be used rather than the circle-point curve. Thus, a pole circle is constructed on the center-point curve with the rotation outside that circle being ijk if poles P_{ij}, P_{jk} and P_{ik} are used. To avoid the necessity of constructing the center-point curve and pole circle, as well as the circle-point curve and image pole circle, it is necessary to determine which areas of the circle-point plane correspond to regions within the pole circle, and likewise which areas correspond to regions outside the pole circle.

Figure 5.2-1 shows an image pole circle for P'_{ij}, P'_{jk} and P'_{ik} with the image pole triangle inscribed. Since only three of the four positions are used for both the image pole and pole circles, the circle-points on the image pole circle have center points at infinity. Conversely, the center-points on the pole circle have corresponding circle-points at infinity. In other words, the pole circle maps into a circle at infinity on the circle-point plane.

If we take one of the image poles and locate all three of its positions in the fixed frame, two positions are the

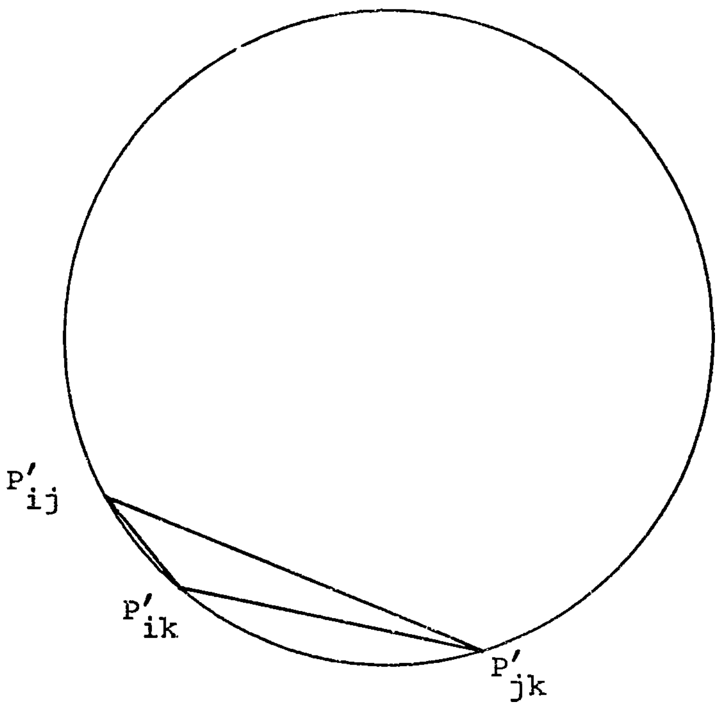

Image pole for P'_{ij}, P'_{jk} and P'_{jk} with inscribed image pole triangle

Fig. 5.2-1

same. Thus there are only two distinct positions through which the crank must pass. Therefore, the fixed pivot of the crank may be any point along the perpendicular bisector of these two positions. Figure 5.2-2 shows image pole P'_{23} in all three positions (in this case positions 2 and 3 are the same point, namely P_{23}). The perpendicular bisector of the two points is a line passing through the poles P_{12} and P_{13} since by definition the image pole P'_{23} is the image of the pole P_{23} with respect to a line through poles P_{12} and P_{13}. Thus the locus of fixed pivots for the moving pivot P'_{23} is any point along the line through poles P_{12} and P_{13}. In other words, the image pole P'_{23} maps into the line passing through poles P_{12} and P_{13} in the fixed lamina (center-point plane). Using this procedure the image poles P'_{12} and P'_{13} map into the lines $P_{13}P_{23}$ and $P_{12}P_{23}$ respectively in the center point plane. Figure 5.2-3 shows the results of this mapping process.

Now it is necessary to determine which regions of the circle-point plane correspond to regions inside and outside of the pole circle. From Figure 5.2-3(a) the area within the pole circle is made up of areas A, B, C, and D. Note that the area within the pole triangle, A, is bounded by the line $P_{12}P_{13}$ which maps into the point P'_{23}, the line

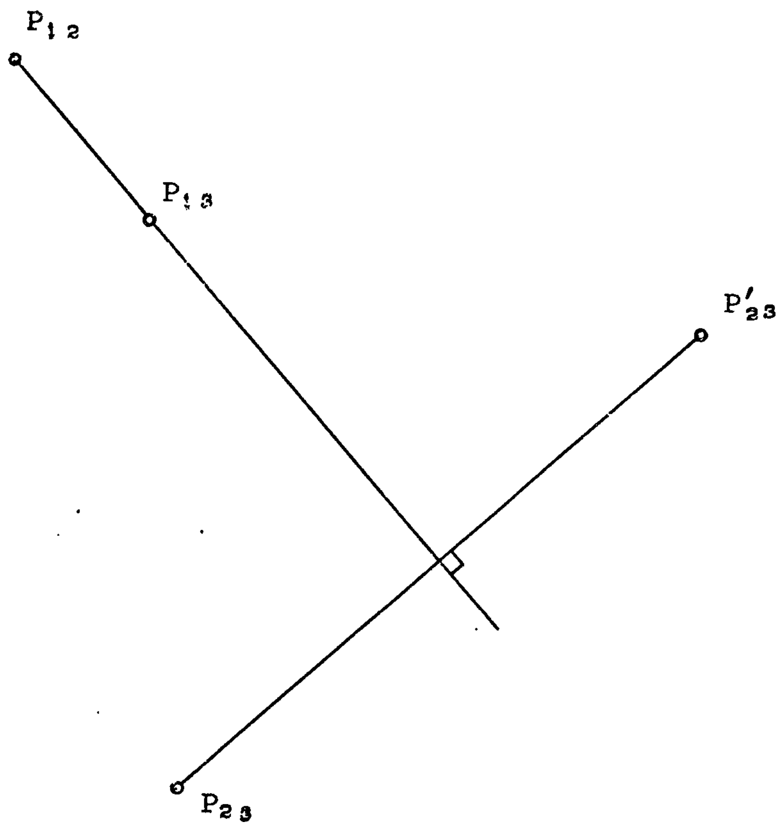

Loci of fixed pivots if P'_{23} is chosen moving pivot

Fig. 5.2-2

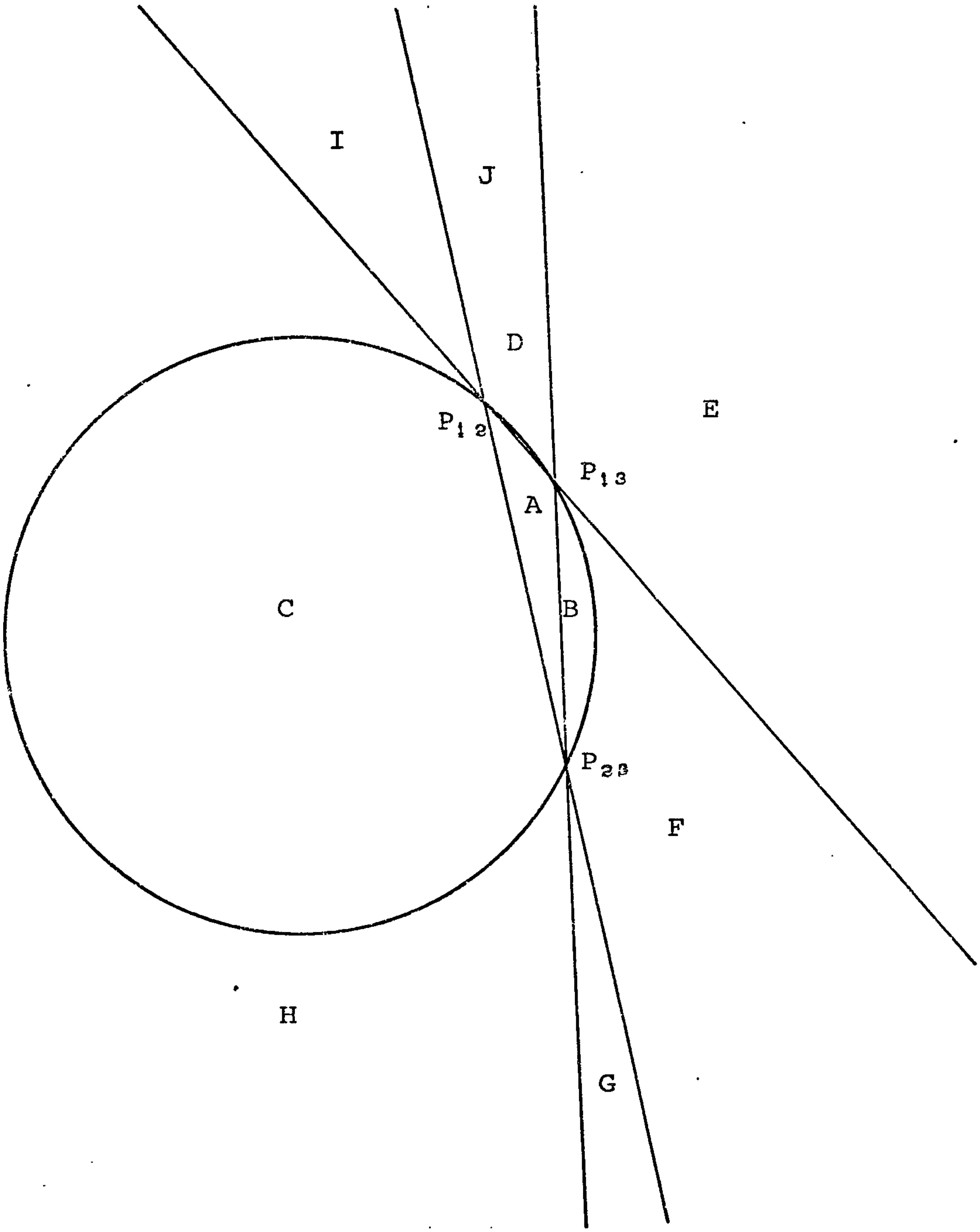

Regions of center-point plane inside and outside of pole circle

Fig. 5.2-3(a)

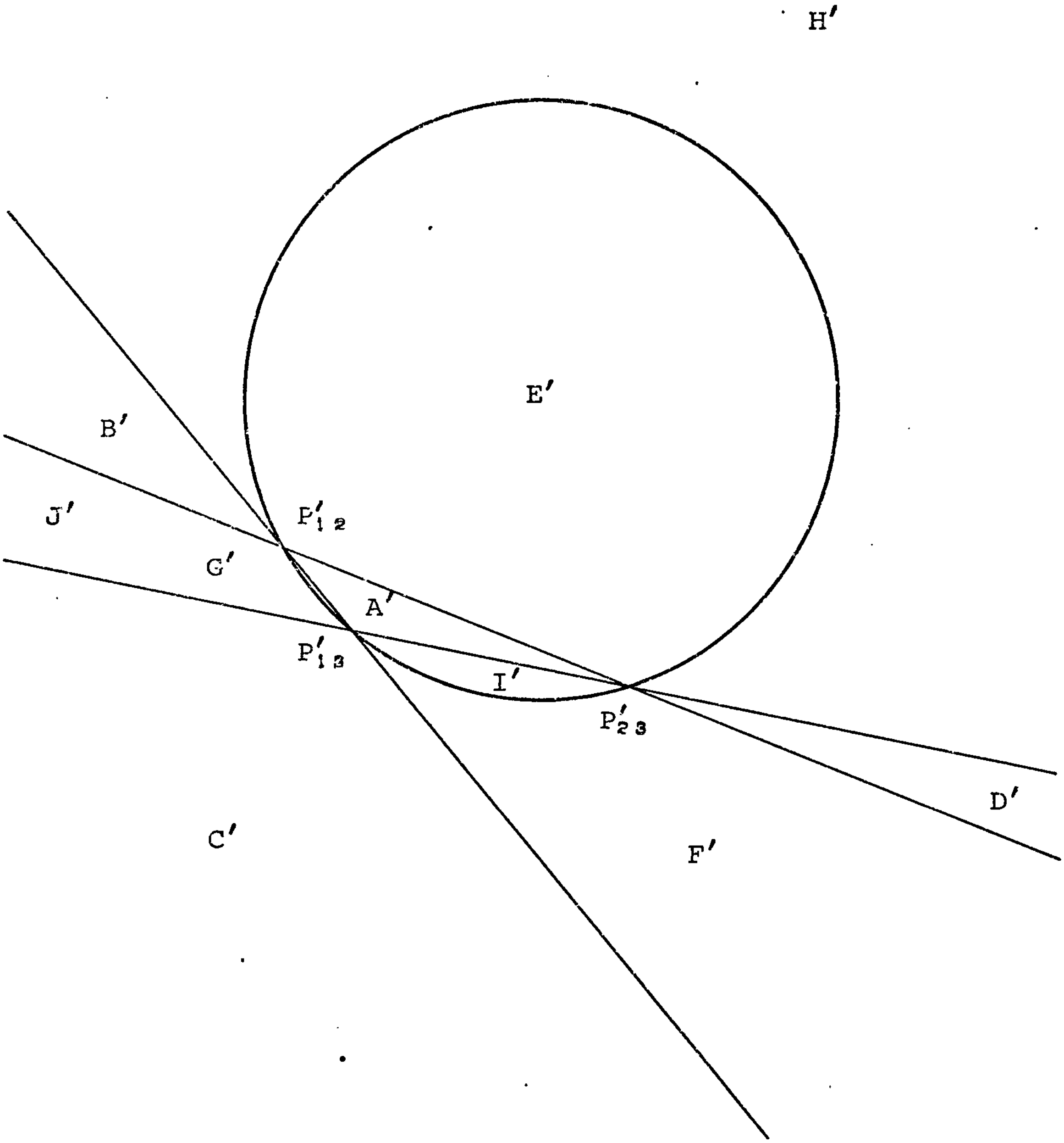

Regions of circle-point plane inside and outside of image pole circle

Fig. 5.2-3(b)

$P_{12}P_{23}$ which maps into P'_{13} and the line $P_{13}P_{23}$ which maps into P'_{12}. Also the diagram has the three poles at the corners of the area which map into the three lines $P'_{13}P'_{23}$, $P'_{12}P'_{23}$ and $P'_{12}P'_{13}$. Thus the area within the pole triangle maps into the area within the image pole triangle and is designated A′ in Figure 5.2-3(b). Area C is bounded by the pole circle which maps into a circle at infinity and the line $P_{12}P_{23}$ which maps into the image pole P'_{13}. The corners are poles P_{12} and P_{23} which map into lines $P'_{13}P'_{23}$ and $P'_{12}P'_{13}$. This area is designated by C′ in Figure 5.2-3(b). The remaining areas are found by the same method and are indicated in Figures 5.2-3(a) and 5.2-3(b), with the prime given to each corresponding area of the circle-point plane. Remember that the areas within the pole circle must give rotation of coupler relative to crank opposite to the sequence ijk or, in this case, 132. Thus the areas A′, B′, C′ and D′ will have sequence 132, while all the remaining areas will give sequence 123. The Q_{ij} points are the bounds for the regions of constant order.

Using the example in Chapter 3, the order and sequence for each segment of the circle-point curve may be determined by merely using the existing data in the manner just outlined. The region between Q_{12} and Q_{13} must have position 1 located between positions 2 and 3. Thus the order is either 1342 or 1243. Since this is one of the areas outside the pole circle, the order of positions 1, 2 and 3 has to be 123. Therefore the proper sequence is 1243. Now the remaining sequences on the closed loop branch may be determined by merely reversing the sequence of those positions which correspond to the subscripts of the Q_{ij} encountered as one proceeds along the curve. For the open branch segment note that the region between Q_{23} and Q_{24} lies in an area which corresponds to an area inside the pole circle so the sequence will be 132. Thus the sequence is 1324. The remaining segments are determined by the same method as for the closed loop branch except that the order is reversed at infinity rather than the Ball point as was the use in Chapter 3. Figure 5.2-4 shows the results of applying this method to the same example used in Section 3.3.

Comparison of Figures 3.3-3 and 5.2-4 shows that the segment of the circle-point curve bounded by Q_{34} and the Ball point is the only segment with the same order of rotation about both the fixed and moving pivots (1234 for this example). Also there are two segments for which the rotations about the fixed and moving pivots are opposed. One of these is the segment bounded by Q_{12} and P_{14}, for which the rotation of the crank relative to the base is 1234 and the rotation of the coupler relative to the crank is 1432. The other

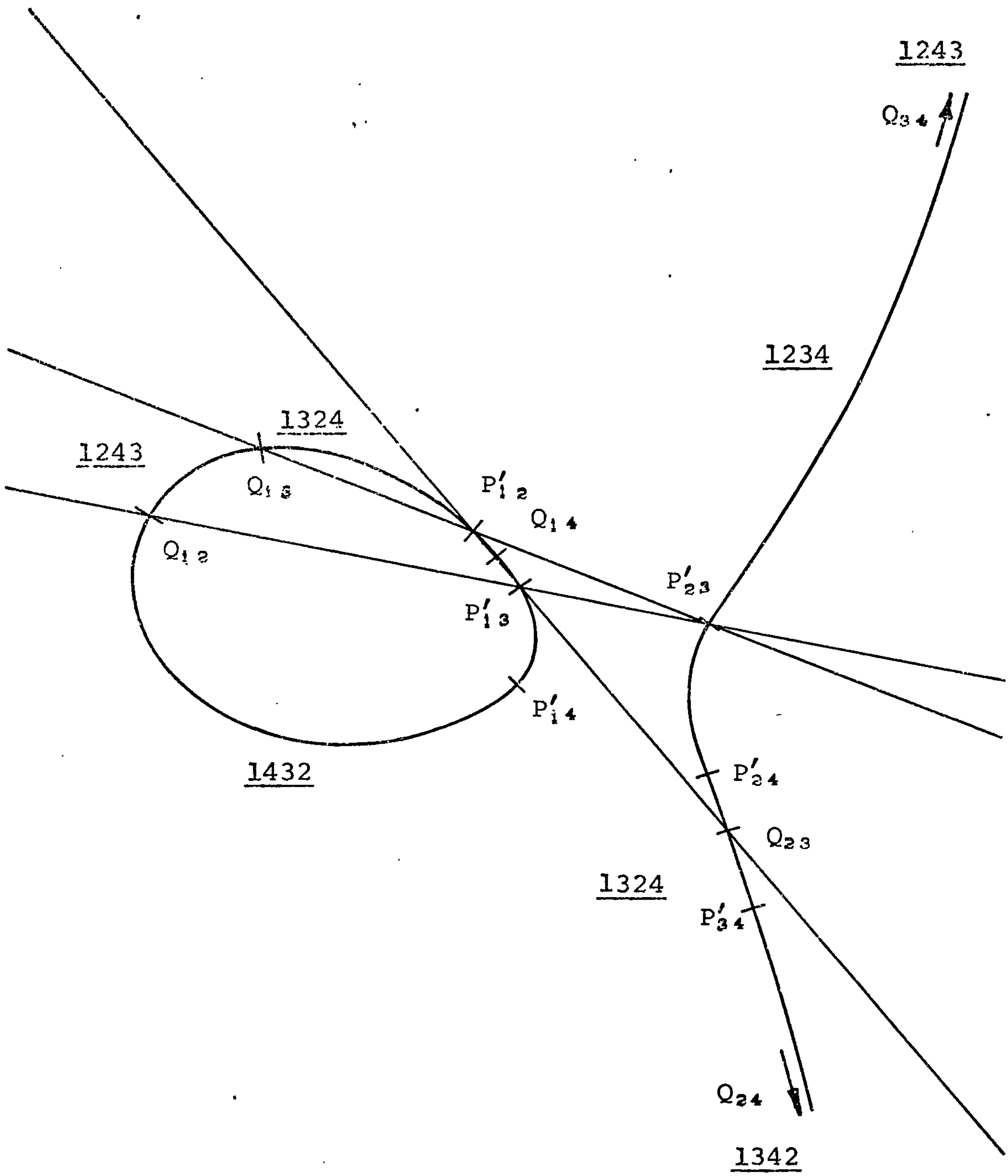

Order of rotation for each segment of circle-point curve

using inverted order solution

Fig. 5.2-4

segment is bounded by the Ball point and P'_{23} with the rotation of the crank relative to the base being 1432 and that of the coupler relative to the crank 1234. For a drag-link, the order of rotation of both cranks relative to the base must be the same, but the rotation of the coupler relative to each crank will vary. Thus the inversion of the order solution provides no new information relevant to the design of a drag-link mechanism. However, for the crank-rocker the rotation of the coupler relative to the driving crank must be opposite to the rotation of the driving crank relative to the base. Therefore for the crank-rocker the moving pivot of the driving crank must be chosen from one of the segments of the circle-point curve for which the orders of rotation about the two pivots are opposed. For the example given here, the only choices for the sequence of the driven crank rotation relative to the base are 1234 along segment Q_{12} to P_{14} and 1432 along segment P'_{23} to $\mathfrak{B}$. The inversion of the order solution has improved the design of the driving crank for a crank-rocker mechanism, since driving crank circle-points chosen anywhere else on the curve cannot possibly give crank-rocker solutions.

5.3 Inverted Branch Solution

As indicated in Section 4.2, the points T_{ij}, U_{ij} are the points on the circle-point curve for which the angular displacement ψ_{ij} of the coupler relative to the crank between positions i and j is 180^{0}. It was also shown that the points T_{ij}, U_{ij} either bound the segments of the curve for which ψ_{ij} is less than, or greater than 180^{0}, or lie on segments for which ψ_{ij} is greater than 180^{0}. Therefore, if the branch solution is inverted, the circle-point curve will be divided into segments for which the rotation of the base (coupler of the inverted linkage) relative to the crank, will be less than, or greater than 180^{0}. Combining the information from both the branch and inverted branch solutions gives an improvement in the design of crank-rockers over that provided by the branch solution as given in Chapter 4.

When the mechanism is inverted the angular displacement of the coupler relative to the crank between positions i and j is the angular displacement of the crank relative to the original base which is φ_{ij}. Since this angular displacement is 180^{0}, the solutions to the circle-point curve for which $\varphi_{ij} = 180^{0}$ need to be determined.

From Figure 2.1-6 which defines the angles θ, φ and ψ the relationship of these angles for the i^{th} position is

$$\theta_i = \varphi_i + \psi_i - \pi \tag{5.3-1}$$

and likewise for the j^{th} position

$$\theta_j = \varphi_j + \psi_j - \pi \tag{5.3-2}$$

The angular displacement for each of these angles between positions i and j (θ_{ij}, φ_{ij} and ψ_{ij}) is the difference between the j^{th} value and the i^{th} value. Thus subtracting equation (5.3-1) from equation (5.3-2) yields

$$\theta_{ij} = \varphi_{ij} + \psi_{ij} \tag{5.3-3}$$

Since θ_{ij} is the angular displacement of the coupler relative to the base between positions i and j, the values for θ_{ij} may be determined from the four design positions. With φ_{ij} = 180° the values for ψ_{ij} may now be determined from

$$\psi_{ij} = \theta_{ij} \mp \pi \tag{5.3-4}$$

The negative is used if θ_{ij} is positive and the positive for negative θ_{ij} such that $-\pi < \psi_{ij} \leq \pi$.

The circle-point curve is constructed graphically by using the two adjacent image pole pairs of an opposite image pole quadrilateral as chords of circles whose radii have the same ratio as that of the length of the lines joining the adjacent image poles [5-1]. This is illustrated in Figure 5.3-1 for the opposite image pole quadrilateral $P'_{12}P'_{23}P'_{34}P'_{14}$. The angle $P'_{12}C_2P'_{23}$ is equal to the angle $P'_{14}C_4P'_{34}$ since the two triangles formed by these same points are similar

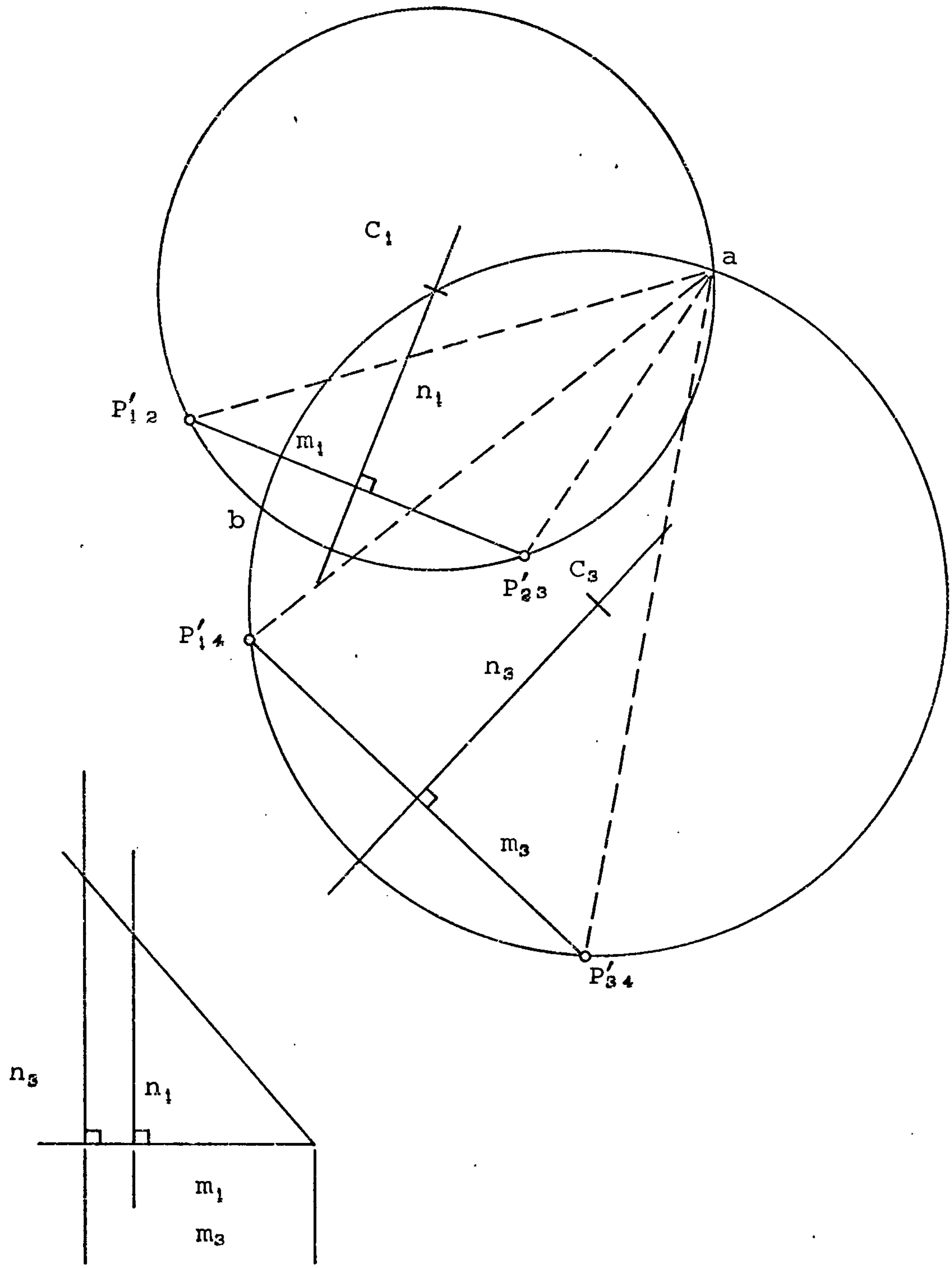

Graphical construction of circle-point curve using opposite image pole quadrilateral $P'_{12}P'_{23}P'_{34}P'_{14}$

Fig. 5.3-1

triangles. From Ref. [5-2] we get the following

$$\measuredangle P'_{14}aP'_{34} = \measuredangle P'_{14}bP'_{34} = \measuredangle P'_{12}aP'_{23} = \measuredangle P'_{12}bP'_{23} = \frac{\psi_{13}}{2} \quad (5.3\text{-}5)$$

However, from Euclidean plane geometry we know that the angle formed by using the chord of a circle with the circle center as the apex of that angle is twice the value of an angle using the same chord but with the apex any point on the circle. Thus

$$\measuredangle P'_{14}C_4P'_{34} = \measuredangle P'_{12}C_2P'_{23} = \psi_{13} \quad (5.3\text{-}6)$$

When ψ_{ij} is determined from equation (5.3-4) the two intersections (if they exist) are labelled T^*_{ij} and U^*_{ij}. Note that when $\psi_{ij} = 180°$ we get the points T_{ij}, U_{ij} since the chords joining the adjacent image poles then become the diameters of the circles. Thus all T^*_{ij} and U^*_{ij} points which exist may be located, up to a maximum of six pairs if all six pairs of circles intersect.

In the case of the T_{ij} and U_{ij} points we looked for the Q_{ij} points which bounded them and used their subscripts to determine the T_{ij} and U_{ij} points which formed the boundary between segments for which ψ_{ij} was greater than $180°$ and segments for which ψ_{ij} was less than $180°$. Section 4.2 indicated that the segments of constant rotation order, for the crank relative to the base or, in other words, the inverted linkage, are bounded by the image poles P'_{ij}. The procedure used in Section 4.2 to determine those segments of the circle-point curve where ψ_{ij} is less than 180° is used here to determine the segments where φ_{ij} is less than 180° for the inverted linkage.

Figure 5.3-2 shows all T^*_{ij} and U^*_{ij} points which exist. For the closed branch portion of the curve all U^*_{ij} points are bounded by P'_{13} and P'_{14} with order of either 1324 or 1423. Thus the subscripts for U^*_{ij} which represent boundaries between regions on which the angular range is greater than or less than 180° would be 13, 23, 24 and 14. The subscripts of U^*_{ij} which lie on segments for which the angular range is greater than 180° would be 12 and 34. Thus the segment of the circle-point curve on which U^*_{12} lies has an angular range greater than 180° and U^*_{13} and U^*_{14} mark the limits of this segment. For the open branch segment all T^*_{ij} points lie between P'_{23} and P'_{34}, thus the sequence is either 1234 or 1432. The subscripts for T^*_{ij} where the range is greater than or less than 180° are 12, 23, 34 and 14, and for the range greater than 180° the subscripts are 13 and 24. Therefore the segment of the curve on which T^*_{13} lies has an angular range greater than 180° and T^*_{12} and T^*_{14} are the limits of this segment. The regions for which the angular displacements of the crank relative to the base are less than 180° are indicated on Figure 5.3-3 by the solid lines.

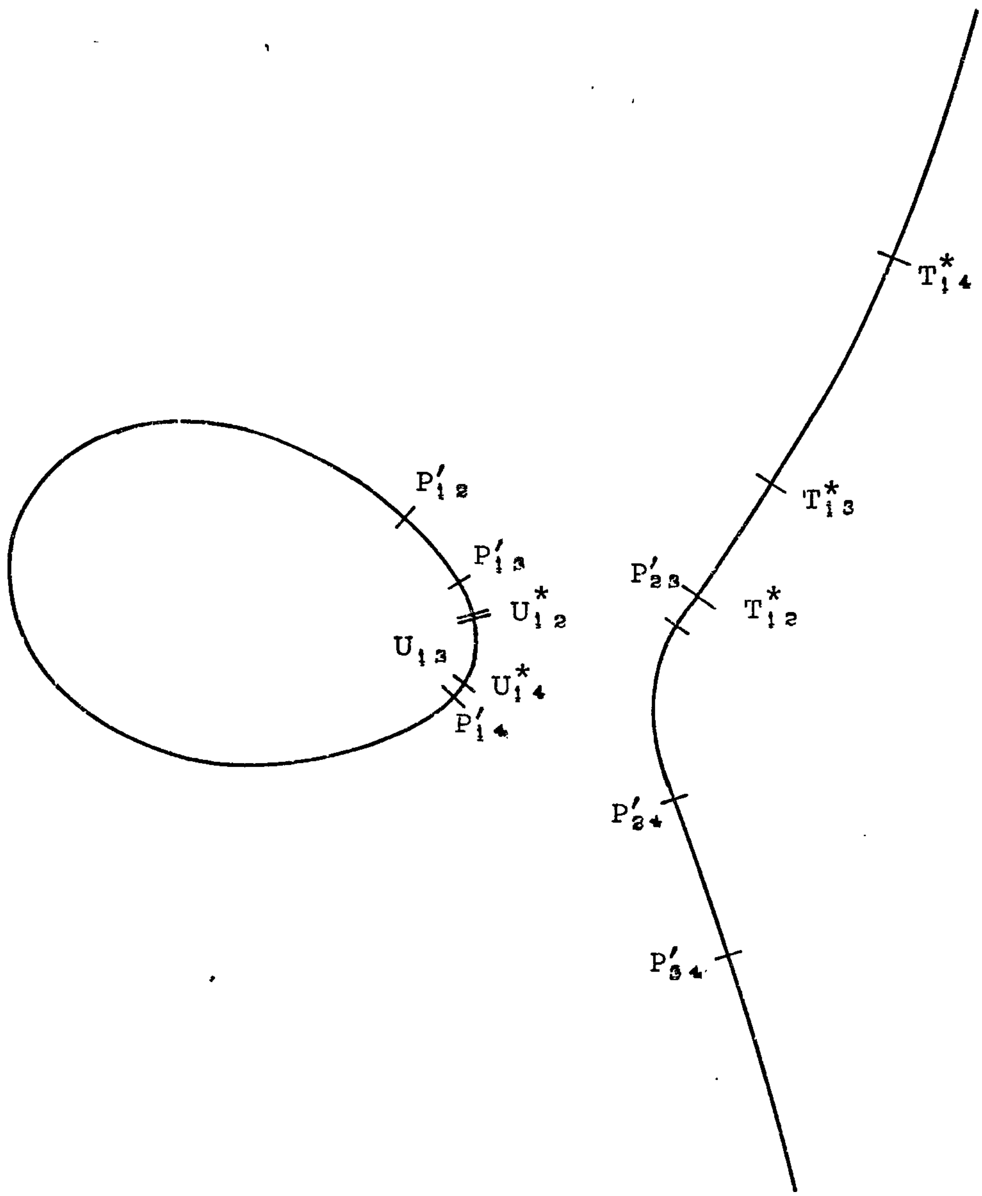

Circle-point curve with P'_{ij}, T^*_{ij}, and U^*_{ij} points used for inverted branch mapping

Fig. 5.3-2

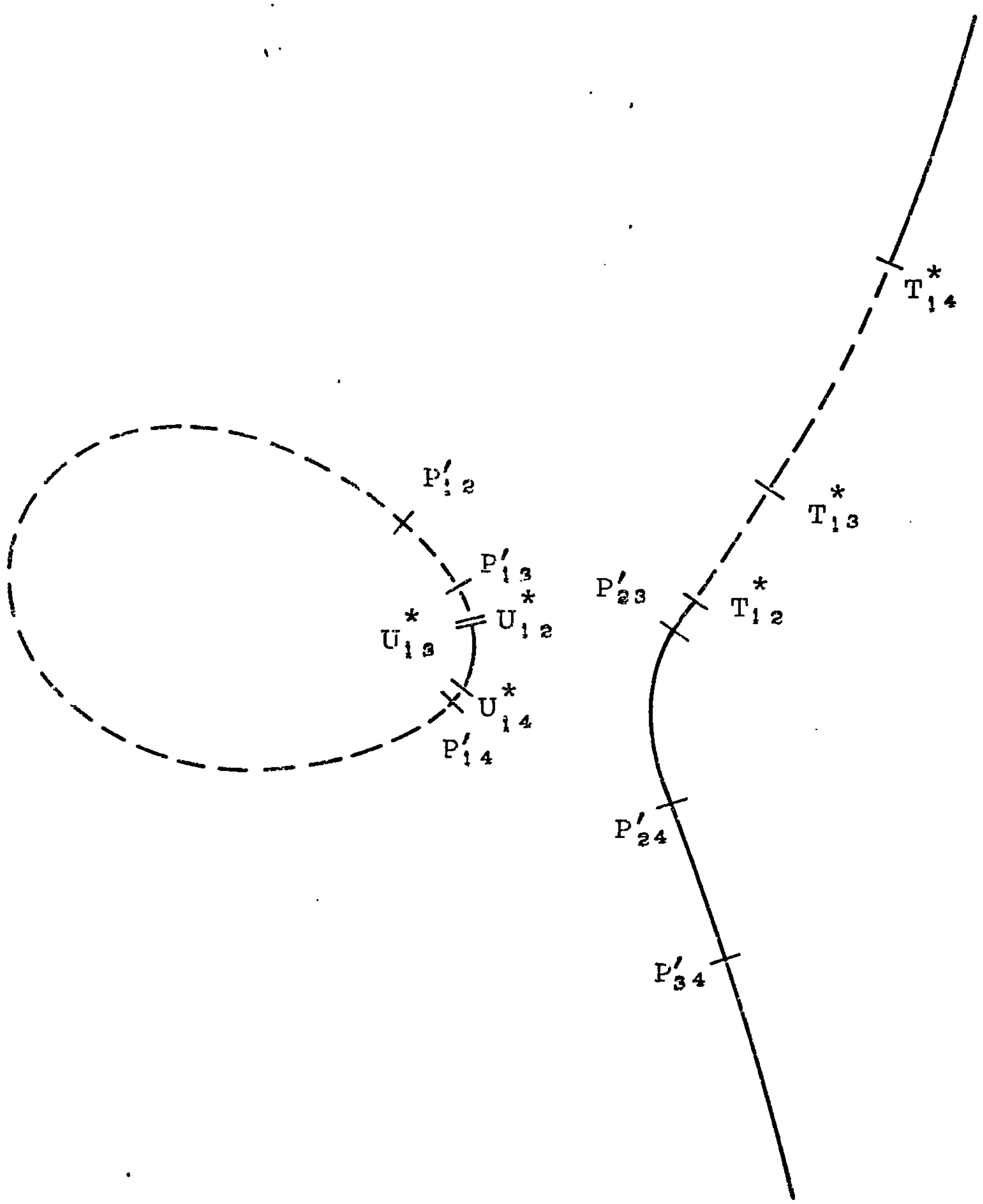

Regions of circle-point curve for $\varphi_{ij} < 180^\circ$

(solid lines)

Fig. 5.3-3

When designing a crank-rocker mechanism the rotation of the driven crank (rocker) relative to the base must be less than 180°. While the rotation of the driven crank relative to the coupler must also be less than 180° in order to satisfy the branch condition. Thus the driven crank moving pivot must be chosen from the segment of the circle-point curve which is solid on both Figures 4.3-2 and 5.3-3. Figure 5.3-4 shows the segments of the circle-point curve, which are satisfied by both these conditions, as the solid segments of the curve.

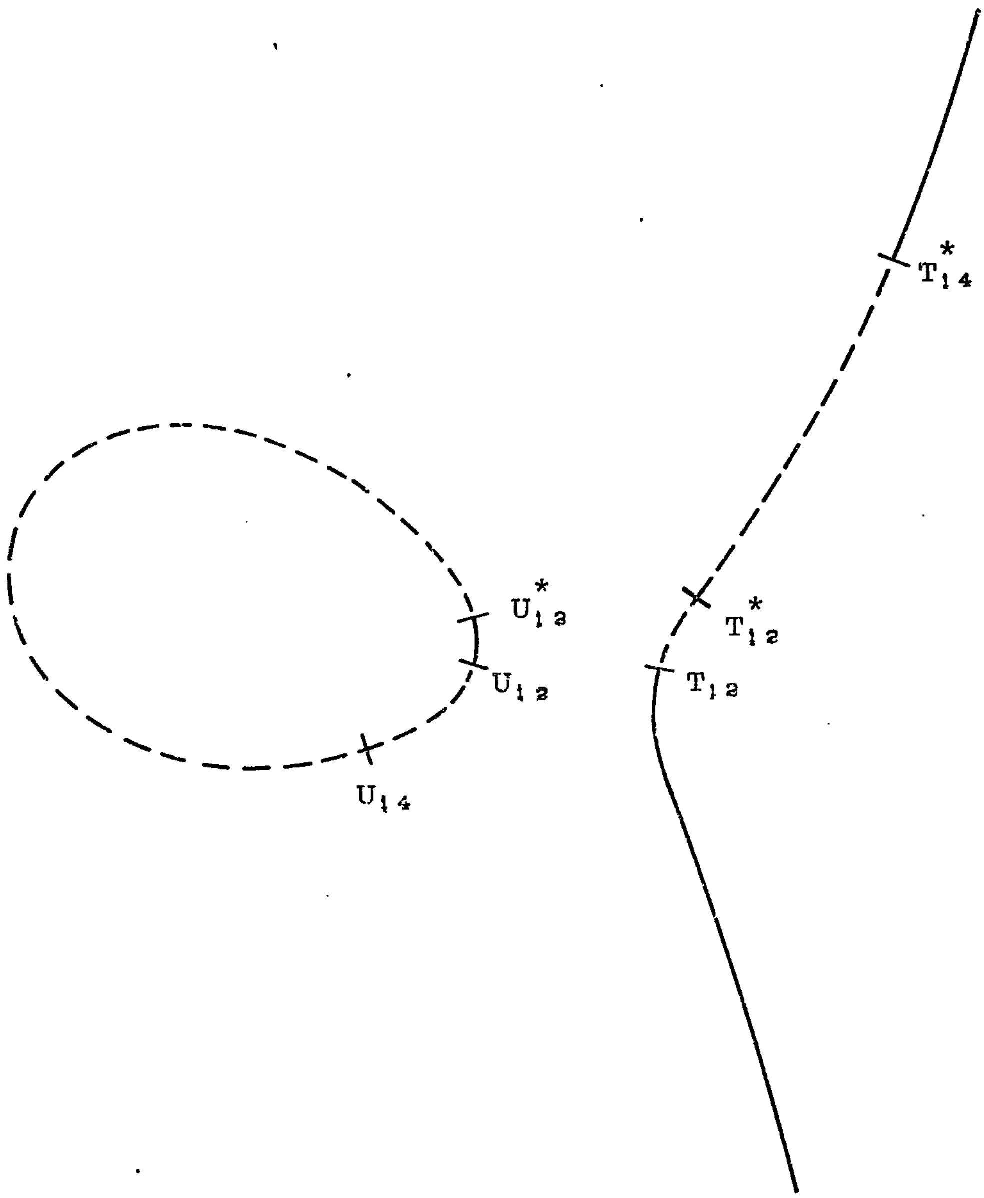

Regions of circle-point curve satisfying both

$\psi_{ij} < 180°$ and $\varphi_{ij} < 180°$ (solid lines)

Fig. 5.3-4

CHAPTER 6

CONCLUSIONS

6.1 Introduction

The techniques developed in Chapters 3, 4 and 5 provide a valuable aid to the designer of four-bar linkages. In Chapter 1 it was shown that the range of the angle between the coupler and the driven crank must be less than 180° to prevent the mechanism from getting into the branch transition position. Strictly speaking, this only applies to linkages in which the driving crank is able to make a full rotation relative to the base. Hence, these techniques apply to only the drag-link and crank-rocker type of mechanisms. However, in most applications of the four-bar linkage it is desirable, if not required, that the input crank be connected to a continuously rotating device such as a motor. Therefore these techniques will be used to first design a drag-link mechanism; and then, a crank-rocker. Also the direction and order of rotation for the driving crank will be specified for both linkages.

6.2 Solution of Drag-Link Mechanism

As indicated in Chapter 5, the inverted order and branch solutions provide no new information for designing a drag-link over that presented in Chapters 3 and 4. A drag-link mechanism is to be designed to move a lamina through four design positions in the order 1234 when driven by a clockwise rotating crank. Thus both cranks must rotate completely in the clockwise direction with order 1234. From Figure 4.3-2 both moving pivots must be chosen from those regions indicated by the solid line and which have order of 1234 as indicated in Figure 3.3-3. The regions which satisfy these conditions are indicated by the solid lines in Figure 6.2-1. Point X_1 is chosen as the driven crank circle-point on the segment $Q_{13}P'_{12}$ with extreme positions of the rotational range being 2 and 4. Figure 6.2-2 shows the location of the corresponding center-point X* and the Filemon lines for the extreme positions 2 and 4 [6-1, 6-2]. Point Y_1 is chosen as driving crank circle-point on the segment $Q_{12}U_{14}$ mapped in Figure 3.3-3 as giving order 1234 and lying outside the region excluded by the Filemon construction. Figure 6.2-3 shows the solution linkage. A check on Grashof's rules [6-3] indicates that the inequality is satisfied. Thus the mechanism is a drag-link, as desired, since the base is the shortest link. Also, Figure 6.2-3 indicates that the clockwise order is 1234, as required.

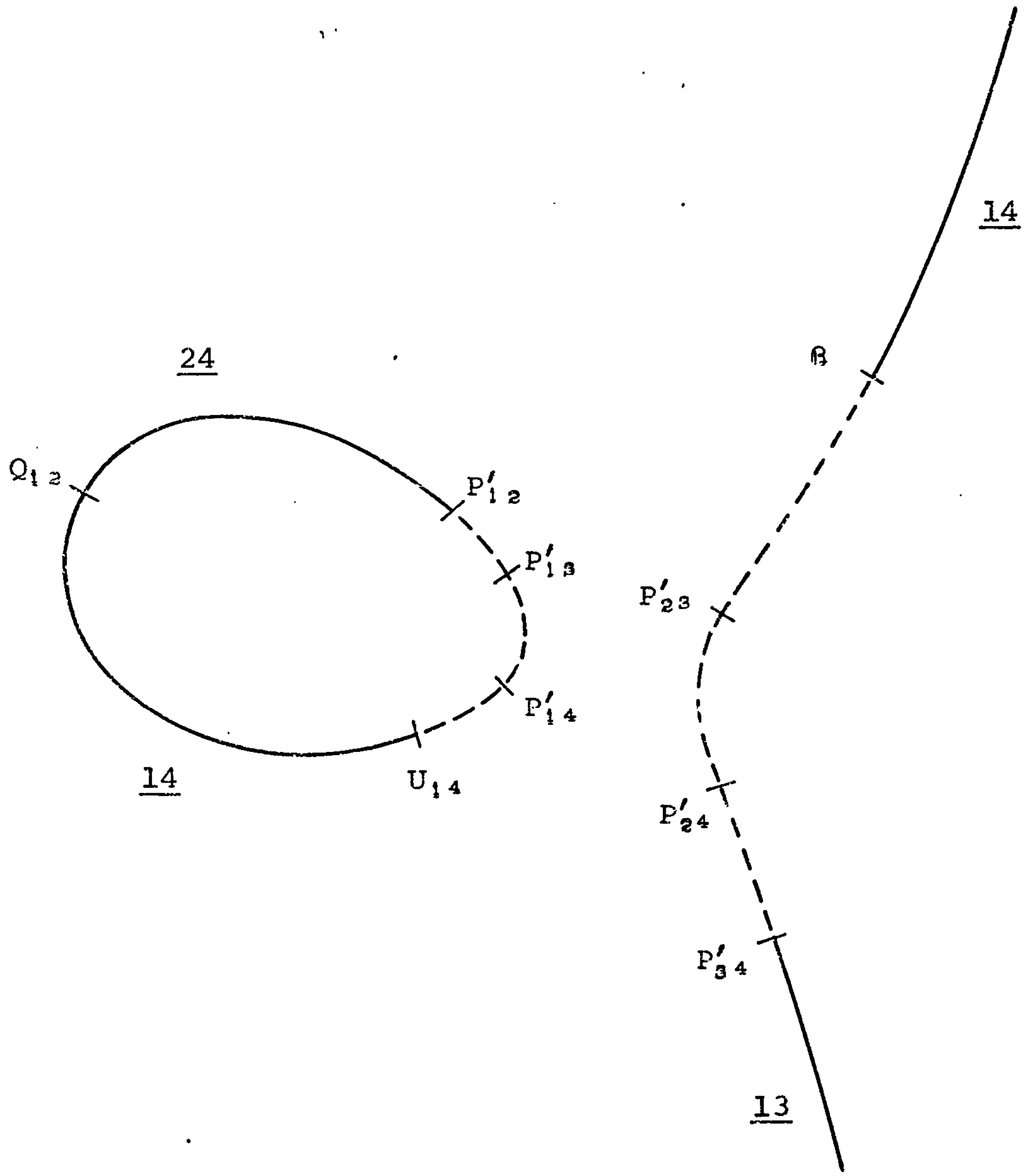

Regions of circle-point curve for $\psi_{ij} < 180^{\circ}$ and order 1234 (solid lines), and extreme positions for those segments

Fig. 6.2-1

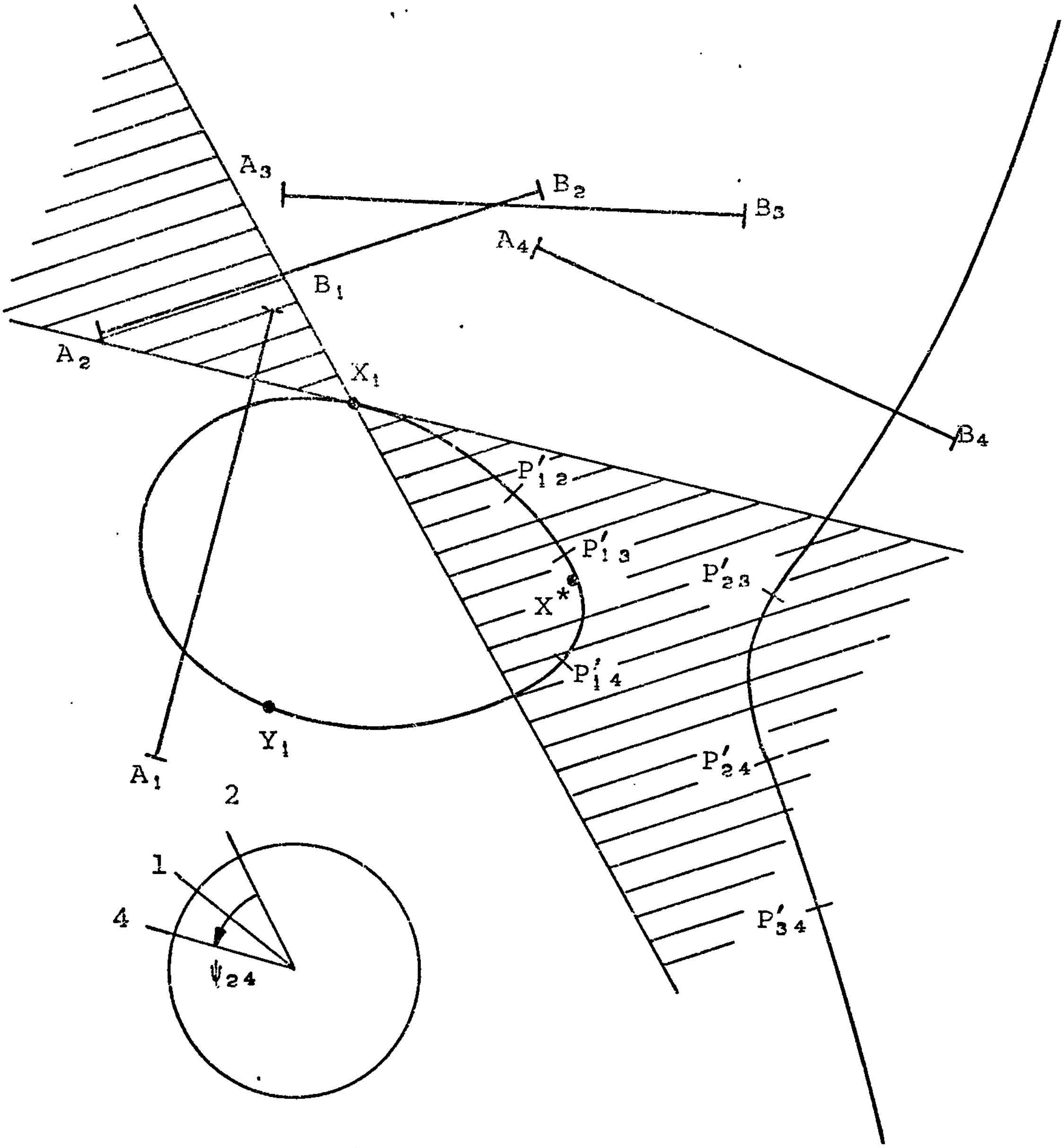

Filemon construction for driven-crank X_1X^* with Y_1 as circle-point for driving crank

Fig. 6.2-2

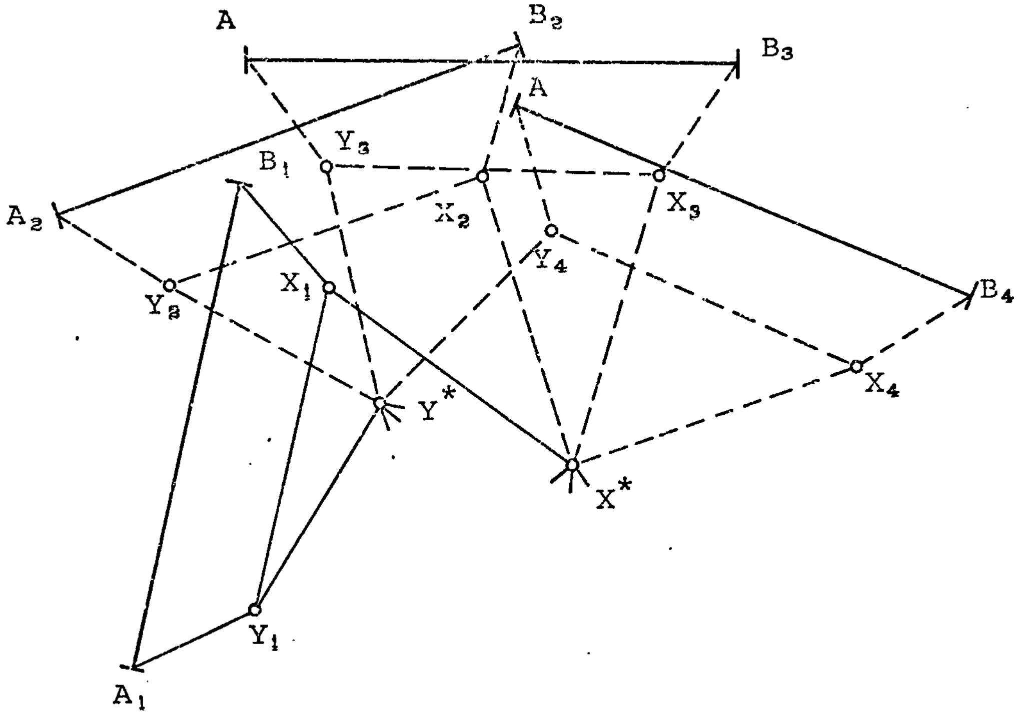

Solution linkage with clockwise order 1234.

Fig. 6.2-3

6.3 Solution of Crank-Rocker Mechanism

If the previous example is used to design a crank-rocker mechanism, one finds that there are no solutions. All solutions either have a Grashof problem, or the driving crank is longer than the driven crank resulting in a double-rocker mechanism. Thus another example will be used to demonstrate the design of a crank-rocker mechanism. For this example the mechanism is to move a lamina through four design positions in a clockwise order of 1342. Figure 6.3-1 shows the design positions, the image poles, Q_{ij}'s, image pole circle (for ijk being 134) and the order of rotation within each segment. Figure 6.3-2 indicates the results of the inverted order problem. Those regions marked by (143) are the mapping of the regions inside the pole circle for poles P_{13}, P_{14} and P_{34}. Since the order must be 1342, then it must be 1243 on Figure 6.3-2. The region which satisfies these conditions is bounded by Q_{34} and Q_{13}. Thus the driving crank circle-point must be chosen from within this region. Figure 6.3-3 shows the results of the order solution with $\psi_{ij} < 180°$ along the solid lines. Likewise, Figure 6.3-4 indicates by the solid lines those regions on which $\varphi_{ij} < 180°$ for the inverted branch solution. As indicated in Section 5.3 the driven crank rotation relative to both the base and the coupler must be less than 180°. The segments of the circle-point curve which satisfy these

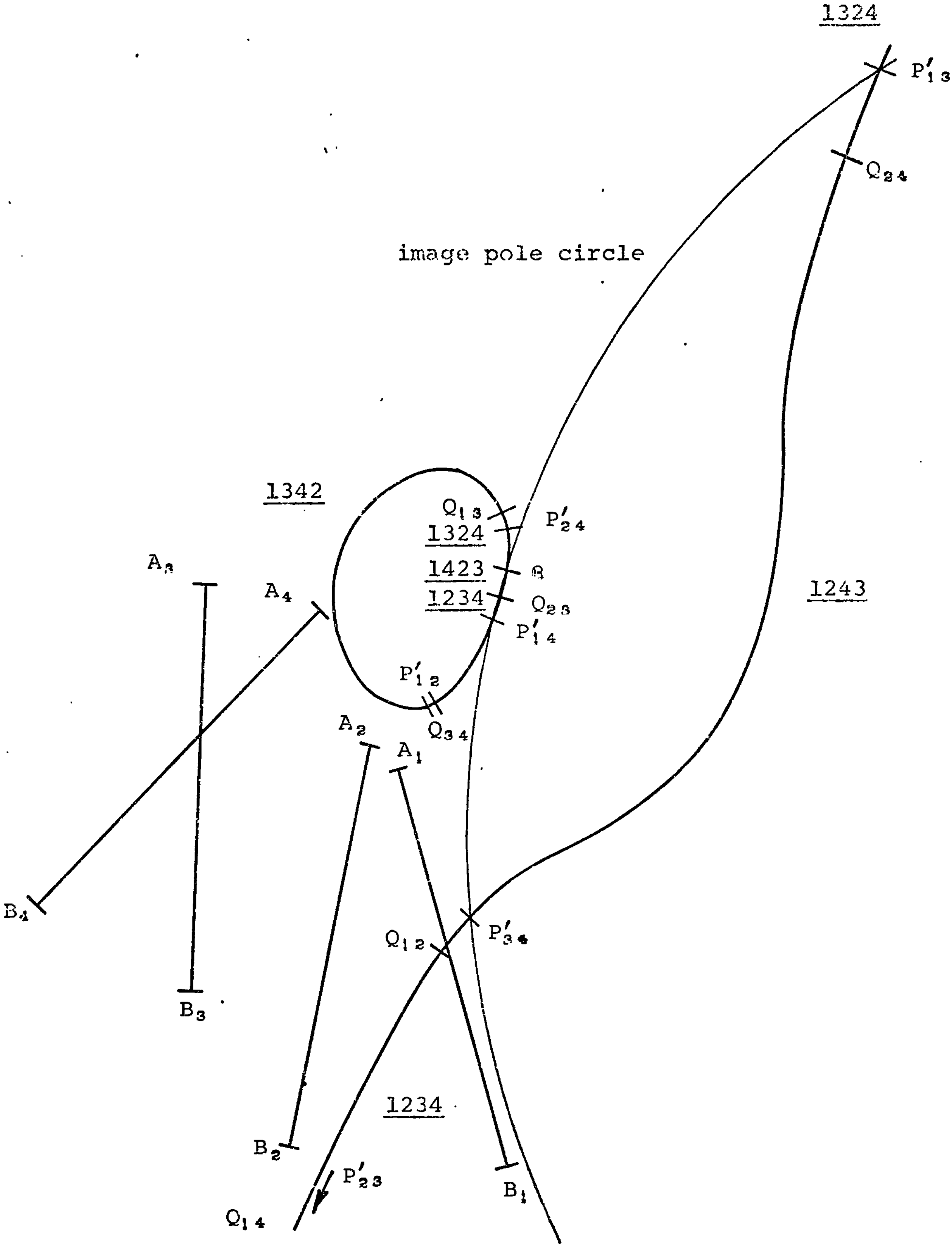

Example for crank-rocker linkage showing design positions, P'_{ij}'s, Q_{ij}'s, image pole circle and order or rotation

Fig. 6.3-1

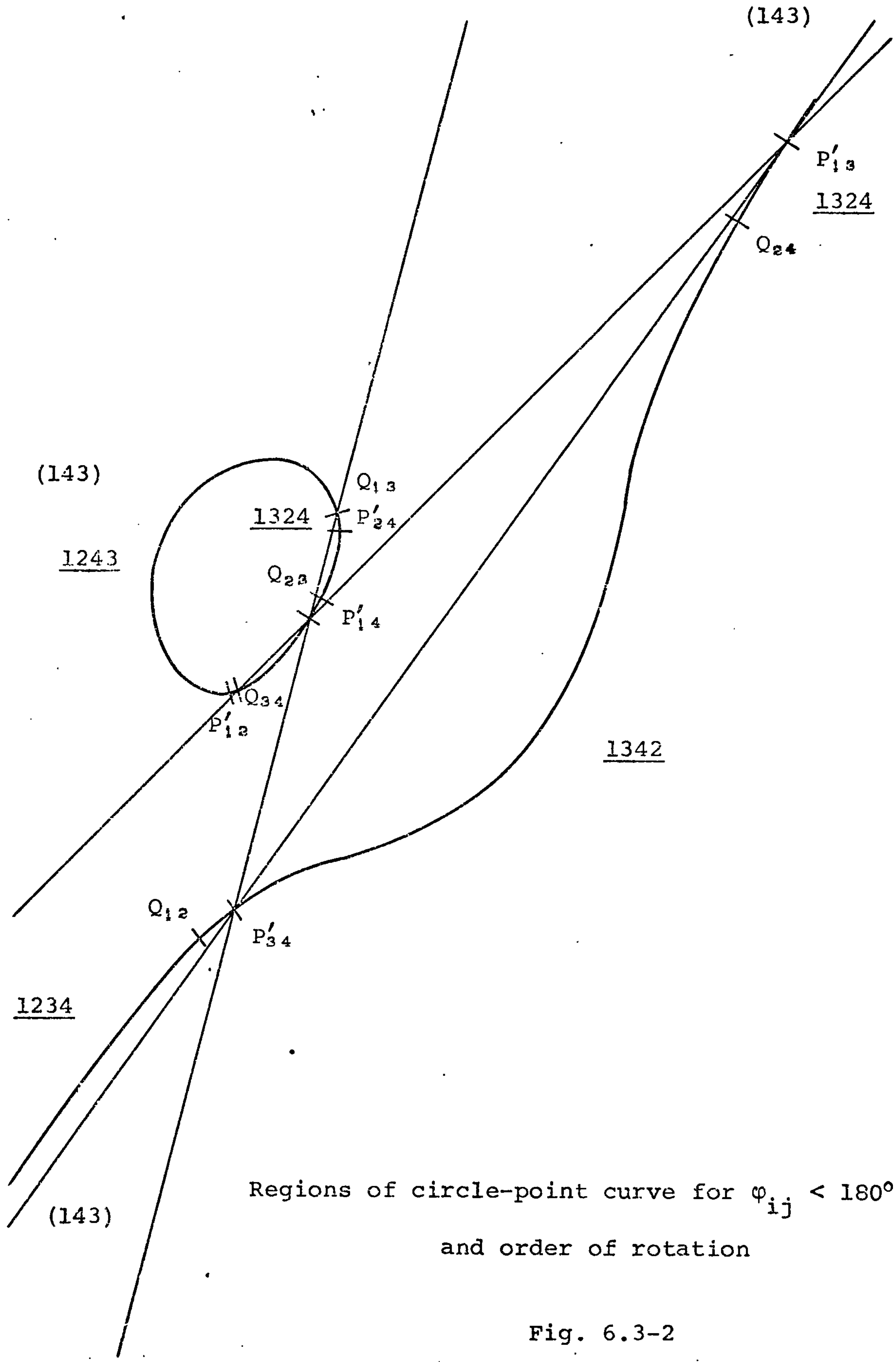

Regions of circle-point curve for $\varphi_{ij} < 180°$

and order of rotation

Fig. 6.3-2

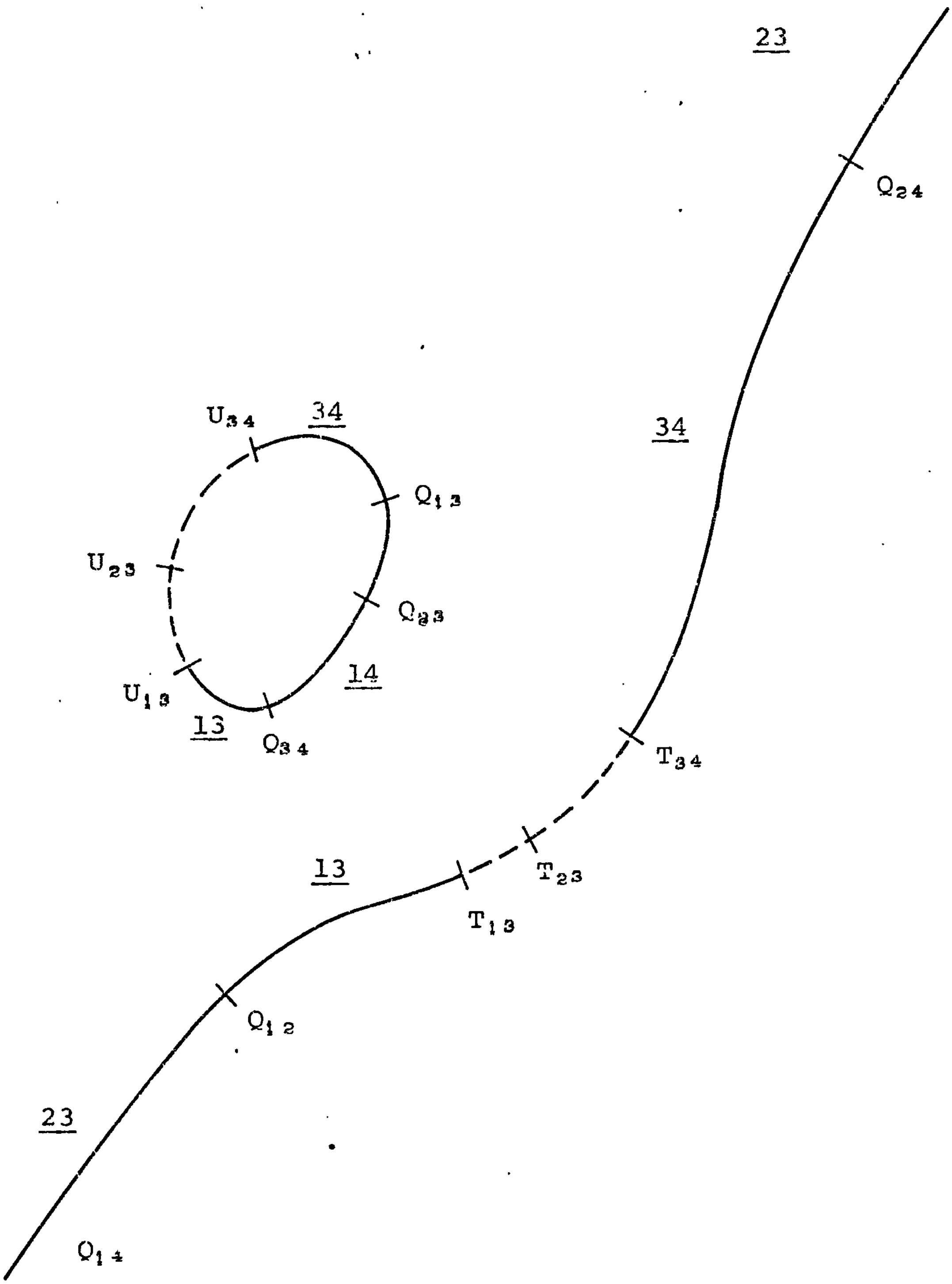

Regions of circle-point curve for $\psi_{ij} < 180^\circ$ (solid lines) and extreme positions

Fig. 6.3-3

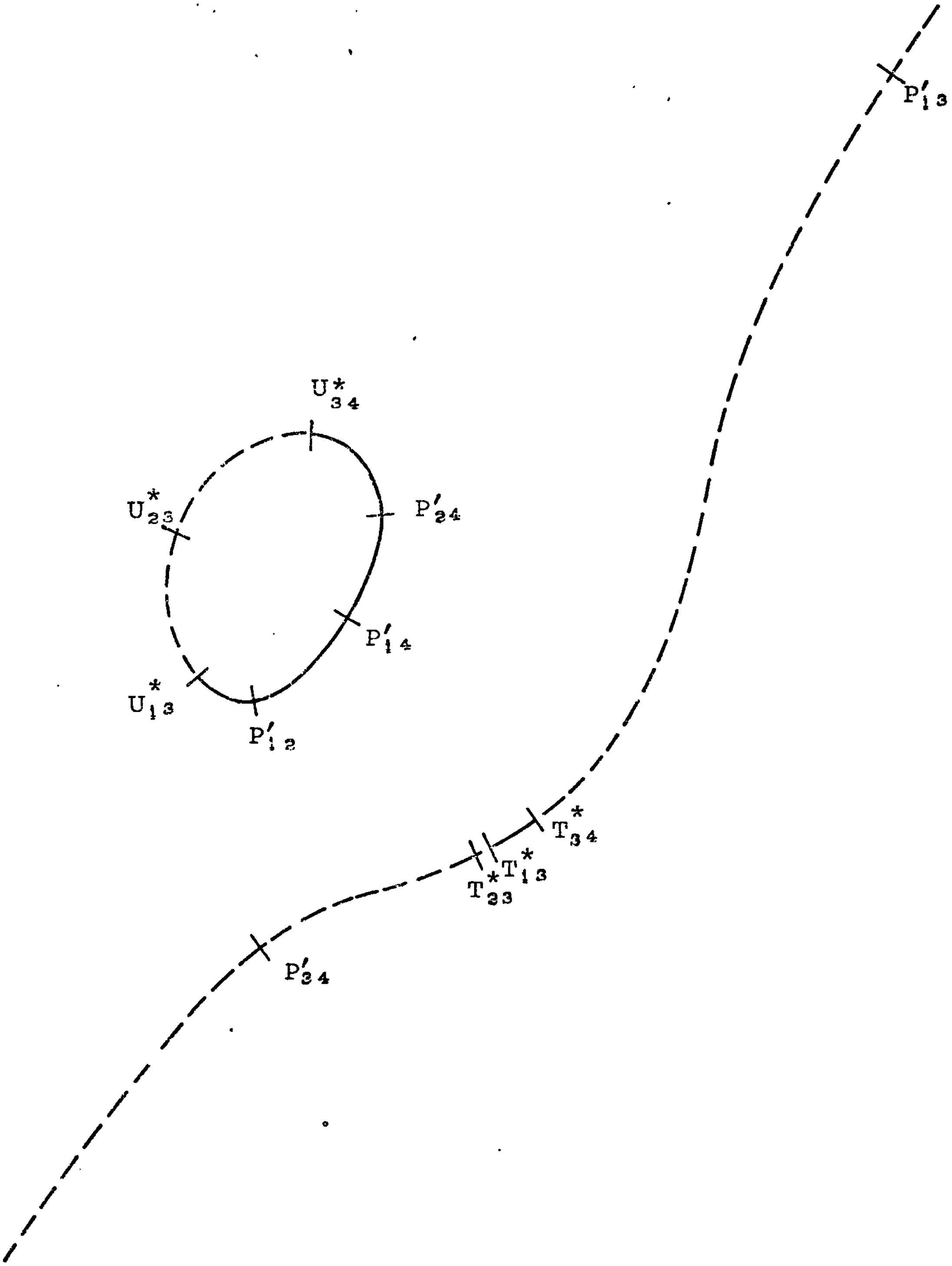

Regions of circle-point curve for $\varphi_{ij} < 180°$ (solid lines)

Fig. 6.3-4

conditions are indicated in Figure 6.3-5 by the solid line. Point V_1 is chosen as the driven crank circle-point on segment $Q_{13}U^*_{34}$ with extreme positions being 3 and 4. Figure 6.3-6 shows the corresponding center-point V* and the extreme position lines. The driving crank circle-point is chosen from that portion of the segment bounded by Q_{34} and Q_{13} which lies outside the region excluded by the Filemon construction. Figure 6.3 7 shows the solution linkage after W* is found. Since Grashof's inequality is satisfied, the mechanism is a crank-rocker, as desired, with clockwise order of 1342.

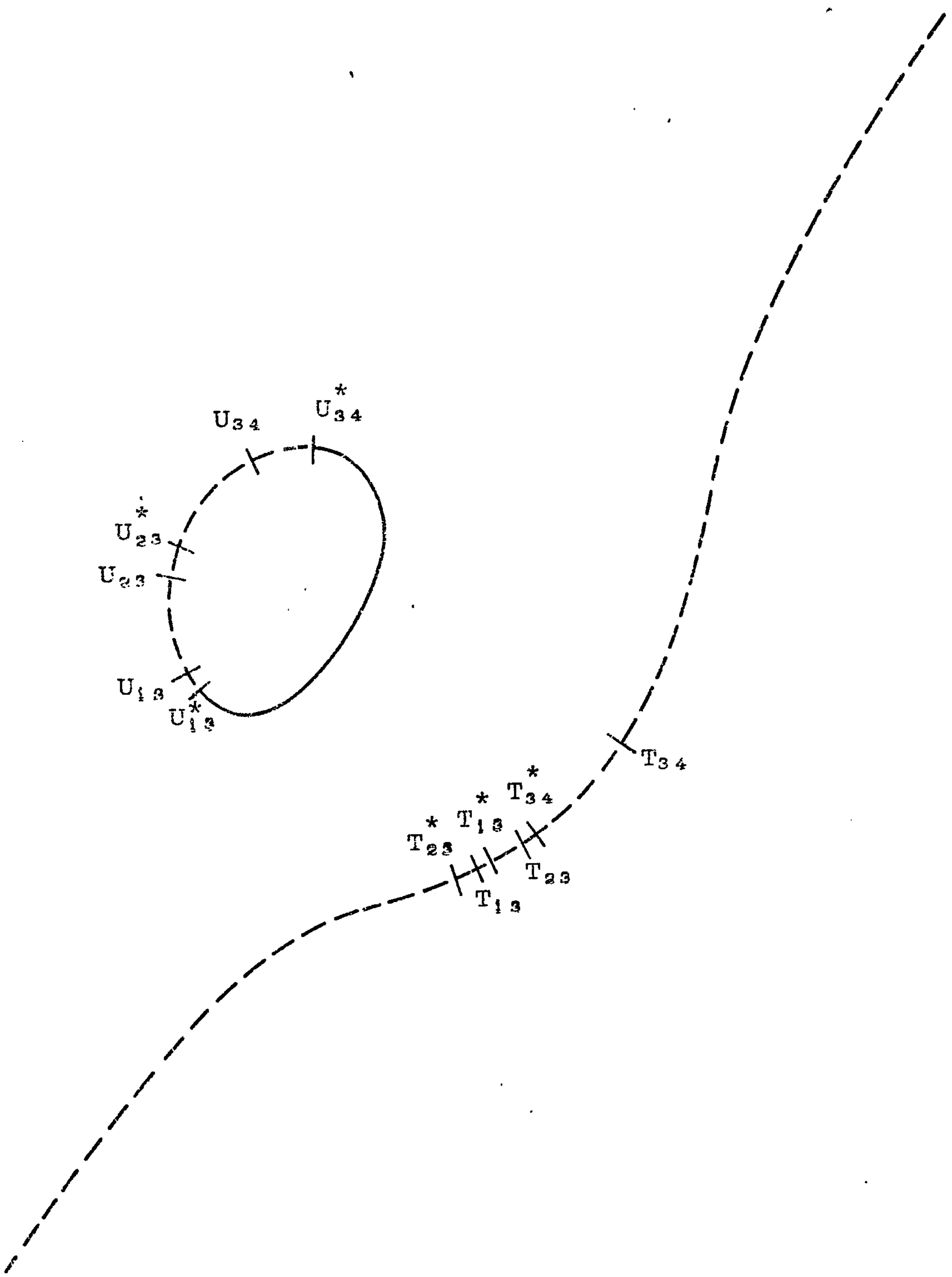

Regions of circle-point curve satisfying both $\psi_{ij} < 180^\circ$ and $\varphi_{ij} < 180^\circ$ (solid lines)

Fig. 6.3-5

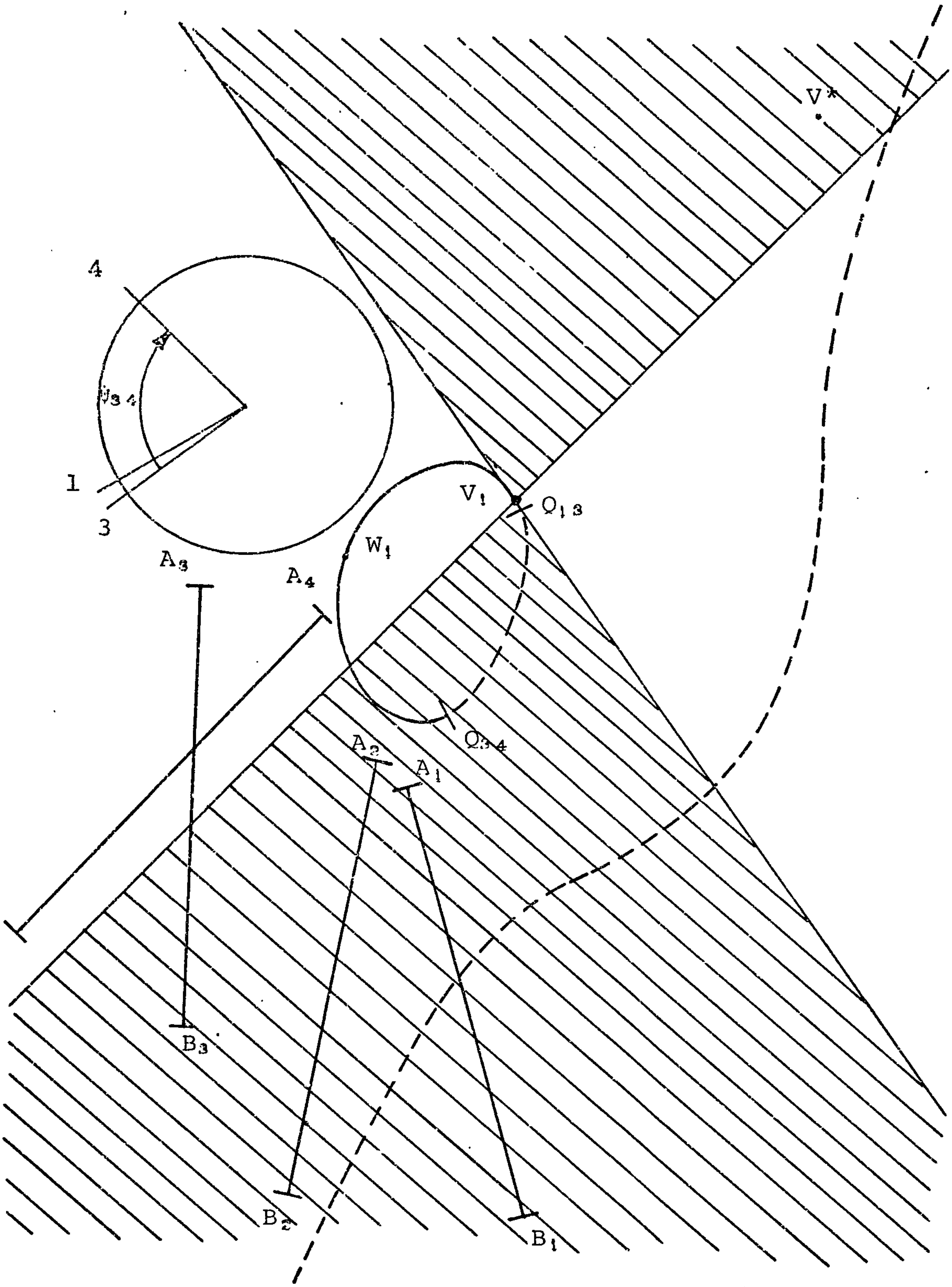

Filemon construction for driven crank V_1V^* with W_1 being the driving crank circle-point

Fig. 6.3-6

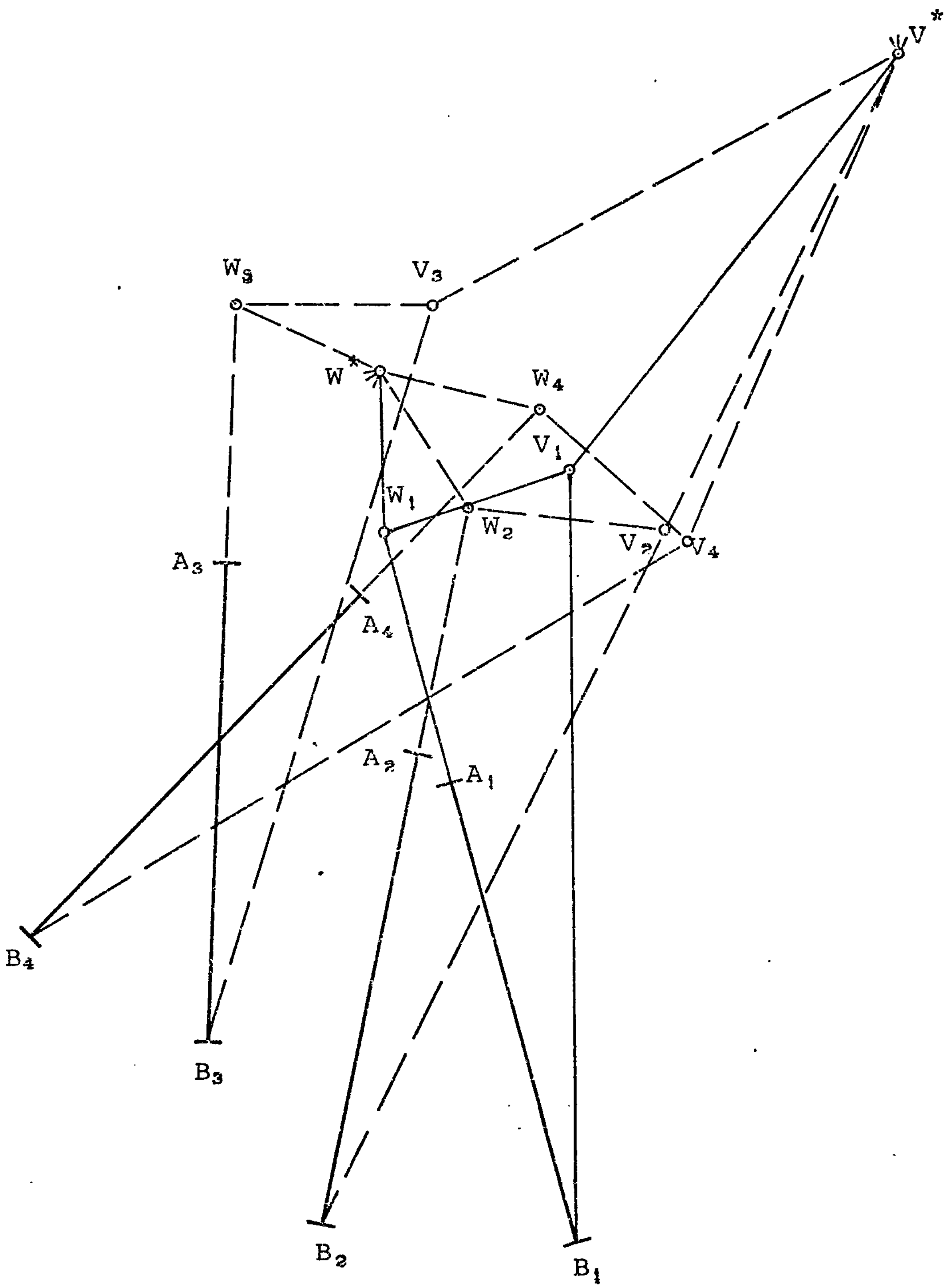

Solution linkage with clockwise order 1342

Fig. 6.3-7

6.4 Statement of Contributions

Because the contribution of this dissertation are intermingled with existing ideas and methods, this section has been added to state the contributions made by this study. The contributions will be stated in the order in which they are presented within the text.

The first contribution is in Chapter 2 regarding the solution to the circle-point curve. Although no new method of solution is presented, an exact generation of the circle-point curve as developed in this dissertation has not been previously published. Instead, most designers have used an approximate solution by means of Newton-Raphson method.

The second contribution comes in Chapter 3 where a new method is presented which makes possible the determination of the order on all segments of the circle-point curve for a given sense of rotation. This method is good for both single and double branch circle-point curves. This eliminates the need to plot the four positions of any point on the closed branch segment in order to determine the order for all segments of the closed branch segment as required by earlier methods. The data required for this new method is the same as was needed for the previous method, namely, P'_{ij}, Q_{ij} and β. Construction of the image pole circle is the only new requirement in this method.

The third contribution is found in Chapter 4 where a new method is presented for solving the branch problem. This method again makes use of the same data required by the previous branch solution, P'_{ij}, Q_{ij}, T_{ij}, U_{ij}. An inspection of the subscripts of points on the curve replaces the cumbersome technique of tabulating the 6 angular displacements ψ_{ij} of the coupler relative to the driven crank as the linkage moves between design positions.

The new methods presented in Chapters 3 and 4 make possible the next two contributions which are found in Chapter 5. Upon invertion of the mechanism the new order and branch solutions may be applied to further improve the design of crank-rocker mechanisms as presented in Sections 5.2 and 5.3.

Therefore the design of drag-link mechanisms is simplified by use of the new order and branch solutions while the design of crank-rockers is not only simplified but improved by means of the inverted order and inverted branch solutions.

APPENDIX A

NUMERICAL ALGORITHM

A.1 Input Data

The only input data required for this program are the coordinates of each end of the line segment representing the rigid body in all four design positions. The data does not have to be presented such that the first design position of end A is at the origin of the coordinate system. The necessary transformation and rotation of the given axes is performed within the program to accomplish this. In addition to the four design positions, it is necessary to input the starting value of the abscissa for the rotated axes, u, and the incremental change, Δu, in this value. The starting value of u must be negative with the increment being positive. The following page shows the input cards for this program.

Input Data for Double Branch Curve

initial

u	Δu
-10.0	1.0

x		y
37.7	(B4)	27.8
13.0	(A4)	32.0
23.5	(B3)	36.5
-1.0	(A3)	31.2
12.3	(B2)	35.0
-8.7	(A2)	21.5
0.0	(B1)	25.0
0.0	(A1)	0.0

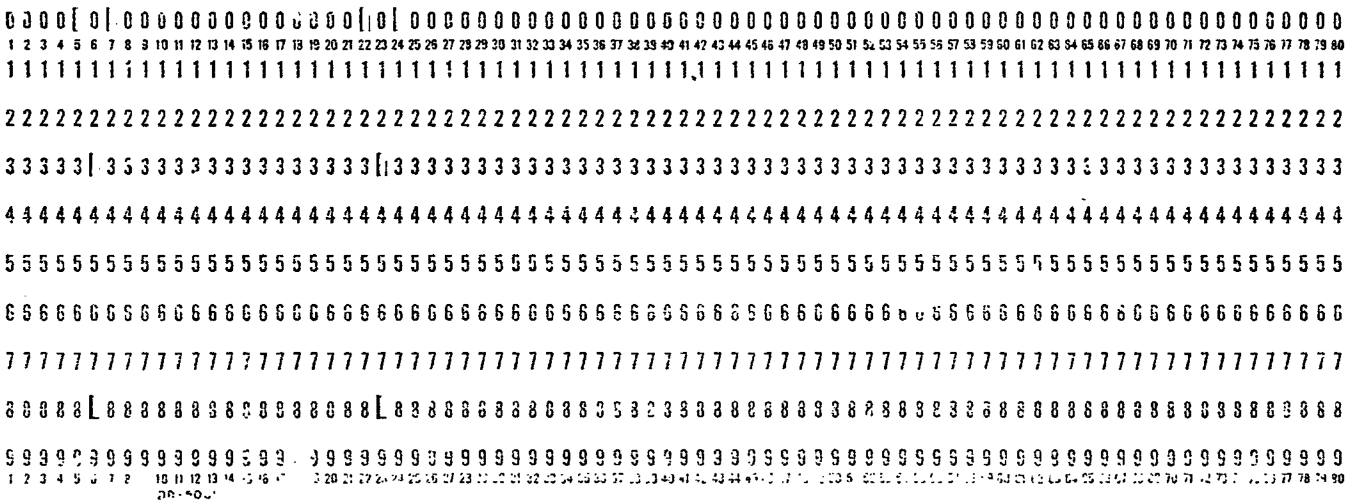

Input Data for Single Branch Curve

initial u	Δu
-10.0	0.5

x		y
13.400	(B4)	-1.898
5.800	(A4)	0.600
4.100	(B3)	-1.356
2.800	(A3)	-9.250
8.300	(B2)	0.784
0.800	(A2)	-2.000
11.000	(B1)	0.000
3.000	(A1)	0.000

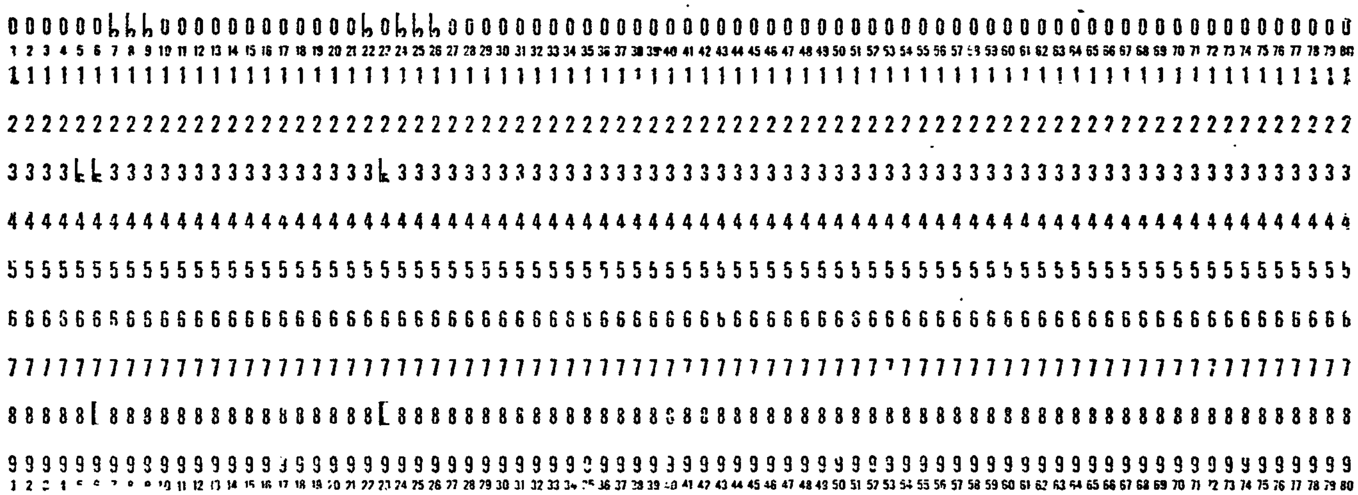

A.2 Algorithm for Determination of Circle-Point Curve and Special Points on That Curve

The following pages present the computer program which translates and rotates the input data to generate the circle-point curve and all the special points on that curve as described in Chapter 2 used in the various methods presented in this dissertation.

```
C
C
C
C
C      THIS PROGRAM FINDS THE SOLUTIONS TO THE CIRCLE-POINT
C      EQUATION, (AX+BY)(X**2+Y**2)+C(X*Y)+D(X**2)+E(Y**2)
C      +FX+GY+H=0, FOR 4 DESIGN POSITIONS.  THE AXES ARE
C      ALIGNED WITH THE FIRST DESIGN POSITION AND THEN THEY ARE
C      ROTATED SO THE ASYMPTOTE IS PARALLEL TO THE ABCISSA.
C      IN ADDITION TO THE CURVE THE PROGRAM COMPUTES THE LOCATION
C      OF THE IMAGE POLES P'(IJ),Q(IJ),T(IJ),U(IJ),
C      TSTAR(IJ), AND USTAR(IJ).
C
C
C
       DIMENSION A(20,20),B(20,20)
       DIMENSION THETA(5),THETAD(5)
       DIMENSION THETA1(4,4),THETA1D(4,4)
       DIMENSION PP(4,4),QQ(4,4)
       DIMENSION AP(4),AQ(4),BP(4),BQ(4)
       DIMENSION PIMGX(4,4),PIMGY(4,4)
       DIMENSION SLOPEK(4,4),SLOPEL(4,4)
       DIMENSION QINCPK(4,4),QINCPL(4,4)
       DIMENSION QX(4,4),QY(4,4)
       DIMENSION MTEST(4,4),NTEST(4,4)
       DIMENSION TX(4,4),TY(4,4),UX(4,4),UY(4,4)
       DIMENSION TSTRX(4,4),TSTRY(4,4),USTRX(4,4),USTRY(4,4)
       DIMENSION A1(4),B1(4),C1(4),D1(4),E1(4)
       DIMENSION AMATX(3,3),BMATX(3,3)
       DIMENSION C1MATX(3,3),C2MATX(3,3),C3MATX(3,3),C4MATX(3,3)
       DIMENSION D1MATX(3,3),D2MATX(3,3),D3MATX(3,3)
       DIMENSION E1MATX(3,3),E2MATX(3,3),E3MATX(3,3)
       DIMENSION F1MATX(3,3),F2MATX(3,3),F3MATX(3,3)
       DIMENSION G1MATX(3,3),G2MATX(3,3),G3MATX(3,3),H1MATX(3,3)
       DIMENSION AU(4),BU(4),AV(4),BV(4)
       DIMENSION PIMGU(4,4),PIMGV(4,4)
       DIMENSION QU(4,4),QV(4,4)
       DIMENSION TU(4,4),TV(4,4),UU(4,4),UV(4,4)
       DIMENSION TSTRU(4,4),TSTRV(4,4),USTRU(4,4),USTRV(4,4)
       DIMENSION U1(250),V1(250)
       DIMENSION U11(250),U12(250),U13(250)
       DIMENSION V11(250),V12(250),V13(250)
       DIMENSION U2(250),V2(250)
     7 CONTINUE
       PI=3.141592654
C
C    READ IN DESIGN POSITIONS  (A'S AND B'S)
C
       DO 10 I=1,4
       READ(5,100,END=600)(A(I,J),J=1,2)
       READ(5,100)(B(I,J),J=1,2)
   100 FORMAT(2F20.3)
```

```
   10 CONTINUE
C
C      CHECK A'S AND B'S
C
       WRITE(6,1000)
 1000  FORMAT(///,40X,'DESIGN POSITIONS (X,Y)',/)
       WRITE(6,1005)
 1005  FORMAT(50X,'X',9X,'Y',/)
       DO 20I=1,4
       WRITE(6,1010)I,(A(I,J),J=1,2)
       WRITE(6,1020)I,(B(I,J),J=1,2)
 1010  FORMAT (40X,'A',I1,'= ',2F10.4)
 1020  FORMAT (40X,'B',I1,'= ',2F10.4)
   20  CONTINUE
       AX1=A(1,1)
       AY1=A(1,2)
       BX1=B(1,1)
       BY1=B(1,2)
C
C    CALCULATING THETA(1) THROUGH THETA(4)
C
       DO 30 I=1,4
       DELY=B(I,2)-A(I,2)
       DELX=B(I,1)-A(I,1)
       IF(DELX)801,802,801
  802  THETA(I)=1.570796327
       GO TO 8
  801  THETA(I)=ATAN((DELY)/(DELX))
    8  CONTINUE
   30  CONTINUE
       THETAD(1)=((THETA(1))*180.)/PI
       WRITE(6,1040) THETAD(1)
 1040  FORMAT (/,40X,'THETA(1)= ',F10.4,//)
C
C      CALCULATING THETA(IJ)
C
       DO 35 I=1,3
       JK=I+1
       DO 36 J=JK,4
       THETA1(I,J)= THETA(J)-THETA(I)
       THETA1D(I,J)=((THETA1(I,J))*180.)/PI
       THETA1(J,I)=THETA1(I,J)
       WRITE (6,1055)(I,J,THETA1D(I,J))
 1055  FORMAT (40X,'THETA(',I1,I1,')= ',F10.4)
   36  CONTINUE
   35  CONTINUE
C
C      P AND Q ARE THE ABCISSA AND ORDINATE, RESPECTIVELY,OF THE
C      AXES ALIGNED WITH THE FIRST DESIGN POSITION USING A1
C      AS THE ORIGIN.
C
C
```

```
C      DESIGN POSITIONS IN P-Q AXES
C
       WRITE (6,2010)
  2010 FORMAT (///,40X,'DESIGN POSITIONS (P,Q)',/)
       WRITE (6,2020)
  2020 FORMAT (50X,'P',10X,'Q',/)
       DO 48 I=1,4
       AP(I)=(COS(THETA(1)))*(A(I,1)-AX1)+(SIN(THETA(1)))*
      1(A(I,2)-AY1)
       AQ(I)=(-SIN(THETA(1)))*(A(I,1)-AX1)+(COS(THETA(1)))*
      1(A(I,2)-AY1)
       BP(I)=(COS(THETA(1)))*(B(I,1)-AX1)+(SIN(THETA(1)))*
      1(B(I,2)-AY1)
       BQ(I)=(-SIN(THETA(1)))*(B(I,1)-AX1)+(COS(THETA(1)))*
      1(B(I,2)-AY1)
    48 CONTINUE
       DO 49 I=1,4
       WRITE (6,2030)(I,AP(I),AQ(I))
       WRITE (6,2040)(I,BP(I),BQ(I))
  2030 FORMAT (40X,'A',I1,'= ',F10.4,1X,F10.4)
  2040 FORMAT (40X,'B',I1,'= ',F10.4,1X,F10.4,/)
    49 CONTINUE
C
C      CALCULATION OF IMAGE POLES IN P-Q AXES
C
       THETA1(1,1)=0.
       WRITE (6,2041)
  2041 FORMAT (///,40X,'IMAGE POLES IN P-Q AXES',/,51X,'P',13X,'Q',/)
       DO 55 I=1,3
       JK=I+1
       DO 56 J=JK,4
       PP(I,J)=AP(J)-AP(I)
       QQ(I,J)=AQ(J)-AQ(I)
       PIMGX(I,J)=((COS(THETA1(1,I))-COS(THETA1(1,J)))*(PP(I,J))
      1+(SIN(THETA1(1,I))-SIN(THETA1(1,J)))*(QQ(I,J)))/
      2(2.*(1.-COS(THETA1(I,J))))
       PIMGY(I,J)=((-SIN(THETA1(1,I))+SIN(THETA1(1,J)))*(PP(I,J))
      1+(COS(THETA1(1,I))-COS(THETA1(1,J)))*(QQ(I,J)))/
      2(2.*(1.-COS(THETA1(I,J))))
       WRITE (6,2042)(I,J,PIMGX(I,J),PIMGY(I,J))
  2042 FORMAT(40X,'P',I1,I1,'= ',F10.4,4X,F10.4,/)
       PIMGX(J,I)=PIMGX(I,J)
       PIMGY(J,I)=PIMGY(I,J)
    56 CONTINUE
    55 CONTINUE
C
C      CALCULATION OF Q(IJ) IN P-Q AXES WHERE Q(IJ) IS THE
C      INTERSECTION OF THE LINES FORMED BY P'(IK)--P'(JK) AND
C      P'(IL)--P'(JL).  THE SLOPE IS DENOTED BY SLOPEK OR SLOPEL
C      AND THE Q INTERCEPT BY QINCPK OR QINCPL.
C
       CALL QXQY(1,2,3,4,PIMGX,PIMGY,SLP1,QIN1,SLP2,QIN2,QQX,QQY)
```

```
      SLOPEK(1,2)=SLP1
      QINCPK(1,2)=QIN1
      SLOPEL(1,2)=SLP2
      QINCPL(1,2)=QIN2
      QX(1,2)=QQX
      QY(1,2)=QQY
      CALL QXQY(1,3,2,4,PIMGX,PIMGY,SLP1,QIN1,SLP2,QIN2,QQX,QQY)
      SLOPEK(1,3)=SLP1
      QINCPK(1,3)=QIN1
      SLOPEL(1,3)=SLP2
      QINCPL(1,3)=QIN2
      QX(1,3)=QQX
      QY(1,3)=QQY
      CALL QXQY(1,4,2,3,PIMGX,PIMGY,SLP1,QIN1,SLP2,QIN2,QQX,QQY)
      SLOPEK(1,4)=SLP1
      QINCPK(1,4)=QIN1
      SLOPEL(1,4)=SLP2
      QINCPL(1,4)=QIN2
      QX(1,4)=QQX
      QY(1,4)=QQY
      CALL QXQY(2,3,1,4,PIMGX,PIMGY,SLP1,QIN1,SLP2,QIN2,QQX,QQY)
      SLOPEK(2,3)=SLP1
      QINCPK(2,3)=QIN1
      SLOPEL(2,3)=SLP2
      QINCPL(2,3)=QIN2
      QX(2,3)=QQX
      QY(2,3)=QQY
      CALL QXQY(2,4,1,3,PIMGX,PIMGY,SLP1,QIN1,SLP2,QIN2,QQX,QQY)
      SLOPEK(2,4)=SLP1
      QINCPK(2,4)=QIN1
      SLOPEL(2,4)=SLP2
      QINCPL(2,4)=QIN2
      QY(2,4)=QQY
      QX(2,4)=QQX
      CALL QXQY(3,4,1,2,PIMGX,PIMGY,SLP1,QIN1,SLP2,QIN2,QQX,QQY)
      SLOPEK(3,4)=SLP1
      QINCPK(3,4)=QIN1
      SLOPEL(3,4)=SLP2
      QINCPL(3,4)=QIN2
      QX(3,4)=QQX
      QY(3,4)=QQY
      DO 65 I=1,3
      JK=I+1
      DO 66 J=JK,4
      SLOPEK(J,I)=SLOPEK(I,J)
      QINCPK(J,I)=QINCPK(I,J)
      SLOPEL(J,I)=SLOPEL(I,J)
      QINCPL(J,I)=QINCPL(I,J)
      QX(J,I)=QX(I,J)
      QY(J,I)=QY(I,J)
   66 CONTINUE
   65 CONTINUE
```

```
C
C     CALCULATION OF T(IJ) AND U(IJ) WHICH ARE THE INTERSECTIONS
C     --IF THEY EXIST-- OF CIRCLES USING IMAGE POLES
C     P'(IK)--P'(JK) AND P'(IL)--P'(JL) AS DIAMETERS.
C
      CALL CIRIN1(1,2,3,4,PIMGX,PIMGY,MM,X1,Y1,X2,Y2)
      MTEST(1,2)=MM
      TX(1,2)=X1
      TY(1,2)=Y1
      UX(1,2)=X2
      UY(1,2)=Y2
      CALL CIRIN1(1,3,2,4,PIMGX,PIMGY,MM,X1,Y1,X2,Y2)
      MTEST(1,3)=MM
      TX(1,3)=X1
      TY(1,3)=Y1
      UX(1,3)=X2
      UY(1,3)=Y2
      CALL CIRIN1(1,4,2,3,PIMGX,PIMGY,MM,X1,Y1,X2,Y2)
      MTEST(1,4)=MM
      TX(1,4)=X1
      TY(1,4)=Y1
      UX(1,4)=X2
      UY(1,4)=Y2
      CALL CIRIN1(2,3,1,4,PIMGX,PIMGY,MM,X1,Y1,X2,Y2)
      MTEST(2,3)=MM
      TX(2,3)=X1
      TY(2,3)=Y1
      UX(2,3)=X2
      UY(2,3)=Y2
      CALL CIRIN1(2,4,1,3,PIMGX,PIMGY,MM,X1,Y1,X2,Y2)
      MTEST(2,4)=MM
      TX(2,4)=X1
      TY(2,4)=Y1
      UX(2,4)=X2
      UY(2,4)=Y2
      CALL CIRIN1(3,4,1,2,PIMGX,PIMGY,MM,X1,Y1,X2,Y2)
      MTEST(3,4)=MM
      TX(3,4)=X1
      TY(3,4)=Y1
      UX(3,4)=X2
      UY(3,4)=Y2
      DO 57 I=1,3
      JK=I+1
      DO 58 J=JK,4
      MTEST(J,I)=MTEST(I,J)
      TX(J,I)=TX(I,J)
      TY(J,I)=TY(I,J)
      UX(J,I)=UX(I,J)
      UY(J,I)=UY(I,J)
   58 CONTINUE
   57 CONTINUE
C
```

```
C     CALCULATION OF TSTAR(IJ) AND USTAR(IJ) WHICH ARE --IF THEY
C     EXIST-- THE INTERSECTIONS OF TWO CIRCLES ON WHICH
C     P'(IK), P'(JK) AND P'(IL),P'(IL) LIE SUCH THAT THE  ANGLE
C     WHICH THE TWO IMAGE POLES MAKE WITH THEIR RESPECTIVE
C     CENTERS IS PSI(IJ).
C
      CALL TUSTR (1,2,3,4,THETA1,SLOPEK,SLOPEL,PIMGX,PIMGY,
     1NN,XK1,YK1,XL1,YL1)
      NTEST(1,2)=NN
      TSTRX(1,2)=XK1
      TSTRY(1,2)=YK1
      USTRX(1,2)=XL1
      USTRY(1,2)=YL1
      CALL TUSTR (1,3,2,4,THETA1,SLOPEK,SLOPEL,PIMGX,PIMGY,
     1NN,XK1,YK1,XL1,YL1)
      NTEST(1,3)=NN
      TSTRX(1,3)=XK1
      TSTRY(1,3)=YK1
      USTRX(1,3)=XL1
      USTRY(1,3)=YL1
      CALL TUSTR (1,4,2,3,THETA1,SLOPEK,SLOPEL,PIMGX,PIMGY,
     1NN,XK1,YK1,XL1,YL1)
      NTEST(1,4)=NN
      TSTRX(1,4)=XK1
      TSTRY(1,4)=YK1
      USTRX(1,4)=XL1
      USTRY(1,4)=YL1
      CALL TUSTR (2,3,1,4,THETA1,SLOPEK,SLOPEL,PIMGX,PIMGY,
     1NN,XK1,YK1,XL1,YL1)
      NTEST(2,3)=NN
      TSTRX(2,3)=XK1
      TSTRY(2,3)=YK1
      USTRX(2,3)=XL1
      USTRY(2,3)=YL1
      CALL TUSTR (2,4,1,3,THETA1,SLOPEK,SLOPEL,PIMGX,PIMGY,
     1NN,XK1,YK1,XL1,YL1)
      NTEST(2,4)=NN
      TSTRX(2,4)=XK1
      TSTRY(2,4)=YK1
      USTRX(2,4)=XL1
      USTRY(2,4)=YL1
      CALL TUSTR (3,4,1,2,THETA1,SLOPEK,SLOPEL,PIMGX,PIMGY,
     1NN,XK1,YK1,XL1,YL1)
      NTEST(3,4)=NN
      TSTRX(3,4)=XK1
      TSTRY(3,4)=YK1
      USTRX(3,4)=XL1
      USTRY(3,4)=YL1
      DO 67 I=1,3
      JK=I+1
      DO 68 J=JK,4
      NTEST(J,I)=NTEST(I,J)
```

```
      TSTRX(J,I)=TSTRX(I,J)
      TSTRY(J,I)=TSTRY(I,J)
      USTRX(J,I)=USTRX(I,J)
      USTRY(J,I)=USTRY(I,J)
   68 CONTINUE
   67 CONTINUE
C
C   BEGINNING OF CALCULATIONS FOR COEFFICIENTS
C
      DO 50 I=1,3
      J=I+1
      A1(J)=1.-COS(THETA1(1,J))
      B1(J)=SIN(THETA1(1,J))
      C1(J)=AP( J)*COS(THETA1(1,J))+AQ( J)*SIN(THETA1(1,J))
      D1(J)=-AP( J)*SIN(THETA1(1,J))+AQ( J)*COS(THETA1(1,J))
      E1(J)=(AP( J)**2+AQ( J)**2)/2.
   50 CONTINUE
      DO 60I=1,3
      J=I+1
      AMATX(I,1)=A1(J)
      AMATX(I,2)=B1(J)
      AMATX(I,3)=C1(J)
      BMATX(I,1)=B1(J)
      BMATX(I,2)=A1(J)
      BMATX(I,3)=D1(J)
      C1MATX(I,1)=A1(J)
      C1MATX(I,2)=AQ(J)
      C1MATX(I,3)=D1(J)
      C2MATX(I,1)=B1(J)
      C2MATX(I,2)=AQ(J)
      C2MATX(I,3)=C1(J)
      C3MATX(I,1)=AP(J)
      C3MATX(I,2)=B1(J)
      C3MATX(I,3)=D1(J)
      C4MATX(I,1)=AP(J)
      C4MATX(I,2)=A1(J)
      C4MATX(I,3)=C1(J)
      D1MATX(I,1)=A1(J)
      D1MATX(I,2)=B1(J)
      D1MATX(I,3)=E1(J)
      D2MATX(I,1)=A1(J)
      D2MATX(I,2)=AQ(J)
      D2MATX(I,3)=C1(J)
      D3MATX(I,1)=AP(J)
      D3MATX(I,2)=B1(J)
      D3MATX(I,3)=C1(J)
      E1MATX(I,1)=B1(J)
      E1MATX(I,2)=A1(J)
      E1MATX(I,3)=E1(J)
      E2MATX(I,1)=B1(J)
      E2MATX(I,2)=AQ(J)
      E2MATX(I,3)=D1(J)
```

```
      E3MATX(I,1)=AP(J)
      E3MATX(I,2)=A1(J)
      E3MATX(I,3)=D1(J)
      F1MATX(I,1)=A1(J)
      F1MATX(I,2)=AQ(J)
      F1MATX(I,3)=E1(J)
      F2MATX(I,1)=AP(J)
      F2MATX(I,2)=B1(J)
      F2MATX(I,3)=E1(J)
      F3MATX(I,1)=AP(J)
      F3MATX(I,2)=AQ(J)
      F3MATX(I,3)=C1(J)
      G1MATX(I,1)=B1(J)
      G1MATX(I,2)=AQ(J)
      G1MATX(I,3)=E1(J)
      G2MATX(I,1)=AP(J)
      G2MATX(I,2)=A1(J)
      G2MATX(I,3)=E1(J)
      G3MATX(I,1)=AP(J)
      G3MATX(I,2)=AQ(J)
      G3MATX(I,3)=D1(J)
      H1MATX(I,1)=AP(J)
      H1MATX(I,2)=AQ(J)
      H1MATX(I,3)=E1(J)
   60 CONTINUE
      CALL DETERM(AMATX,G)
      A2=-G
      CALL DETERM(BMATX,G)
      B2=G
      CALL DETERM(C1MATX,G1)
      CC1=G1
      CALL DETERM(C2MATX,G2)
      CC2=G2
      CALL DETERM(C3MATX,G3)
      CC3=G3
      CALL DETERM(C4MATX,G4)
      CC4=G4
      C2=-CC1-CC2+CC3-CC4
      CALL DETERM(D1MATX,G1)
      DD1=G1
      CALL DETERM(D2MATX,G2)
      DD2=G2
      CALL DETERM(D3MATX,G3)
      DD3=G3
      D2=-DD1-DD2+DD3
      CALL DETERM(E1MATX,G1)
      EE1=G1
      CALL DETERM(E2MATX,G2)
      EE2=G2
      CALL DETERM(E3MATX,G3)
      EE3=G3
      E2=EE1-EE2-EE3
```

```
          CALL DETERM(F1MATX,G1)
          FF1=G1
          CALL DETERM(F2MATX,G2)
          FF2=G2
          CALL DETERM(F3MATX,G3)
          FF3=G3
          F2=-FF1+FF2+FF3
          CALL DETERM(G1MATX,G1)
          GG1=G1
          CALL DETERM(G2MATX,G2)
          GG2=G2
          CALL DETERM(G3MATX,G3)
          GG3=G3
          G2=-GG1-GG2+GG3
          CALL DETERM(H1MATX,G1)
          H2=G1
          WRITE (6,2050)A2,B2,C2,D2,E2,F2,G2,H2
     2050 FORMAT (///,40X,'A= ',F10.4,/,40X,'B= ',F10.4,/,40X,'C= ',F10.4,/,
         140X,'D= ',F10.4,/,40X,'E= ',F10.4,/,40X,'F= ',F10.4,/,
         140X,'G= ',F10.4,/,40X,'H= ',F10.4)
    C
    C     P-Q AXES ARE ROTATED TO U-V AXES THROUGH THE ANGLE
    C     ALPHA=ARCTAN(-A/B) SUCH THAT THE ASYMPTOTE OF THE
    C     CIRCLE-POINT CURVE IS PARALLEL WITH THE U-AXIS.
    C     THE COEFFICIENTS IN THE ROTATED AXES ARE DENOTED BY PRIM.
    C

          ALPHA1=ATAN(-A2/B2)
          IF (B2) 110,111,111
      110 ALPHA2=ALPHA1+PI
          GO TO 113
      111 ALPHA2=ALPHA1
          GO TO 113
      113 CONTINUE
          ALPHAD=(ALPHA2*180.)/PI
          WRITE (6,2060) ALPHAD
     2060 FORMAT (///,40X,'ALPHA (DEG)= ',F10.4)
          WRITE (6,2070)
     2070 FORMAT (///,30X,'THE FOLLOWING DATA ARE IN THE U-V AXES'
         1,//)
          BPRIM=SQRT(A2**2+B2**2)
          CPRIM=(C2*(B2**2-A2**2)+2.*A2*B2*D2-2.*A2*B2*E2)/(BPRIM**2)
          DPRIM=((E2*A2**2)+(D2*B2**2)-(A2*B2*C2))/(BPRIM**2)
          EPRIM=((D2*A2**2)+(E2*B2**2)+(A2*B2*C2))/(BPRIM**2)
          FPRIM=((B2*F2)-(A2*G2))/(BPRIM)
          GPRIM=((A2*F2)+(B2*G2))/(BPRIM)
          HPRIM=H2
          WRITE (6,3000)BPRIM,CPRIM,DPRIM,EPRIM,FPRIM,GPRIM,HPRIM
     3000 FORMAT (///,40X,'BPRIM= ',F10.4,/,40X,'CPRIM= ',F10.4,/,40X,
         1'DPRIM= ',F10.4,/,40X,'EPRIM= 'F10.4,/,40X,'FPRIM= ',F10.4,/,
         140X,'GPRIM= ',F10.4,/,40X,'HPRIM= ',F10.4)
    C
```

```
C      INTERCEPT OF ASYMPTOTE WITH V-AXIS
C
       ASMTOT=-DPRIM/BPRIM
       WRITE (6,3010) ASMTOT
  3010 FORMAT (//,40X,'ASYMPTOTE= ',F10.4)
C
C      ROTATION OF DESIGN POSITIONS, IMAGE POLES P'(IJ),Q(IJ),
C      T(IJ),U(IJ),TSTAR(IJ) AND USTAR(IJ) INTO U-V AXES
C
       WRITE (6,3020)
  3020 FORMAT (///,42X,'DESIGN POSITIONS (U,V)',/)
       WRITE (6,3030)
  3030 FORMAT (50X,'U',10X,'V',/)
       DO 75 I=1,4
       FP1=AP(I)
       FQ1=AQ(I)
       CALL ROTAT (ALPHA2,FP1,FQ1,FU1,FV1)
       AU(I)=FU1
       AV(I)=FV1
       FP1=BP(I)
       FQ1=BQ(I)
       CALL ROTAT (ALPHA2,FP1,FQ1,FU1,FV1)
       BU(I)=FU1
       BV(I)=FV1
       WRITE (6,2030) (I,AU(I),AV(I))
       WRITE (6,2040) (I,BU(I),BV(I))
    75 CONTINUE
       WRITE (6,3035)
  3035 FORMAT (///,42X,'IMAGE POLES IN U-V AXES',/)
       WRITE (6,3025)
  3025 FORMAT (54X,'U',10X,'V',/)
       DO 85 I=1,3
       JK=I+1
       DO 86 J=JK,4
       FP1=PIMGX(I,J)
       FQ1=PIMGY(I,J)
       CALL ROTAT (ALPHA2,FP1,FQ1,FU1,FV1)
       PIMGU(I,J)=FU1
       PIMGV(I,J)=FV1
       WRITE (6,3040) (I,J,PIMGU(I,J),PIMGV(I,J))
    86 CONTINUE
    85 CONTINUE
  3040 FORMAT (40X,'P',I1,I1,'IMG= ',F10.4,1X,F10.4)
       WRITE (6,3050)
  3050 FORMAT (///,51X,'U',10X,'V',/)
       DO 95 I=1,3
       JK=I+1
       DO 96 J=JK,4
       FP1=QX(I,J)
       FQ1=QY(I,J)
       CALL ROTAT (ALPHA2,FP1,FQ1,FU1,FV1)
       QU(I,J)=FU1
```

```
      QV(I,J)=FV1
      WRITE (6,3060) (I,J,QU(I,J),QV(I,J))
 3060 FORMAT (40X,'Q',I1,I1,'= ',F10.4,1X,F10.4)
   96 CONTINUE
   95 CONTINUE
      WRITE (6,3050)
      DO 105 I=1,3
      JK=I+1
      DO 106 J=JK,4
      FP1=TX(I,J)
      FQ1=TY(I,J)
      CALL ROTAT (ALPHA2,FP1,FQ1,FU1,FV1)
      TU(I,J)=FU1
      TV(I,J)=FV1
      FP1=UX(I,J)
      FQ1=UY(I,J)
      CALL ROTAT (ALPHA2,FP1,FQ1,FU1,FV1)
      UU(I,J)=FU1
      UV(I,J)=FV1
      IF (MTEST(I,J).EQ.0) GO TO 3065
      WRITE (6,3070) (I,J,TU(I,J),TV(I,J))
      WRITE (6,3071) (I,J,UU(I,J),UV(I,J))
 3070 FORMAT (40X,'T',I1,I1,'= ',F10.4,1X,F10.4)
 3071 FORMAT (40X,'U',I1,I1,'= ',F10.4,1X,F10.4,//)
      GO TO 106
 3065 CONTINUE
      WRITE (6,3066) (I,J,I,J)
 3066 FORMAT (//,40X,'T(',I1,I1,') AND U(',I1,I1,')'
     1'DO NOT EXIST',//)
  106 CONTINUE
  105 CONTINUE
      DO 115 I=1,3
      JK=I+1
      DO 116 J=JK,4
      FP1=TSTRX(I,J)
      FQ1=TSTRY(I,J)
      CALL ROTAT (ALPHA2,FP1,FQ1,FU1,FV1)
      TSTRU(I,J)=FU1
      TSTRV(I,J)=FV1
      FP1=USTRX(I,J)
      FQ1=USTRY(I,J)
      CALL ROTAT (ALPHA2,FP1,FQ1,FU1,FV1)
      USTRU(I,J)=FU1
      USTRV(I,J)=FV1
      IF (NTEST(I,J).EQ.0) GO TO 3075
      WRITE (6,3080) (I,J,TSTRU(I,J),TSTRV(I,J))
      WRITE (6,3081) (I,J,USTRU(I,J),USTRV(I,J))
 3080 FORMAT (40X,'TSTR',I1,I1,'= ',F10.4,1X,F10.4)
 3081 FORMAT (40X,'USTR',I1,I1,'= ',F10.4,1X,F10.4,//)
      GO TO 116
 3075 CONTINUE
      WRITE (6,3076) (I,J,I,J)
```

```
 3076 FORMAT (//,40X,'TSTR(',I1,I1,') AND USTR(',I1,I1,')'
     1'DO NOT EXIST',//)
  116 CONTINUE
  115 CONTINUE
C
C      READING IN U AND DELU WHERE U IS NEGATIVE AND DELU IS POSITIVE
C
    9 READ(5,200,END=500)U,DELU
      TEST=U
  200 FORMAT(F10.3,F10.7)
      I=1
      K=1
      L=1
      IX=I
    1 CONTINUE
      AA1=EPRIM/BPRIM
      AA2=((BPRIM*U**2)+(CPRIM*U)+GPRIM)/BPRIM
      AA3=((DPRIM*U**2)+(FPRIM*U)+HPRIM)/BPRIM
      Q1=((3.*AA2)-(AA1**2))/9.
      R1=((9.*AA1*AA2)-(27.*AA3)-(2.*AA1**3))/54.
      R2=ABS(R1)
      Q2=ABS(Q1)
      D=(SIGN(1,Q1)*(Q2**3))+(R2**2)
      IF(D)101,101,102
  102 SS=SQRT(D)
      DS1=R1+SS
      DT1=R1-SS
      DS2=ABS(DS1)
      DT2=ABS(DT1)
      S1=(SIGN(1,DS1))*(DS2**.333333)
      T1=(SIGN(1,DT1))*(DT2**.333333)
      IF(I.NE.1)GO TO 104
      U1(I)=U
      V=S1+T1-AA1/3.
      V1(I)=V
      U=U+DELU
      I=I+1
      GO TO 1
  104 U1(I)=U
      V=S1+T1-AA1/3.
      V1(I)=V
      Z=V1(I)
      U=U+DELU
      I=I+1
      IX=I
      GO TO 1
  101 DELV=Z-ASMTOT
      PHI=ARCOS(R1/SQRT(Q2**3))
      PHID=(180./PI)*PHI
      R3=2.*SQRT(Q2)
      VV1=R3*COS(PHI/3.)-AA1/3.
      VV2=R3*COS(PHI/3.+(2.*PI/3.))-AA1/3.
```

```
      VV3=R3*COS(PHI/3.+(4.*PI/3.))-AA1/3.
  202 U11(K)=U
      U12(K)=U
      U13(K)=U
      IF(K.NE.1)GO TO 207
      V11(K)=VV1
      V12(K)=VV2
      V13(K)=VV3
      U=U+(DELU/10.)
      K=K+1
      GO TO 2
  207 V11(K)=VV1
      V12(K)=VV2
      V13(K)=VV3
      U=U+(DELU/10.)
      K=K+1
      KK=K
      GO TO 2
    2 CONTINUE
      AA1=EPRIM/BPRIM
      AA2=((BPRIM*U**2)+(CPRIM*U)+(GPRIM))/BPRIM
      AA3=((DPRIM*U**2)+(FPRIM*U)+(HPRIM))/(BPRIM)
      Q1=((3.*AA2)-(AA1**2))/9.
      R1=((9.*AA1*AA2)-(27.*AA3)-(2.*AA1**3))/54.
      R2=ABS(R1)
      Q2=ABS(Q1)
      D=(SIGN(1,Q1)*(Q2**3))+(R2**2)
      IF(D)101,101,103
  103 SS=SQRT(D)
      DS1=R1+SS
      DT1=R1-SS
      DS2=ABS(DS1)
      DT2=ABS(DT1)
      S1=(SIGN(1,DS1))*(DS2**.333333)
      T1=(SIGN(1,DT1))*(DT2**.333333)
      IF(L.NE.1)GO TO 351
      U2(L)=U
      V=S1+T1-AA1/3.
      V2(L)=V
      U=U+DELU
      L=L+1
      GO TO 2
  351 U2(L)=U
      V=S1+T1-AA1/3.
      V2(L)=V
      IF(LL.GE.IX) GO TO 6000
      U=U+DELU
      L=L+1
      LL=L
      GO TO 2
 6000 CONTINUE
 6050 CONTINUE
```

```
      BB1=4.*(BPRIM**2)
      BB2=(4*(BPRIM)*(DPRIM+EPRIM))/4.
      BB3=(-(CPRIM**2)+(4.*BPRIM*GPRIM)+(4.*DPRIM*EPRIM))/6.
      BB4=(-2.*(CPRIM*FPRIM)+(4.*BPRIM*HPRIM)+(4.*DPRIM*GPRIM))/4.
      BB5=-(FPRIM**2)+(4.*DPRIM*HPRIM)
      TEST1=(((BB1*BB5)-(4.*BB2*BB4)+(3.*BB3**2))**3)-27.*((BB1*BB3*BB5
     1+(2*BB2*BB3*BB4)-(BB1*BB4**2)-(BB5*BB2**2)-(BB3**3))**2)
      IF(TEST1.LT.0) GO TO 3
      WRITE(6,9021)
 9021 FORMAT(///,47X,'DOUBLE BRANCH CURVE',///,47X,
     1'OPEN BRANCH SEGMENT',//,46X,'U',19X,'V',/)
      IK=IX-1
      DO 350 I=1,IK
      WRITE(6,9011)(U1(I),V1(I))
 9011 FORMAT(40X,F10.5,10X,F10.5)
  350 CONTINUE
      KL=KK-1
      DO 360 I=1,KL
      WRITE (6,9011) (U12(I),V12(I))
  360 CONTINUE
      DO 370 I=1,LL
      WRITE (6,9011) (U2(I),V2(I))
  370 CONTINUE
      WRITE (6,9022)
 9022 FORMAT (//,44X,'CLOSED BRANCH SEGMENT',//,46X,'U',18X,'V1',18X,
     1'V2',/)
      KL=KK-1
      DO 380 I=1,KL
      WRITE (6,9012) (U11(I),V11(I),V13(I))
 9012 FORMAT (40X,F10.5,10X,F10.5,10X,F10.5)
  380 CONTINUE
      GO TO 480
    3 CONTINUE
      WRITE (6,9031)
 9031 FORMAT (///,47X,'SINGLE BRANCH CURVE',//,46X,'U',19X,'V',/)
      IK=IX-1
      DO 450 I=1,IK
      WRITE (6,9011) (U1(I),V1(I))
  450 CONTINUE
      WRITE (6,9014)
 9014 FORMAT (//,46X,'U',13X,'V1',13X,'V2',12X,'V3',/)
      KL=KK-1
      DO 460 I=1,KL
      WRITE (6,9015) (U11(I),V11(I),V12(I),V13(I))
 9015 FORMAT (40X,F10.5,5X,F10.5,5X,F10.5,5X,F10.5)
  460 CONTINUE
      WRITE (6,9016)
 9016 FORMAT (//,46X,'U',19X,'V',/)
      DO 470 I=1,LL
      WRITE (6,9011) (U2(I),V2(I))
  470 CONTINUE
  480 CONTINUE
```

```
C
C     INSERT GO TO 9 CARD AFTER THIS CARD FOR VARING U AND DELU
C
  500 CONTINUE
C
C     INSERT GO TO 7 CARD AFTER THIS CARD FOR MORE THAN ONE CASE
C
      GO TO 7
  600 CONTINUE
      STOP
      END
```

```
      SUBROUTINE DETERM(A,G)
C
C     THIS SUBROUTINE EXPANDS A 3X3 DETERMINATE
C
      DIMENSION A(3,3)
      Z1=A(1,1)*A(2,2)*A(3,3)+A(1,2)*A(2,3)*A(3,1)+A(1,3)*A(2,1)*A(3,2)
      Z2=A(1,3)*A(2,2)*A(3,1)+A(1,2)*A(2,1)*A(3,3)+A(1,1)*A(2,3)*A(3,2)
      DET=Z1-Z2
      G=DET
      RETURN
      END
```

```
      SUBROUTINE QXQY(I,J,K,L,PIMGX,PIMGY,SLP1,QIN1,SLP2,QIN2,
     1QQX,QQY)
C
C     THIS SUBROUTINE FINDS THE SLOPE AND INTERCEPT FOR TWO
C     STRAIGHT LINES USED IN COMPUTING Q(IJ)
C
      DIMENSION PIMGX(4,4),PIMGY(4,4)
      SLP1=(PIMGY(I,K)-PIMGY(J,K))/(PIMGX(I,K)-PIMGX(J,K))
      QIN1=((PIMGX(I,K))*(PIMGY(J,K))-(PIMGX(J,K))*(PIMGY(I,K)
     1))/(PIMGX(I,K)-PIMGX(J,K))
      SLP2=(PIMGY(I,L)-PIMGY(J,L))/(PIMGX(I,L)-PIMGX(J,L))
      QIN2=((PIMGX(I,L))*(PIMGY(J,L))-(PIMGX(J,L))*(PIMGY(I,L)
     1))/(PIMGX(I,L)-PIMGX(J,L))
      QQX=(QIN1-QIN2)/(SLP2-SLP1)
      QQY=((QIN1*SLP2)-(QIN2*SLP1))/(SLP2-SLP1)
      RETURN
      END
```

```
      SUBROUTINE CIRIN1(I,J,K,L,PIMGX,PIMGY,MM,X1,Y1,X2,Y2)
C
C     THIS SUBROUTINF FINDS THE INTERSECTIONS-- IF THEY EXIST--
C     OF TWO CIRCLES WHERE P(IK)--P(JK) AND P(IL)--P(JL) ARE
C     THE DIAMETERS.  THE INTERSECTIONS ARE T(IJ) AND U(IJ).
C
      DIMENSION PIMGX(4,4),PIMGY(4,4)
      XCK=(PIMGX(I,K)+PIMGX(J,K))/2.
      YCK=(PIMGY(I,K)+PIMGY(J,K))/2.
      RK=((PIMGX(J,K)-PIMGX(I,K))**2+(PIMGY(J,K)-PIMGY(I,K))
     1**2)/4.
      XCL=(PIMGX(I,L)+PIMGX(J,L))/2.
      YCL=(PIMGY(I,L)+PIMGY(J,L))/2.
      RL=((PIMGX(J,L)-PIMGX(I,L))**2+(PIMGY(J,L)-PIMGY(I,L))
     1**2)/4.
      XCK2=XCK*XCK
      YCK2=YCK*YCK
      XCL2=XCL*XCL
      YCL2=YCL*YCL
          DX=XCL-XCK
      DY=YCK-YCL
      C1=DY/DX
      C2=(XCL2-XCK2+YCL2-YCK2+RK-RL)/(2.*DX)
      BB=(YCK+XCK*C1-C1*C2)/(1.+C1**2)
      CC=(XCK2+YCK2-RK-2.*XCK*C2+C2**2)/(1.+C1**2)
      DD=(BB**2)-CC
      IF (DD) 101,102,102
  101 CONTINUE
      MM=0
      X1=999.9999
      Y1=999.9999
      X2=999.9999
      Y2=999.9999
      GO TO 10
  102 CONTINUE
      MM=1
      Y1=BB+SQRT(DD)
      Y2=BB-SQRT(DD)
      X1=(C1*Y1)+C2
      X2=(C1*Y2)+C2
   10 CONTINUE
      RETURN
      END
```

```
      SUBROUTINE TUSTR(I,J,K,L,THETA1,SLOPEK,SLOPFL,PIMGX,
     1PIMGY,NN,XK1,YK1,XL1,YL1)
C
C     THIS SUBROUTINE FINDS THE INTERSECTIONS -- IF THEY EXIST--
C     OF TWO CIRCLES WHERE P(IK)--P(JK) AND P(IL)--P(JL) ARE NOT
C     THE DIAMETERS OF THE CIRCLES.  THE INTERSECTIONS ARE
C     TSTAR(IJ) AND USTAR(IJ).
C
      DIMENSION THFTA1(4,4),SLOPEK(4,4),SLOPEL(4,4)
      DIMENSION PIMGX(4,4),PIMGY(4,4)
      PI=3.141592654
      IF (THETA1(I,J)) 101,102,102
  101 CONTINUE
      PSI=PI+THETA1(I,J)
      GO TO 10
  102 CONTINUE
      PSI=THETA1(I,J)-PI
   10 CONTINUE
      BETA=(THETA1(I,J))/2.
      PHIK=ATAN(SLOPEK(I,J))
      SLP1K=SIN(PHIK-BETA)/COS(PHIK-BETA)
      YP1K=PIMGY(I,K)-(SLP1K*PIMGX(I,K))
      SLP2K=SIN(PHIK+BETA)/COS(PHIK+BETA)
      YP2K=PIMGY(J,K)-(SLP2K*PIMGX(J,K))
      XK=(YP1K-YP2K)/(SLP2K-SLP1K)
      YK=(SLP2K*YP1K-SLP1K*YP2K)/(SLP2K-SLP1K)
      RRK=((PIMGX(J,K)-PIMGX(I,K))**2+(PIMGY(J,K)-PIMGY(I,K))
     1**2)/(4.*SIN(PSI/2.)*SIN(PSI/2.))
      PHIL=ATAN(SLOPEL(I,J))
      SLP1L=SIN(PHIL-BETA)/COS(PHIL-BETA)
      YP1L=PIMGY(I,L)-(SLP1L*PIMGX(I,L))
      SLP2L=SIN(PHIL+BETA)/COS(PHIL+BETA)
      YP2L=PIMGY(J,L)-(SLP2L*PIMGX(J,L))
      XL=(YP1L-YP2L)/(SLP2L-SLP1L)
      YL=(SLP2L*YP1L-SLP1L*YP2L)/(SLP2L-SLP1L)
      RRL=((PIMGX(J,L)-PIMGX(I,L))**2+(PIMGY(J,L)-PIMGY(I,L))
     1**2)/(4.*SIN(PSI/2.)*SIN(PSI/2.))
      XK2=XK*XK
      YK2=YK*YK
      XL2=XL*XL
      YL2=YL*YL
      DX=XL-XK
      DY=YK-YL
      CC1=DY/DX
      CC2=(XL2-XK2+YL2-YK2+RRK-RRL)/(2.*DX)
      BBB=(YK+XK*CC1-CC1*CC2)/(1.+CC1**2)
      CCC=(XK2+YK2-RRK-2.*XK*CC2+CC2**2)/(1.+CC1**2)
      DDD=(BBB**2)-CCC
      IF (DDD) 105,106,106
  105 CONTINUE
      NN=0
      XK1=999.9999
```

```
      YK1=999.9999
      XL1=999.9999
      YL1=999.9999
      GO TO 20
  106 CONTINUE
      NN=1
      YK1=BBB+SQRT(DDD)
      YL1=BBB-SQRT(DDD)
      XK1=(CC1*YK1)+CC2
      XL1=(CC1*YL1)+CC2
   20 CONTINUE
      RETURN
      END
```

```
      SUBROUTINE ROTAT(ALPHA2,FP1,FQ1,FU1,FV1)
C
C     THIS SUBROUTINE ROTATES THE P-Q AXES THROUGH AN ANGLE
C     ALPHA TO GET THE U-V AXES.
C
      FU1=(COS(ALPHA2))*FP1+(SIN(ALPHA2))*FQ1
      FV1=-(SIN(ALPHA2))*FP1+(COS(ALPHA2))*FQ1
      RETURN
      END
```

A.3 Output Data For Both Single and Double Branch Circle-Point Curves

The data presented in this section are the output data from the numerical algorithm of A.2 for both the single and double branch curves. The data indicates whether it is in the p-q coordinate system which has its origin at end A in the first design position or in the u-v coordinate system which has been rotated such that the asymptote is parallel with the u-axis. The data for the circle-point curve is listed in the u-v coordinate system only.

DESIGN POSITIONS (X,Y)

	X	Y
A1=	0.	0.
B1=	0.	25.0000
A2=	-8.7000	21.5000
B2=	12.3000	35.0000
A3=	-1.0000	31.2000
B3=	23.5000	36.5000
A4=	13.0000	32.0000
B4=	37.7000	27.8000

THETA(1)= 90.0000

THETA(12)=	-57.2648
THETA(13)=	-77.7935
THETA(14)=	-99.6503
THETA(23)=	-20.5287
THETA(24)=	-42.3855
THETA(34)=	-21.8568

DESIGN POSITIONS (P,Q)

	P	Q
A1=	0.	0.
B1=	25.0000	0.0000
A2=	21.5000	8.7000
B2=	35.0000	-12.3000
A3=	31.2000	1.0000
B3=	36.5000	-23.5000
A4=	32.0000	-13.0000
B4=	27.8000	-37.7000

IMAGE POLES IN P-Q AXES

	P	Q
P12=	18.7177	-15.3404
P13=	16.2197	-18.8355
P14=	10.5120	-20.0090
P23=	16.8934	-30.3688
P24=	8.2234	-32.3122
P34=	1.2858	-36.9612

A=	-0.1904
B=	0.7324
C=	-22.3360
D=	47.4868
E=	36.7412
F=	-1109.3788
G=	475.4894
H=	5029.5547

ALPHA (DEG)= 14.5691

THE FOLLOWING DATA ARE IN THE U-V AXES

BPRIM=	0.7567
CPRIM=	-24.7416
DPRIM=	41.3690
EPRIM=	42.8590
FPRIM=	-954.0989
GPRIM=	739.2610
HPRIM=	5029.5547

ASYMPTOTE= -54.6672

DESIGN POSITIONS (U,V)

	U	V
A1=	0.	0.
B1=	24.1961	-6.2887
A2=	22.9971	3.0120
B2=	30.7806	-20.7086
A3=	30.4483	-6.8804
B3=	29.4150	-31.9258
A4=	27.7009	-20.6315
B4=	17.4228	-43.4808

IMAGE POLES IN U-V AXES

	U	V
P12IMG=	14.2570	-19.5555
P13IMG=	10.9602	-22.3099
P14IMG=	5.1407	-22.0099
P23IMG=	8.7110	-33.6418
P24IMG=	-0.1691	-33.3417
P34IMG=	-8.0530	-36.0961

	U	V
Q12=	15.3399	-0.2435
Q13=	19.2010	-6.9986
Q14=	12.6789	-21.0637
Q23=	-3.7362	-34.5880
Q24=	-93.8214	-48.6531
Q34=	652.9236	-55.4073

```
T12=      6.7473   -23.0942
U12=      6.3597   -32.5895

T13=      5.3298   -22.1918
U13=      7.3708   -32.9529

T14=      2.5990   -17.5164
U14=     11.4181   -35.4158


T(23) AND U(23)'DO NOT EXIST


T(24) AND U(24)'DO NOT EXIST


T(34) AND U(34)'DO NOT EXIST

TSTR12=      9.3432   -23.0711
USTR12=     10.1810   -34.5699

TSTR13=      9.3303   -23.0753
USTR13=     15.9257   -38.4822

TSTR14=      5.8945   -22.6452
USTR14=     27.3504   -44.5702


TSTR(23) AND USTR(23)'DO NOT EXIST


TSTR(24) AND USTR(24)'DO NOT EXIST


TSTR(34) AND USTR(34)'DO NOT EXIST


        DOUBLE BRANCH CURVE

        OPEN BRANCH SEGMENT

      U                      V
 -10.00000             -36.73993
  -9.00000             -36.41259
  -8.00000             -36.07816
  -7.00000             -35.73704
  -6.00000             -35.38991
  -5.00000             -35.03776
  -4.00000             -34.68208
  -3.00000             -34.32507
```

-2.00000	-33.96994
-1.00000	-33.62141
0.	-33.28639
1.00000	-32.97504
2.00000	-32.70217
2.10000	-32.67774
2.20000	-32.65392
2.30000	-32.63074
2.40000	-32.60823
2.50000	-32.58641
2.60000	-32.56530
2.70000	-32.54495
2.80000	-32.52537
2.90000	-32.50660
3.00000	-32.48867
3.10000	-32.47161
3.20000	-32.45544
3.30000	-32.44021
3.40000	-32.42595
3.50000	-32.41268
3.60000	-32.40044
3.70000	-32.38927
3.80000	-32.37920
3.90000	-32.37027
4.00000	-32.36250
4.10000	-32.35593
4.20000	-32.35060
4.30000	-32.34653
4.40000	-32.34377
4.50000	-32.34234
4.60000	-32.34227
4.70000	-32.34360
4.80000	-32.34635
4.90000	-32.35056
5.00000	-32.35624
5.10000	-32.36342
5.20000	-32.37213
5.30000	-32.38239
5.40000	-32.39421
5.50000	-32.40761
5.60000	-32.42261
5.70000	-32.43922
5.80000	-32.45744
5.90000	-32.47729
6.00000	-32.49876
6.10000	-32.52187
6.20000	-32.54660
6.30000	-32.57295
6.40000	-32.60091
6.50000	-32.63048
6.60000	-32.66163
6.70000	-32.69436
6.80000	-32.72864
6.90000	-32.76445
7.00000	-32.80177
7.10000	-32.84057
7.20000	-32.88083
7.30000	-32.92251
7.40000	-32.96558

7.50000	-33.01001
7.60000	-33.05576
7.70000	-33.10280
7.80000	-33.15109
7.90000	-33.20058
8.00000	-33.25125
8.10000	-33.30305
8.20000	-33.35593
8.30000	-33.40987
8.40000	-33.46482
8.50000	-33.52074
8.60000	-33.57758
8.70000	-33.63532
8.80000	-33.69390
8.90000	-33.75329
9.00000	-33.81346
9.10000	-33.87436
9.20000	-33.93595
9.30000	-33.99821
9.40000	-34.06108
9.50000	-34.12455
9.60000	-34.18857
9.70000	-34.25312
9.80000	-34.31816
9.90000	-34.38365
10.00000	-34.44958
10.10000	-34.51591
10.20000	-34.58261
10.30000	-34.64966
10.40000	-34.71702
10.50000	-34.78469
10.60000	-34.85262
10.70000	-34.92080
10.80000	-34.98921
10.90000	-35.05782
11.00000	-35.12662
11.10000	-35.19558
11.20000	-35.26468
11.30000	-35.33391
11.40000	-35.40325
11.50000	-35.47269
11.60000	-35.54220
11.70000	-35.61178
11.80000	-35.68140
11.90000	-35.75106
12.00000	-35.82074
12.10000	-35.89042
12.20000	-35.96011
12.30000	-36.02978
12.40000	-36.09942
12.50000	-36.16903
12.60000	-36.23859
12.70000	-36.30810
12.80000	-36.37754
12.90000	-36.44691
13.00000	-36.51620
13.10000	-36.58540
13.20000	-36.65451
13.30000	-36.72351

13.40000	-36.79241
13.50000	-36.86119
13.60000	-36.92984
13.70000	-36.99837
13.80000	-37.06677
13.90000	-37.13503
14.00000	-37.20315
14.10000	-37.27112
14.20000	-37.33894
14.30000	-37.40660
14.40000	-37.47411
14.50000	-37.54145
14.60000	-37.60863
14.70000	-37.67564
14.80000	-37.74248
14.90000	-37.80914
15.00000	-37.87562
15.10000	-37.94192
15.20000	-38.00804
15.30000	-38.07397
15.40000	-38.13972
15.50000	-38.20528
15.60000	-38.27065
15.70000	-38.33582
15.80000	-38.40080
15.90000	-38.46559
16.00000	-38.53017
16.10000	-38.59456
16.20000	-38.65875
16.30000	-38.72274
16.40000	-38.78652
16.50000	-38.85010
16.60000	-38.91348
16.70000	-38.97666
16.80000	-39.03963
16.90000	-39.10239
17.00000	-39.16495
17.10000	-39.22730
17.20000	-39.28945
17.30000	-39.35138
17.40000	-39.41311
17.50000	-39.47463
17.60000	-39.53594
17.70000	-39.59705
17.80000	-39.65794
17.90000	-39.71863
18.00000	-39.77911
18.10000	-39.83937
18.20000	-39.89943
18.30000	-39.95928
18.40000	-40.01892
18.50000	-40.07836
18.60000	-40.13758
18.70000	-40.19660
18.80000	-40.25541
18.90000	-40.31401
19.00000	-40.37240
19.10000	-40.43059
19.20000	-40.48856

19.30000	-40.54629
20.30000	-41.11274
21.30000	-41.65903
22.30000	-42.18574
23.30000	-42.69350
24.30000	-43.18297
25.30000	-43.65483
26.30000	-44.10973
27.30000	-44.54835
28.30000	-44.97131
29.30000	-45.37922
30.30000	-45.77266
31.30000	-46.15221

CLOSED BRANCH SEGMENT

U	V1	V2
2.00000	-8.74335	-15.19060
2.10000	-8.27010	-15.68828
2.20000	-7.85717	-16.12503
2.30000	-7.48745	-16.51793
2.40000	-7.15073	-16.87716
2.50000	-6.84032	-17.20939
2.60000	-6.55157	-17.51924
2.70000	-6.28108	-17.81009
2.80000	-6.02627	-18.08447
2.90000	-5.78515	-18.34436
3.00000	-5.55611	-18.59133
3.10000	-5.33786	-18.82665
3.20000	-5.12932	-19.05135
3.30000	-4.92960	-19.26630
3.40000	-4.73794	-19.47223
3.50000	-4.55369	-19.66974
3.60000	-4.37629	-19.85938
3.70000	-4.20525	-20.04159
3.80000	-4.04014	-20.21678
3.90000	-3.88057	-20.38528
4.00000	-3.72622	-20.54740
4.10000	-3.57678	-20.70340
4.20000	-3.43199	-20.85353
4.30000	-3.29159	-20.99799
4.40000	-3.15537	-21.13697
4.50000	-3.02314	-21.27064
4.60000	-2.89470	-21.39914
4.70000	-2.76989	-21.52263
4.80000	-2.64856	-21.64121
4.90000	-2.53056	-21.75500
5.00000	-2.41577	-21.86410
5.10000	-2.30407	-21.96862
5.20000	-2.19535	-22.06863
5.30000	-2.08950	-22.16423
5.40000	-1.98643	-22.25548
5.50000	-1.88604	-22.34246
5.60000	-1.78826	-22.42524
5.70000	-1.69301	-22.50388
5.80000	-1.60022	-22.57846
5.90000	-1.50981	-22.64902
6.00000	-1.42172	-22.71563

6.10000	-1.33590	-22.77835
6.20000	-1.25228	-22.83724
6.30000	-1.17081	-22.89236
6.40000	-1.09144	-22.94376
6.50000	-1.01413	-22.99150
6.60000	-0.93883	-23.03565
6.70000	-0.86550	-23.07626
6.80000	-0.79410	-23.11338
6.90000	-0.72458	-23.14708
7.00000	-0.65692	-23.17742
7.10000	-0.59108	-23.20446
7.20000	-0.52703	-23.22825
7.30000	-0.46474	-23.24887
7.40000	-0.40417	-23.26636
7.50000	-0.34531	-23.28079
7.60000	-0.28812	-23.29223
7.70000	-0.23259	-23.30072
7.80000	-0.17868	-23.30635
7.90000	-0.12638	-23.30915
8.00000	-0.07566	-23.30920
8.10000	-0.02651	-23.30656
8.20000	0.02109	-23.30127
8.30000	0.06717	-23.29341
8.40000	0.11173	-23.28303
8.50000	0.15480	-23.27018
8.60000	0.19639	-23.25492
8.70000	0.23651	-23.23731
8.80000	0.27518	-23.21739
8.90000	0.31240	-23.19522
9.00000	0.34820	-23.17086
9.10000	0.38258	-23.14434
9.20000	0.41555	-23.11572
9.30000	0.44713	-23.08504
9.40000	0.47731	-23.05234
9.50000	0.50612	-23.01768
9.60000	0.53355	-22.98109
9.70000	0.55961	-22.94261
9.80000	0.58432	-22.90228
9.90000	0.60767	-22.86013
10.00000	0.62968	-22.81621
10.10000	0.65034	-22.77055
10.20000	0.66966	-22.72317
10.30000	0.68764	-22.67410
10.40000	0.70430	-22.62339
10.50000	0.71962	-22.57105
10.60000	0.73361	-22.51711
10.70000	0.74628	-22.46159
10.80000	0.75762	-22.40452
10.90000	0.76763	-22.34592
11.00000	0.77631	-22.28581
11.10000	0.78367	-22.22421
11.20000	0.78970	-22.16114
11.30000	0.79440	-22.09660
11.40000	0.79776	-22.03062
11.50000	0.79979	-21.96322
11.60000	0.80047	-21.89439
11.70000	0.79982	-21.82415
11.80000	0.79781	-21.75252
11.90000	0.79444	-21.67950

12.00000	0.78972	-21.60510
12.10000	0.78362	-21.52931
12.20000	0.77615	-21.45216
12.30000	0.76730	-21.37363
12.40000	0.75705	-21.29374
12.50000	0.74540	-21.21248
12.60000	0.73233	-21.12986
12.70000	0.71785	-21.04586
12.80000	0.70192	-20.96050
12.90000	0.68455	-20.87375
13.00000	0.66572	-20.78563
13.10000	0.64541	-20.69612
13.20000	0.62360	-20.60521
13.30000	0.60029	-20.51289
13.40000	0.57545	-20.41916
13.50000	0.54907	-20.32400
13.60000	0.52112	-20.22740
13.70000	0.49159	-20.12934
13.80000	0.46046	-20.02980
13.90000	0.42769	-19.92877
14.00000	0.39326	-19.82623
14.10000	0.35716	-19.72216
14.20000	0.31934	-19.61652
14.30000	0.27979	-19.50930
14.40000	0.23847	-19.40047
14.50000	0.19534	-19.29000
14.60000	0.15038	-19.17786
14.70000	0.10354	-19.06401
14.80000	0.05478	-18.94842
14.90000	0.00406	-18.83104
15.00000	-0.04865	-18.71184
15.10000	-0.10342	-18.59077
15.20000	-0.16029	-18.46778
15.30000	-0.21932	-18.34282
15.40000	-0.28056	-18.21584
15.50000	-0.34407	-18.08676
15.60000	-0.40993	-17.95554
15.70000	-0.47820	-17.82209
15.80000	-0.54897	-17.68635
15.90000	-0.62231	-17.54822
16.00000	-0.69831	-17.40764
16.10000	-0.77706	-17.26449
16.20000	-0.85868	-17.11869
16.30000	-0.94327	-16.97011
16.40000	-1.03096	-16.81863
16.50000	-1.12188	-16.66413
16.60000	-1.21618	-16.50646
16.70000	-1.31400	-16.34545
16.80000	-1.41554	-16.18094
16.90000	-1.52098	-16.01274
17.00000	-1.63055	-15.84062
17.10000	-1.74446	-15.66435
17.20000	-1.86301	-15.48366
17.30000	-1.98647	-15.29826
17.40000	-2.11520	-15.10780
17.50000	-2.24958	-14.91190
17.60000	-2.39004	-14.71013
17.70000	-2.53710	-14.50196
17.80000	-2.69135	-14.28682

17.90000	-2.85348	-14.06400
18.00000	-3.02432	-13.83269
18.10000	-3.20486	-13.59188
18.20000	-3.39632	-13.34036
18.30000	-3.60021	-13.07662
18.40000	-3.81844	-12.79875
18.50000	-4.05351	-12.50425
18.60000	-4.30880	-12.18973
18.70000	-4.58903	-11.85049
18.80000	-4.90119	-11.47952
18.90000	-5.25649	-11.06561
19.00000	-5.67505	-10.58866
19.10000	-6.20095	-10.00457
19.20000	-6.98772	-9.15983

DESIGN POSITIONS (X,Y)

	X	Y
A1=	3.0000	0.
B1=	11.0000	0.
A2=	0.8000	-2.0000
B2=	8.3000	0.7840
A3=	2.8000	-9.2500
B3=	4.1000	-1.3560
A4=	5.8000	0.6000
B4=	13.4000	-1.8980

THETA(1)= 0.

THETA(12)=	20.3649
THETA(13)=	80.6484
THETA(14)=	-18.1949
THETA(23)=	60.2834
THETA(24)=	-38.5598
THETA(34)=	-98.8432

DESIGN POSITIONS (P,Q)

	P	Q
A1=	0.	0.
B1=	8.0000	0.
A2=	-2.2000	-2.0000
B2=	5.3000	0.7840
A3=	-0.2000	-9.2500
B3=	1.1000	-1.3560
A4=	2.8000	0.6000
B4=	10.4000	-1.8980

IMAGE POLES IN P-Q AXES

	P	Q
P12=	4.4675	-7.1243
P13=	5.3490	-4.7428
P14=	3.2735	-8.4430
P23=	6.1281	-4.3044
P24=	3.7931	-7.4447

P34= 4.5211 -5.0505

A=	0.0488
B=	0.0352
C=	0.0851
D=	-0.9532
E=	0.9328
F=	6.2942
G=	8.9793
H=	12.5533

ALPHA (DEG)= -54.2019

THE FOLLOWING DATA ARE IN THE U-V AXES

BPRIM=	0.0602
CPRIM=	-1.8164
DPRIM=	0.2472
EPRIM=	-0.2675
FPRIM=	-3.6013
GPRIM=	10.3574
HPRIM=	12.5533

ASYMPTOTE= -4.1051

DESIGN POSITIONS (U,V)

	U	V
A1=	0.	0.
B1=	4.6794	6.4887
A2=	0.3353	-2.9542
B2=	2.4642	4.7573
A3=	7.3855	-5.5728
B3=	1.7433	0.0990
A4=	1.1512	2.6220
B4=	7.6227	7.3251

IMAGE POLES IN U-V AXES

	U	V
P12IMG=	8.3916	-0.5437
P13IMG=	6.9756	1.5642
P14IMG=	8.7627	-2.2835
P23IMG=	7.0757	2.4526
P24IMG=	8.4192	-1.3951
P34IMG=	6.7409	0.7128

	U	V
Q12=	7.0432	2.1638
Q13=	9.8880	-3.9511
Q14=	8.1812	5.9379
Q23=	11.9017	-5.7688
Q24=	7.3967	4.1202
Q34=	8.6286	-1.9947

U V

T(12) AND U(12)'DO NOT EXIST

T13=	6.2624	0.2384
U13=	9.2195	0.2693

T(14) AND U(14)'DO NOT EXIST

T23=	6.4240	0.3506
U23=	8.8682	0.0534

T(24) AND U(24)'DO NOT EXIST

T34=	5.7790	0.0020
U34=	9.7851	0.5507

TSTR(12) AND USTR(12)'DO NOT EXIST

TSTR13=	6.8957	1.1180
USTR13=	11.1241	1.1713

TSTR(14) AND USTR(14)'DO NOT EXIST

TSTR23=	6.8276	0.8979
USTR23=	9.7060	0.5135

TSTR(24) AND USTR(24)'DO NOT EXIST

TSTR34=	6.8735	1.0353
USTR34=	12.9928	2.2184

[illegible]

U	V
-10.00000	-2.07275
-9.50000	-2.04092
-9.00000	-2.00808
-8.50000	-1.97421
-8.00000	-1.93923
-7.50000	-1.90309
-7.00000	-1.86574
-6.50000	-1.82712
-6.00000	-1.78715
-5.50000	-1.74575
-5.00000	-1.70286
-4.50000	-1.65838
-4.00000	-1.61223
-3.50000	-1.56428
-3.00000	-1.51444
-2.50000	-1.46259
-2.00000	-1.40857
-1.50000	-1.35224
-1.00000	-1.29343
-0.50000	-1.23194
0.	-1.16754
0.50000	-1.09998
1.00000	-1.02895
1.50000	-0.95408
2.00000	-0.87492
2.50000	-0.79088
3.00000	-0.70119
3.50000	-0.60481
4.00000	-0.50018
4.50000	-0.38485
5.00000	-0.25452
5.50000	-0.10066
6.00000	0.09763
6.50000	0.41451
7.00000	1.76479
7.50000	4.45363
8.00000	5.61988

U	V1	V2	V3
8.50000	6.41733	-1.66322	-0.31071
8.55000	6.48495	-1.80122	-0.24034
8.60000	6.55078	-1.92694	-0.18045
8.65000	6.61491	-2.04372	-0.12781
8.70000	6.67740	-2.15354	-0.08047
8.75000	6.73832	-2.25772	-0.03721
8.80000	6.79773	-2.35718	0.00284
8.85000	6.85568	-2.45260	0.04030
8.90000	6.91223	-2.54448	0.07564
8.95000	6.96742	-2.63323	0.10920
9.00000	7.02129	-2.71918	0.14128
9.05000	7.07390	-2.80259	0.17208
9.10000	7.12528	-2.88369	0.20180
9.15000	7.17546	-2.96265	0.23057
9.20000	7.22449	-3.03964	0.25854
9.25000	7.27239	-3.11480	0.28580
9.30000	7.31219	-3.18824	0.31243

9.35000	7.36492	-3.26007	0.33853
9.40000	7.40962	-3.33038	0.36415
9.45000	7.45330	-3.39927	0.38935
9.50000	7.49599	-3.46679	0.41419
9.55000	7.53771	-3.53302	0.43870
9.60000	7.57848	-3.59803	0.46293
9.65000	7.61833	-3.66186	0.48692
9.70000	7.65727	-3.72457	0.51068
9.75000	7.69532	-3.78620	0.53426
9.80000	7.73251	-3.84680	0.55768
9.85000	7.76883	-3.90641	0.58096
9.90000	7.80432	-3.96506	0.60412
9.95000	7.83898	-4.02279	0.62719
10.00000	7.87284	-4.07962	0.65017
10.05000	7.90589	-4.13560	0.67309
10.10000	7.93816	-4.19074	0.69596
10.15000	7.96966	-4.24507	0.71880
10.20000	8.00040	-4.29863	0.74161
10.25000	8.03039	-4.35142	0.76442
10.30000	8.05964	-4.40348	0.78722
10.35000	8.08816	-4.45481	0.81004
10.40000	8.11596	-4.50546	0.83288
10.45000	8.14305	-4.55542	0.85576
10.50000	8.16943	-4.60472	0.87867
10.55000	8.19512	-4.65337	0.90163
10.60000	8.22013	-4.70140	0.92466
10.65000	8.24445	-4.74881	0.94774
10.70000	8.26810	-4.79562	0.97090
10.75000	8.29109	-4.84185	0.99415
10.80000	8.31341	-4.88750	1.01748
10.85000	8.33508	-4.93259	1.04090
10.90000	8.35610	-4.97713	1.06442
10.95000	8.37647	-5.02114	1.08805
11.00000	8.39620	-5.06462	1.11180
11.05000	8.41530	-5.10758	1.13567
11.10000	8.43377	-5.15004	1.15966
11.15000	8.45161	-5.19200	1.18378
11.20000	8.46883	-5.23348	1.20804
11.25000	8.48542	-5.27448	1.23244
11.30000	8.50140	-5.31501	1.25699
11.35000	8.51677	-5.35508	1.28170
11.40000	8.53152	-5.39470	1.30657
11.45000	8.54566	-5.43387	1.33160
11.50000	8.55920	-5.47261	1.35680
11.55000	8.57212	-5.51092	1.38218
11.60000	8.58445	-5.54881	1.40775
11.65000	8.59617	-5.58628	1.43350
11.70000	8.60728	-5.62334	1.45944
11.75000	8.61780	-5.66000	1.48559
11.80000	8.62771	-5.69626	1.51194
11.85000	8.63702	-5.73214	1.53850
11.90000	8.64573	-5.76763	1.56528
11.95000	8.65384	-5.80274	1.59228
12.00000	8.66134	-5.83747	1.61952
12.05000	8.66825	-5.87184	1.64698
12.10000	8.67454	-5.90585	1.67469
12.15000	8.68023	-5.93950	1.70265
12.20000	8.68531	-5.97279	1.73087
12.25000	8.68979	-6.00574	1.75934

12.30000	8.69365	-6.03835	1.78809
12.35000	8.69689	-6.07061	1.81711
12.40000	8.69952	-6.10254	1.84641
12.45000	8.70152	-6.13414	1.87601
12.50000	8.70290	-6.16542	1.90590
12.55000	8.70366	-6.19637	1.93610
12.60000	8.70378	-6.22701	1.96662
12.65000	8.70326	-6.25733	1.99746
12.70000	8.70210	-6.28734	2.02863
12.75000	8.70029	-6.31704	2.06014
12.80000	8.69782	-6.34644	2.09201
12.85000	8.69470	-6.37554	2.12423
12.90000	8.69091	-6.40435	2.15683
12.95000	8.68644	-6.43286	2.18981
13.00000	8.68129	-6.46108	2.22318
13.05000	8.67545	-6.48902	2.25695
13.10000	8.66892	-6.51667	2.29114
13.15000	8.66167	-6.54405	2.32576
13.20000	8.65370	-6.57114	2.36083
13.25000	8.64501	-6.59796	2.39634
13.30000	8.63557	-6.62451	2.43233
13.35000	8.62538	-6.65080	2.46880
13.40000	8.61442	-6.67681	2.50578
13.45000	8.60268	-6.70257	2.54327
13.50000	8.59015	-6.72806	2.58130
13.55000	8.57680	-6.75329	2.61988
13.60000	8.56263	-6.77827	2.65903
13.65000	8.54761	-6.80300	2.69878
13.70000	8.53172	-6.82748	2.73915
13.74999	8.51494	-6.85170	2.78015
13.79999	8.49725	-6.87569	2.82182
13.84999	8.47863	-6.89943	2.86418
13.89999	8.45905	-6.92293	2.90726
13.94999	8.43848	-6.94619	2.95110
13.99999	8.41688	-6.96921	2.99571
14.04999	8.39424	-6.99200	3.04114
14.09999	8.37051	-7.01455	3.08743
14.14999	8.34565	-7.03688	3.13461
14.19999	8.31963	-7.05898	3.18274
14.24999	8.29238	-7.08085	3.23185
14.29999	8.26388	-7.10249	3.28200
14.34999	8.23405	-7.12392	3.33325
14.39999	8.20285	-7.14512	3.38566
14.44999	8.17019	-7.16611	3.43930
14.49999	8.13601	-7.18687	3.49425
14.54999	8.10023	-7.20743	3.55058
14.59999	8.06275	-7.22777	3.60840
14.64999	8.02347	-7.24790	3.66781
14.69999	7.98227	-7.26781	3.72893
14.74999	7.93901	-7.28752	3.79190
14.79999	7.89355	-7.30703	3.85687
14.84999	7.84570	-7.32633	3.92402
14.89999	7.79525	-7.34542	3.99356
14.94999	7.74197	-7.36432	4.06573
14.99999	7.68556	-7.38301	4.14084
15.04999	7.62567	-7.40151	4.21923
15.09999	7.56186	-7.41981	4.30133
15.14999	7.49361	-7.43791	4.38768
15.19999	7.42023	-7.45582	4.47898

15.24999	7.34081	-7.47354	4.57612
15.29999	7.25413	-7.49106	4.68032
15.34999	7.15846	-7.50840	4.79333
15.39999	7.05119	-7.52555	4.91774
15.44999	6.92805	-7.54251	5.05785
15.49999	6.78109	-7.55928	5.22158
15.54999	6.59161	-7.57587	5.42764
15.59999	6.27565	-7.59228	5.76002

U	V
15.64999	-7.60849
16.14999	-7.76105
16.64999	-7.89679
17.14999	-8.01678
17.64999	-8.12200
18.14999	-8.21335
18.64999	-8.29166
19.14999	-8.35768
19.64999	-8.41214
20.14999	-8.45574
20.64999	-8.48913
21.14999	-8.51294
21.64999	-8.52779
22.14999	-8.53427
22.64999	-8.53296
23.14999	-8.52447
23.64999	-8.50919
24.14999	-8.48782
24.64999	-8.46084
25.14999	-8.42876
25.64999	-8.39207
26.14999	-8.35124
26.64999	-8.30675
27.14999	-8.25903
27.64999	-8.20851
28.14999	-8.15559
28.64999	-8.10065
29.14999	-8.04403
29.64999	-7.98608
30.14999	-7.92710
30.64999	-7.86738
31.14999	-7.80716
31.64999	-7.74670
32.14999	-7.68619
32.64999	-7.62583
33.14999	-7.56579
33.64999	-7.50621
34.14999	-7.44722

REFERENCES

CHAPTER 1

[1-1] Burmester, L., Lehrbuch der Kinematik, Leipzig, A. Felix Verlag, 1888.

[1-2] Alt, H., "Zur Synthese der Ebenen Mechanismen," ZAMM 1, 373-398, 1921.

[1-3] Beyer, R., The Kinematic Synthesis of Mechanisms, translated by H. Kuenzel, McGraw-Hill Book Co., Inc., New York, 1963.

[1-4] Hain, K., "Applied Kinematics," McGraw-Hill Book Co., Inc., New York, 1967.

[1-5] Tesar, D., in collaboration with W. K. Kubitza, J. C. Wolford and W. Meyer zur Capellen, "(Translations of) papers (by R. Mueller) on geometrical theory of motion applied to approximate straight-line motion,"

[1-6] Tesar, D., "The Generalized Concept of Three Multiply Separated Positions in Coplanar Motion," Journal of Mechanisms, Vol. 2, 1967, pp. 461-474.

[1-7] Tesar, D., "The Generalized Concept of Four Multiply Separated Positions in Coplanar Motion," Journal of Mechanisms, Vol. 3, 1967, pp. 11-23.

[1-8] Tesar, D., and Sparks, J. W., "The Generalized Concept of Five Multiply Separated Positions in Coplanar Motion," Journal of Mechanisms, Vol. 3, 1968, pp. 25-33.

[1-9] Myklebust, A., and Tesar, D., "The Analytical Synthesis of Complex Mechanisms for Combinations of Specified Geometric or Time Derivatives up to the Fourth Order," JOURNAL OF ENGINEERING FOR INDUSTRY, TRANS. ASME, Series B, Vol. 97, No. 2, 1975, pp. 714-722.

[1-10] Sparks, J. W., Walters, W. T., Tesar, D., "Multiply Separated Position Synthesis - Parts I and II," ASME Paper No. 68-Mech-66, presented at Mechanisms Conference, Atlanta, Oct. 1968.

[1-11] Tesar, D., and Eschenbach, P. W., "Four Multiply Separated Positions in Coplanar Motion," JOURNAL OF ENGINEERING FOR INDUSTRY, TRANS. ASME, Series B, Vol. 89, No. 2, 1967, pp. 231-234.

[1-12] Volmer, J., "Die Sonderfälle der Burmesterchen Mittelpunktkurve mit Doppelpunkt und ihre Getriebetechnische Bedeutung," Revue de Mécanique Appliquée, Vol. 4, No. 2, 1959, Editions de l'Académie de la Republique Populaire Roumaine.

[1-13] Dijksman, E. A., "Geometrical Treatment of the PP-P case in Coplanar Motion," Journal of Mechanisms, Vol. 4, 1969, pp. 375-389.

[1-14] Waldron, K. J., "Graphical Solution of the Branch and Order Problems of Linkage Synthesis for Multiply Separated Positions," JOURNAL OF ENGINEERING FOR INDUSTRY, TRANS. ASME, Series B, Vol. 99, No. 3, 1977, pp. 591-597.

[1-15] Tesar, D., and Carrero, G., "Graphical Procedures for Kinematic Synthesis of Mechanisms," University of Florida, Department of Mechanical Engineering Report, 1975.

[1-16] Tao, D. C., Applied Linkage Synthesis, Addison-Wesley Publishing Co., Inc., Reading, Mass., 1964.

[1-17] Hartenberg, R. S., and Denavit, J., Kinematic Synthesis of Linkages, McGraw-Hill Book Co., Inc., New York, 1964.

[1-18] Filemon, E., "In Addition to the Burmester Theory," Proceedings of Third World Congress for Theory of Machines and Mechanisms, Kupari, Yugoslavia, Vol. D, 1971, pp. 63-78.

[1-19] Waldron, K. J., "The Order Problem of Burmester Linkage Synthesis," JOURNAL OF ENGINEERING FOR INDUSTRY, TRANS. ASME, Series B, Vol. 97, 1975, pp. 1405-1406.

[1-20] Waldron, K. J., "Elimination of the Branch Problem in Graphical Burmester Mechanism Synthesis of Four Finitely Separated Positions," JOURNAL OF ENGINEERING FOR INDUSTRY, TRANS. ASME, Series B, Vol. 98, No. 1, 1976, pp. 176-182.

[1-21] Modler, K. H., "Reinhenfolge der homologen Punkte," Maschinenbautechnik, Vol. 21, 1972, pp. 258-265.

[1-22] Waldron, K. J., and Strong, R. T., "Improved Solutions of the Branch and Order Problems of Burmester Linkage Synthesis," Mechanism and Machine Theory, Vol. 13, No. 2, 1978, pp. 199-208.

CHAPTER 2

[2-1] Beyer, R., The Kinematic Synthesis of Mechanisms, translated by H. Kuenzel, McGraw-Hill Book Co., Inc., New York, 1963.

[2-2] Waldron, K. J., "Elimination of the Branch Problem in Graphical Burmester Mechanism Synthesis for Four Finitely Separated Positions," JOURNAL OF ENGINEERING FOR INDUSTRY, TRANS. ASME, Series B, Vol. 98, No. 1, 1976, pp. 176-182.

CHAPTER 3

[3-1] Waldron, K. J., "Elimination of the Branch Problem in Graphical Burmester Mechanism Synthesis for Four Finitely Separated Positions," JOURNAL OF ENGINEERING FOR INDUSTRY, TRANS. ASME, Series B, Vol. 98, No. 1, 1976, pp. 176-182.

[3-2] Waldron, K. J., "The Order Problem of Burmester Linkage Synthesis," JOURNAL OF ENGINEERING FOR INDUSTRY, TRANS. ASME, Series B, Vol. 97, 1975, pp. 1405-1406.

[3-3] Modler, K. H., "Reinhenfolge der homologen Punkte," Maschinenbautechnik, Vol. 21, 1972, pp. 258-265.

[3-4] Hartenberg, R. S., and Denavit, J., Kinematic Synthesis of Linkages, McGraw-Hill Book Co., Inc., New York, 1964.

CHAPTER 4

[4-1] Waldron, K. J., "Elimination of the Branch Problem in Graphical Burmester Mechanism Synthesis for Four Finitely Separated Positions," JOURNAL OF ENGINEERING FOR INDUSTRY, TRANS. ASME, Series B, Vol. 98, No. 1, 1976, pp. 176-182.

[4-2] Waldron, K. J., "The Order Problem of Burmester Linkage Synthesis," JOURNAL OF ENGINEERING FOR INDUSTRY, TRANS. ASME, Series B, Vol. 97, 1975, pp. 1405-1406.

[4-3] Filemon, E., "In Addition to the Burmester Theory," Proceedings of Third World Congress for Theory of Machines and Mechanisms, Kupari, Yugoslavia, Vol. D, 1971, pp. 63-78.

CHAPTER 5

[5-1] Beyer, R., The Kinematic Synthesis of Mechanisms, translated by H. Kuenzel, McGraw-Hill Book Co., Inc., New York, 1963.

[5-2] Waldron, K. J., "Elimination of the Branch Problem in Graphical Burmester Mechanism Synthesis of Four Finitely Separated Positions," JOURNAL OF ENGINEERING FOR INDUSTRY, TRANS. ASME, Series B, Vol. 98, No. 1, 1976, pp. 176-182.

CHAPTER 6

[6-1] Waldron, K. J., "Elimination of the Branch Problem in Graphical Burmester Mechanism Synthesis of Four Finitely Separated Positions," JOURNAL OF ENGINEERING FOR INDUSTRY, TRANS. ASME, Series B, Vol. 98, No. 1, 1976, pp. 176-182.

[6-2] Filemon, E., "In Addition to the Burmester Theory," Proceedings of Third World Congress for Theory of Machines and Mechanisms, Kupari, Yugoslavia, Vol. D, 1971, pp. 63-78.

[6-3] Hartenberg, R. S., and Denavit, J., Kinematic Synthesis of Linkages, McGraw-Hill Book Co., Inc., New York, 1964.